USARTL-TR-78-53

ADVANCED COMPOSITE ROTOR HUB PRELIMINARY DESIGN

Elliot F. Olster
Sikorsky Aircraft
Division of United Technologies Corp.
Stratford, Conn. 06497

January 1980

Final Report for Period October 1977 - July 1979

Prepared for

APPLIED TECHNOLOGY LABORATORY
U. S. ARMY RESEARCH AND TECHNOLOGY LABORATORIES (AVRADCOM)
Fort Eustis, Va. 23604

APPLIED TECHNOLOGY LABORATORY POSITION STATEMENT

This report provides insight into the benefits to be gained through the application of composite materials to the main rotor hub of the UH-60A helicopter. It is noted, however, that the results are based on a preliminary design and analysis, and findings from related research programs. Final verification will be possible only through full-scale testing, manufacturing and flight demonstration of the composite hub system.

Mr. Harold K. Reddick, Structures Technical Area, Aeronautical Technology Division, served as project engineer for this effort.

Unclassified

SECURITY CLASSIFICATION OF THIS PAGE (When Data Entered)

(19) REPORT DOCUMENTATION PAGE

READ INSTRUCTIONS BEFORE COMPLETING FORM

1. REPORT NUMBER (18) USARTL-TR-78-53	2. GOVT ACCESSION NO. (9)
3. RECIPIENT'S CATALOG NUMBER	
4. TITLE (and Subtitle) (6) ADVANCED COMPOSITE ROTOR HUB PRELIMINARY DESIGN	5. TYPE OF REPORT & PERIOD COVERED Final Rept. Oct 77 - Jul 79
6. PERFORMING ORG. REPORT NUMBER	
7. AUTHOR(s) (10) Elliot F. Olster	8. CONTRACT OR GRANT NUMBER(s) (15) DAAJ02-77-C-0056
9. PERFORMING ORGANIZATION NAME AND ADDRESS Sikorsky Aircraft Division of United Technologies Corp. Stratford, Conn. 06497 323 800 (16)	10. PROGRAM ELEMENT, PROJECT, TASK AREA & WORK UNIT NUMBERS 62209A 1L262209AH76 00 214 EK (17) 001
11. CONTROLLING OFFICE NAME AND ADDRESS Applied Technology Laboratory, US Army Research and Technology Laboratories (AVRADCOM) Fort Eustis, Virginia 23604 (11)	12. REPORT DATE Jan 80
	13. NUMBER OF PAGES 190
14. MONITORING AGENCY NAME & ADDRESS (if different from Controlling Office) (12) 191	15. SECURITY CLASS. (of this report) Unclassified
	15a. DECLASSIFICATION/DOWNGRADING SCHEDULE

16. DISTRIBUTION STATEMENT (of this Report)

Approved for public release; distribution unlimited.

17. DISTRIBUTION STATEMENT (of the abstract entered in Block 20, if different from Report)

18. SUPPLEMENTARY NOTES

19. KEY WORDS (Continue on reverse side if necessary and identify by block number)

Helicopter
Composite Hub
Main Rotor Hub
Main Rotor Head
Composite Rotor

20. ABSTRACT (Continue on reverse side if necessary and identify by block number)

The design requirements for a UH-60A (BLACK HAWK) main rotor hub are presented. A series of six composite hub configurations were evaluated. The evaluation included a comparison to the design requirements as well as additional goals such as reduced weight, cost, radar cross section, use of existing rotor head components, etc. The best of these hub concepts was subsequently refined and reanalyzed. The results of this study indicated the following:

→ (over)

DD FORM 1 JAN 73 1473 EDITION OF 1 NOV 65 IS OBSOLETE

Unclassified

SECURITY CLASSIFICATION OF THIS PAGE (When Data Entered)

323800

Block 20. Continued.

(1) A composite rotor hub can reduce the weight of an equivalent metal hub by up to 15%.

(2) The production and acquisition costs of a composite hub are 20% less than its metal counterpart.

(3) The life-cycle cost analysis indicated that $690K could be saved if the hub were in production by January 1983. The life-cycle cost savings are significantly affected by the "introduction time", and a 6-month delay would negate the cost savings.

(4) For other benefits, such as an alternate source in case of a shortage of titanium, or to generate limited, in-service, maintenance and repair data on a composite hub, a continued effort was recommended.

TABLE OF CONTENTS

TABLE OF CONTENTS (Cont'd)

LIST OF ILLUSTRATIONS

LIST OF ILLUSTRATIONS (Cont'd)

LIST OF ILLUSTRATIONS (Cont'd)

LIST OF TABLES

LIST OF TABLES (Cont'd)

I. BACKGROUND AND INTRODUCTION

A. Prior Studies

Previous studies to evaluate the benefits of a composite hub as compared to a metal one were aimed at the CH-54B Skycrane. This hub, relative to the BLACK HAWK, is large but, because the aircraft is not as maneuverable, the design loads are significantly lower.

Since a half-scale CH-54B is physically equivalent to a full-scale BLACK HAWK a direct comparison of these loads (see Table 1) demonstrates the much more severe loading requirements for the BLACK HAWK.

Table 1

Design Head Moments for the CH-54B and the UH-60A

Design Condition	Head Moment (in.-lbs.)	
	Aircraft	
	CH-54B Skycrane (half-scale)*	UH-60A BLACK HAWK (full-scale)
Fatigue Design	100,000	180,000
Limit Load	164,250	657,470

*moments reduced by 1/8

Although the design requirements were not as severe, the results of the studies are significant and are summarized here. The first composite hub program resulted in the "Whittaker" hub shown in Figure 1. This hub is composed of many layers of filament-wound fiberglass tension loops which are continuous from one blade attachment lug to the opposite one. This system is inexpensive to manufacture and is structurally efficient for carrying centrifugal loads introduced by the blades. It carries vertical forces, that is shears introduced by blade flapping and coning, as interlaminar shear stresses in the composite. The interlaminar plane is the weakest in the composite, and during tests the hub failed prematurely in an interlaminar mode. The "Kaman" hub is shown in Figure 2. It consists of three relatively easy to manufacture graphite/epoxy plates. This hub carries the vertical shear loads by a truss-type action and thereby loads the composite in an in-plane mode rather than in an interlaminar mode. The Kaman hub is lighter and less costly than its titanium counterpart. A portion of the weight saved is attributable to the bonded joints between titanium and

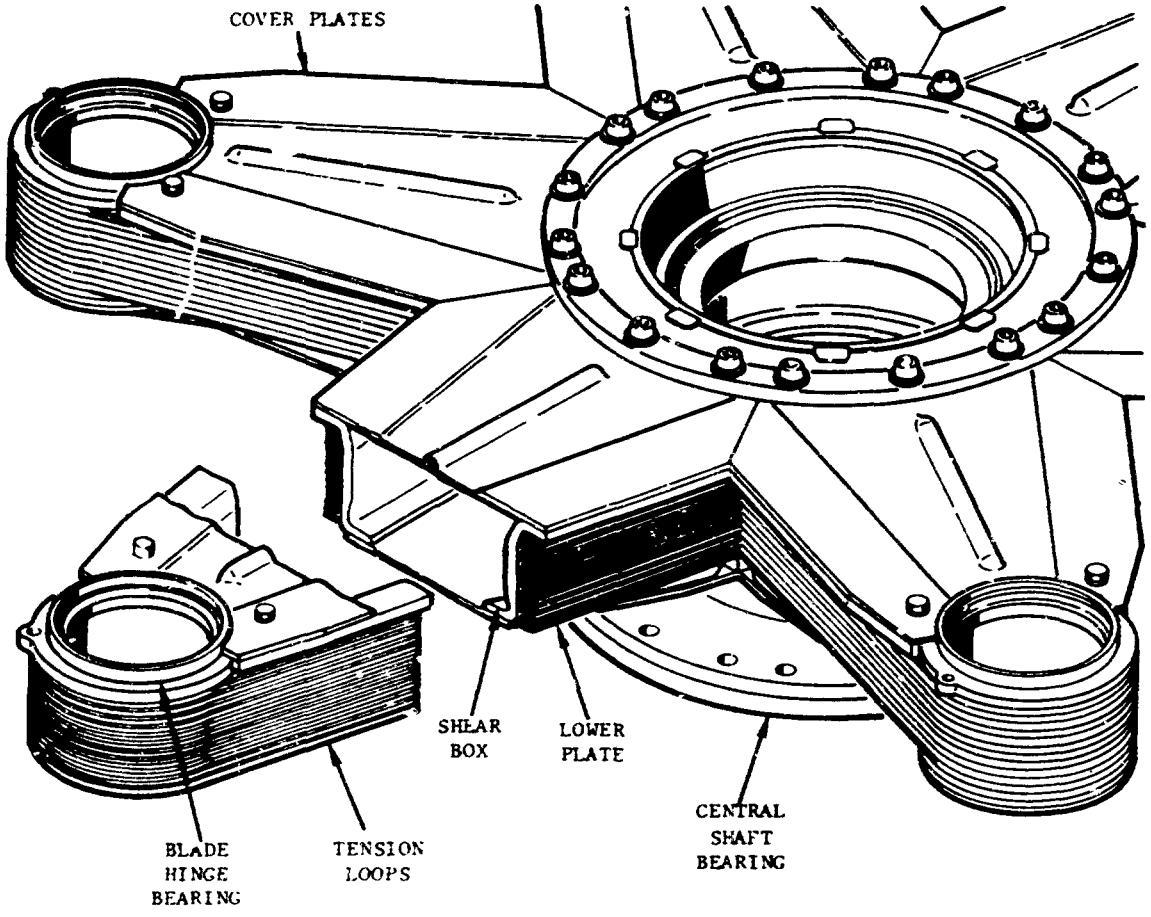

FIGURE 1. SCHEMATIC OF THE "WHITTAKER" HUB

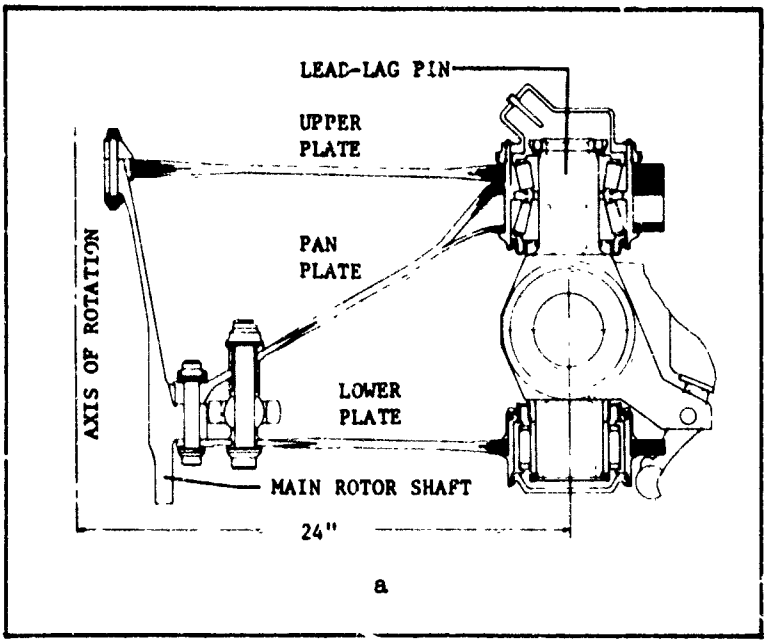

FIGURE 2. CROSS SECTION OF THE "KAMAN" HUB

graphite/epoxy. Although these joints are structurally efficient under normal conditions, there is some question as to their ability to successfully sustain ballistic damage, as will be discussed later.

B. Objectives of the Present Study

The present study was directed toward: (1) summarizing design data for the BLACK HAWK main rotor hub; (2) developing and evaluating a series of composite hub concepts; (3) selecting the best of these hub concepts; and (4) refining its design.

The design data included the geometric constraints, the design loads, the ballistic requirements, and the reliability and maintainability requirements for the present BLACK HAWK rotor hub.

The composite hub concepts were designed to meet the above requirements as well as the following additional design goals:

1. Make maximum use of existing BLACK HAWK rotor head components.

2. Achieve an acquisition cost savings of 25% and an overall reduction in life-cycle costs.

3. Obtain a 15% reduction in weight.

4. Obtain a 98% reduction in radar cross section in the 5 to 15 GHz radar frequency range.

5. Improve the damage tolerance as compared to a titanium hub and design the hub to be field repairable for external damage.

6. Design the hub so that no in-flight testing is required to track and balance when the titanium rotor hub housing is replaced with the composite and so that no in-flight tracking is required when interchanging blades on the composite hub.

One candidate was selected from all those considered by conducting a trade-off study, which included the following parameters:

(1) Cost
(2) Weight
(3) Ballistic Survivability
(4) Reliability
(5) Maintainability

(6) Producibility

(7) Repairability

(8) Radar Reflectivity

(9) Lightning Protection

The hub concept receiving the highest score in the trade-off study was refined and subsequently analyzed more thoroughly. The final evaluation included a more detailed investigation of the parameters listed in the trade-off study as well as a preliminary structural analysis.

II. DESIGN REQUIREMENTS FOR THE BLACK HAWK ROTOR HUB

A. Geometric Requirements

The geometric requirements are described in Figure 3. The centerline of the pitch-flap-lag bearing, with respect to the center of rotation, is shown in the Plan and Elevation View. The arms are offset by 1.83 inches and the face of each arm is preconed 8°. From this position the bearing is free to move up 17° and down 14° in the flap direction and $\pm 10^{\circ}$ in the lead-lag direction. The overall motion of the elastomeric bearing is shown by shaded areas in Figure 3. The movement of the control horn and damper/accumulator system is given in Sections A-A through E-E. The location of the damper bearing is described by offsets in the Plan View, and its vertical position is shown in Section E-E.

For air transport the hub is lowered and the shaft extension is removed (see Figure 4). To meet the present requirements, no portion of the hub can be more than 5.2 inches above the centerline of the arm at Section A-A of Figure 3, i.e., above waterline 318.78. In addition, no portion of the hub can be below waterline 307.62.

B. Design Loads

A schematic of the present BLACK HAWK hub is shown in Figures 5 and 6. The primary design loads are those at the flap/hinge and are designated as P_{HA}, P_{HC}, and P_{HF} for load at the hinge in the axial, chordwise and flatwise directions respectively (refer to Figure 6). These loads are transferred to the bearing end plate through an elastomeric bearing (see Figure 6). The damper, which also serves as a lead/lag stop, introduces loads to the side of each hub arm. These are designated as P_{DA}, P_{DC} and P_{DF} for load at the damper lug in the axial, chordwise, and flatwise directions respectively (refer to Figure 6). When the blade hits the hub stops, either droop or flap, the forces P_{SD} or P_{SF} respectively are developed (see Figure 6). These are reacted by forces at the hinge (P_{HA} and P_{HF}) and develop an axial and shear force as well as a bending moment M_{BEP} at the bearing end plate.

The primary design loads are summarized in Table 2. A more complete description of the loads and load development taken from Reference 1 follows.

---

[1] "Main Rotor Head Structural Analysis, UH-60A," SER-70514, Sikorsky Aircraft.

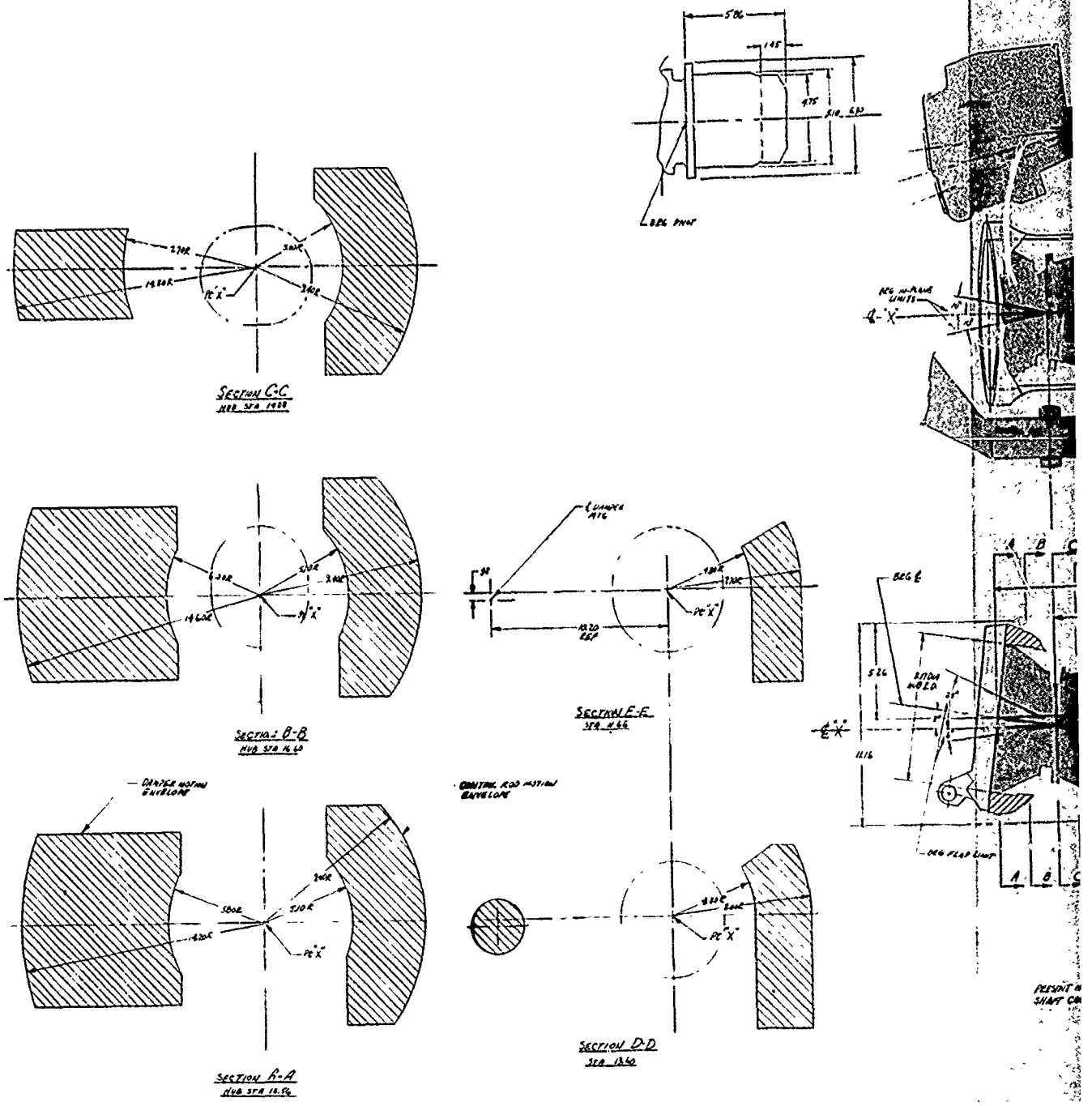

FIGURE 3

GEOMETRIC REQUIREMENTS FOR UH-60A ROTOR HUB

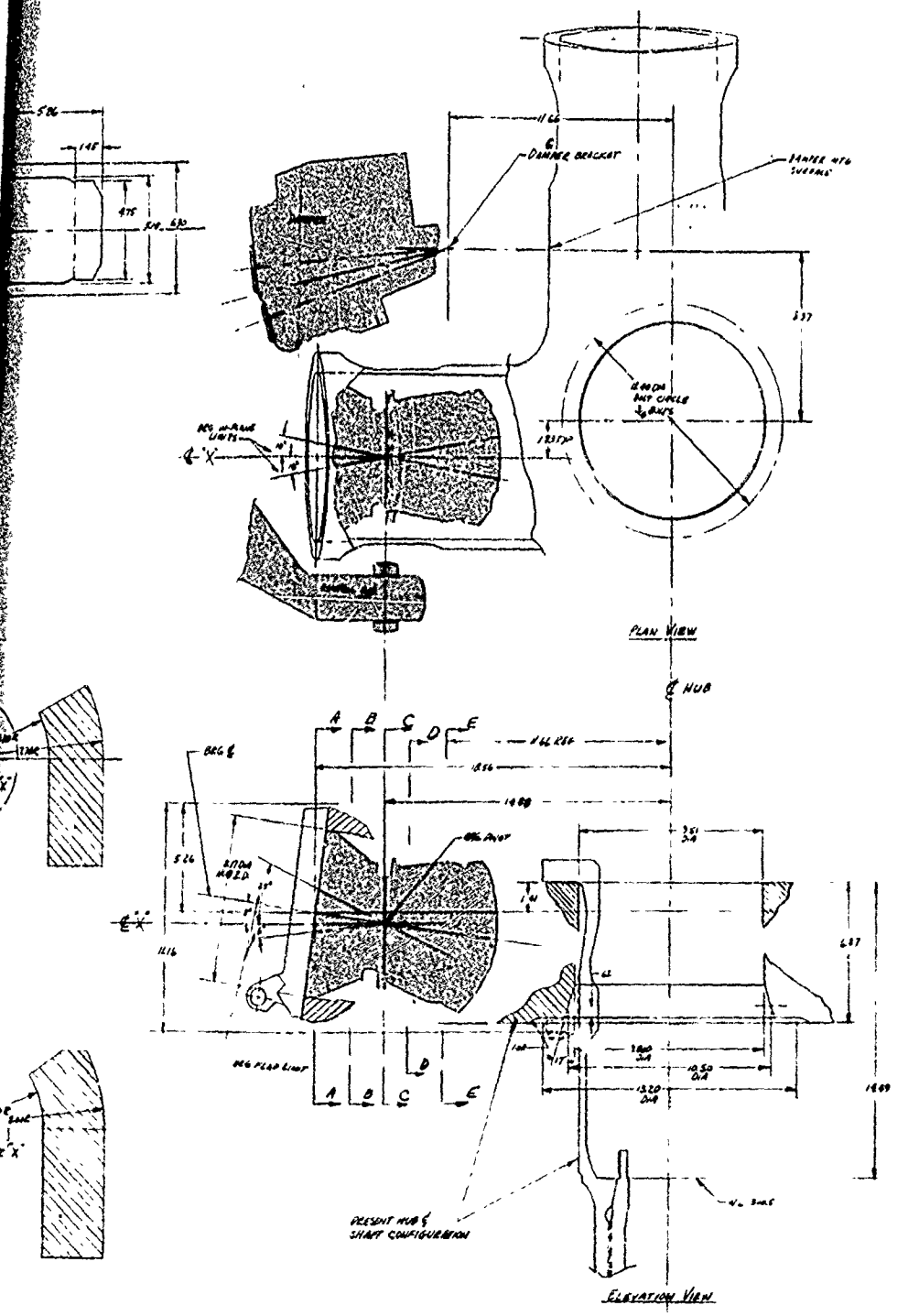

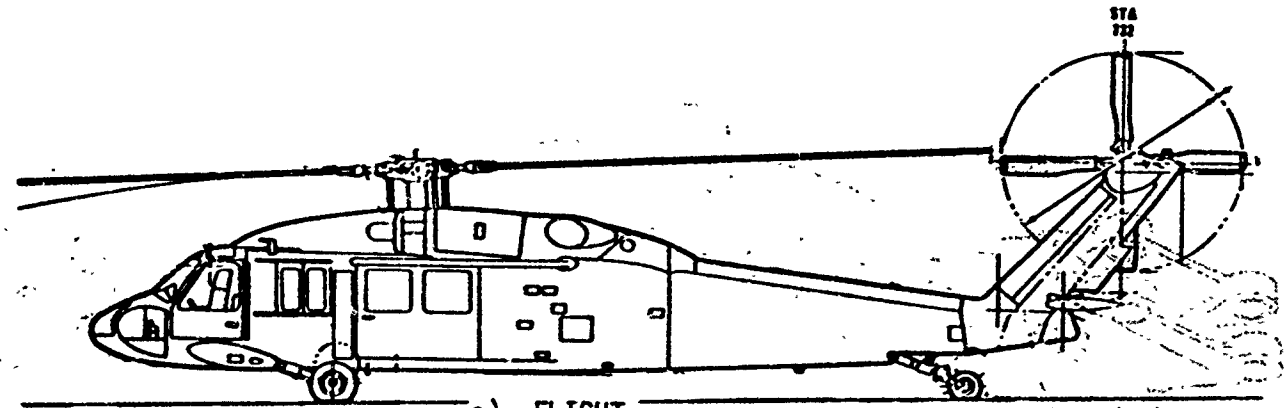

a) FLIGHT

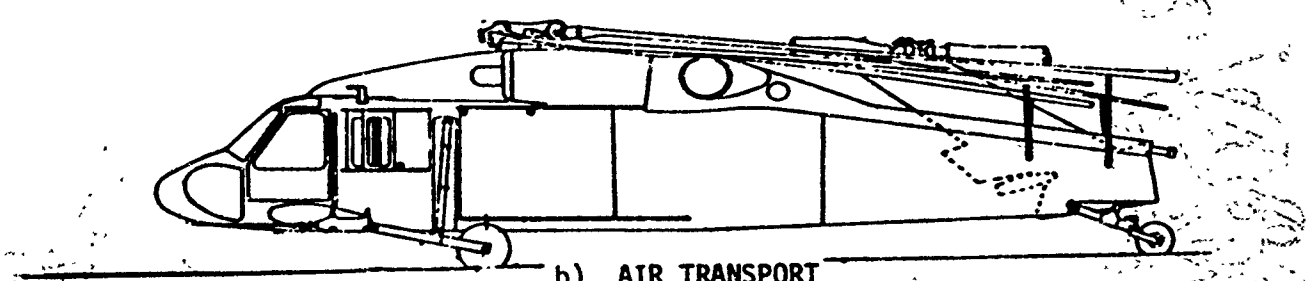

b) AIR TRANSPORT

FIGURE 4. POSITION OF THE HUB DURING a) FLIGHT AND b) AIR TRANSPORT.

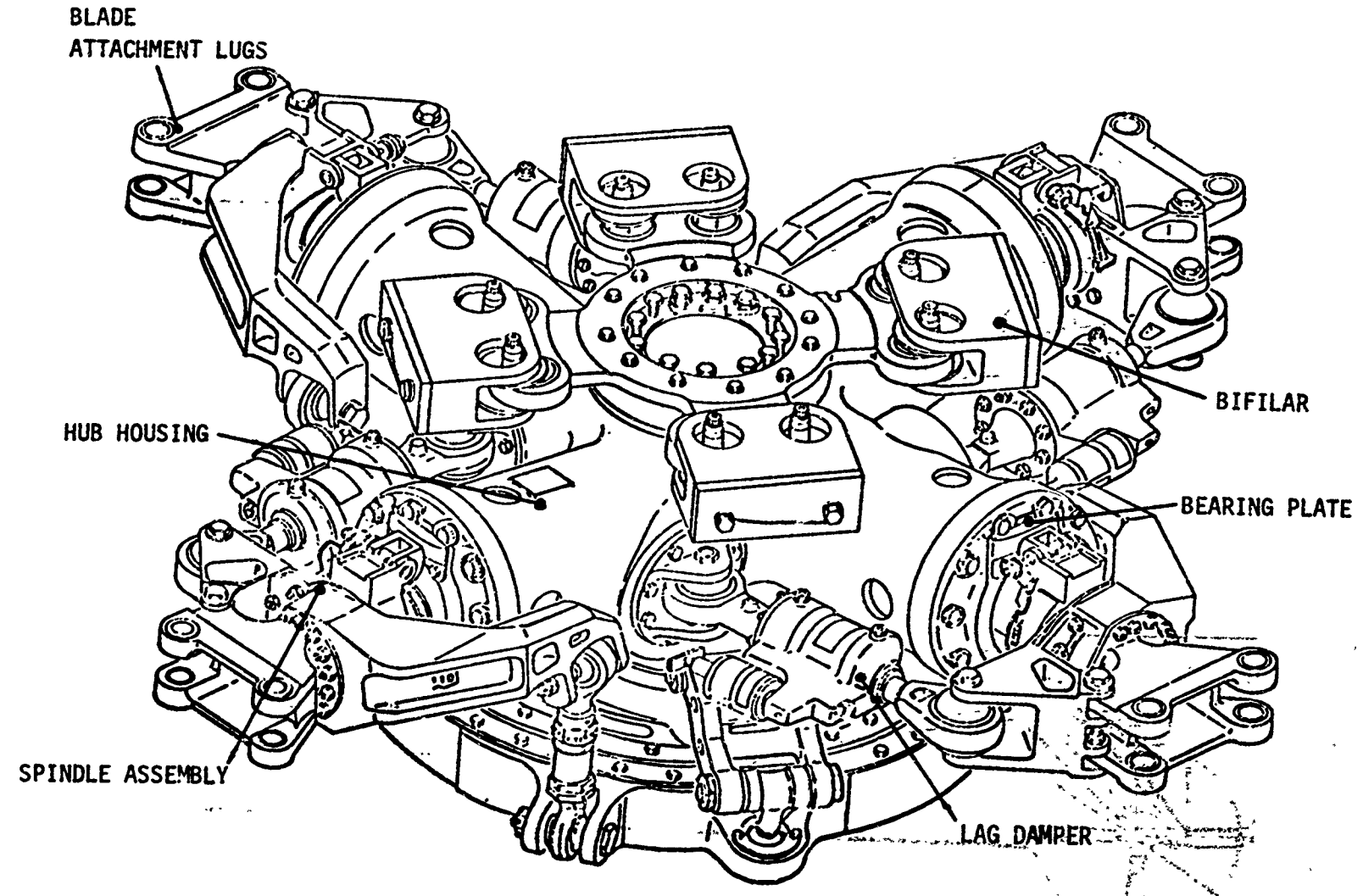

FIGURE 5. UH-60A MAIN ROTOR HUB

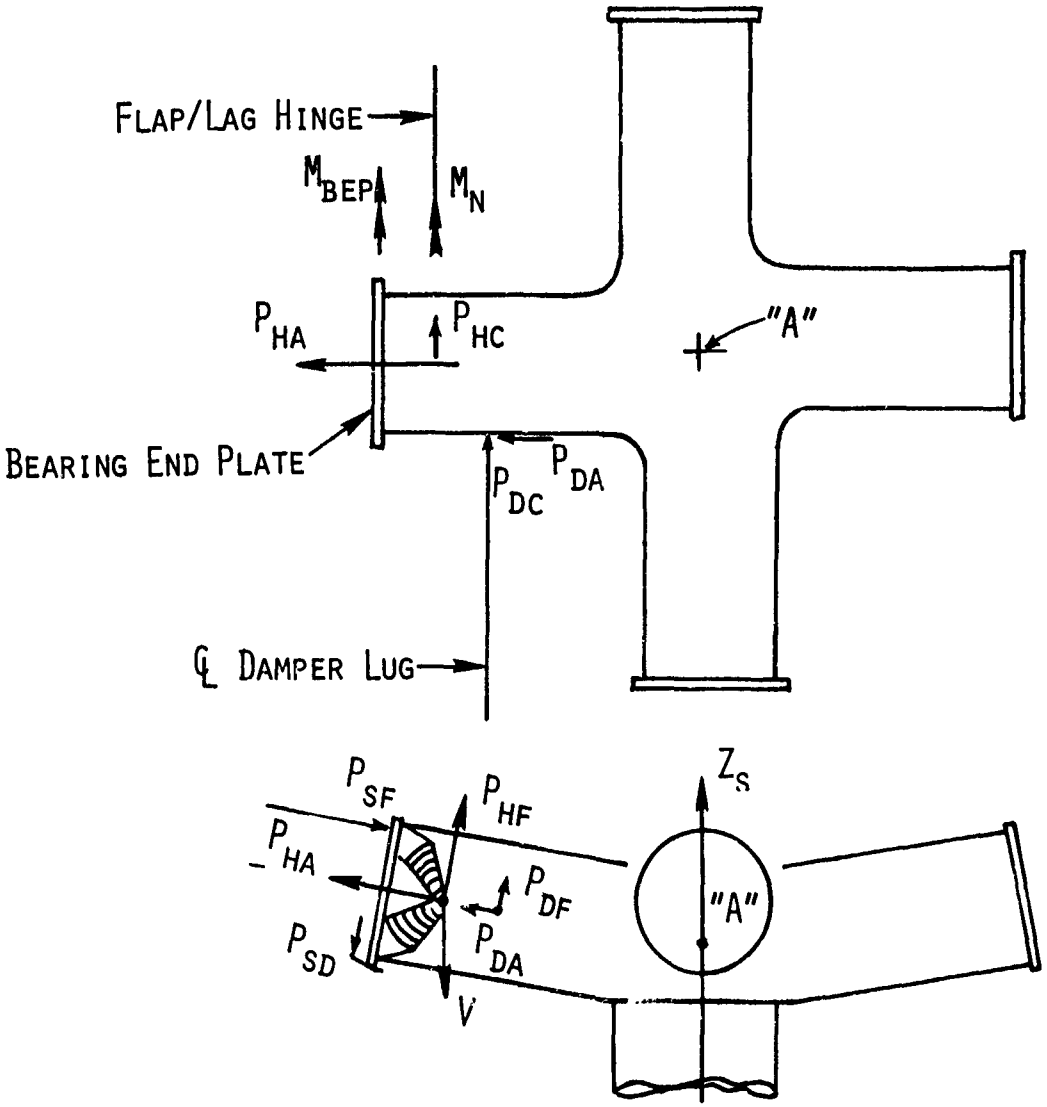

FIGURE 6. HUB CONFIGURATION AND LOADING POINTS

Ground and Handling Loads

- Limit Droop Condition

The droop stop reacts the dead weight of the mass outboard of the flap-lag hinge when the rotor is not turning. An ultimate ground load handling factor of 4g vertical is applied to the loads to determine the ultimate loads. These loads are divided by 1.5 to obtain the limit load.

Moment about the flap-lag hinge:

Mn = Maximum Lifting Moment about spindle
Mn = 250(145.03 - 15)(4/1.5) (From Figures 6 & 7)
Mn = 86,866 in.-lb

TABLE 2
Primary Design Loads Summary

Limit Load

P_{HA} = 108,122 lb

M_T = 486,667 in.-lb

M_H = 657,478 in.-lb

Fatigue Load

P_{HA} = 68,562 $\pm$ 3638 lb

P_{HF} = 4772 $\pm$ 5799 lb

P_{HC} = 10,200 $\pm$ 1850 lb

P_{DC} = 0 $\pm$ 716 lb

P_{DA} = 0 $\pm$ 38 lb

Starting Load

P_{HA} = 23,000 lb

P_{HC} = 406 lb

P_{DA} = 2570 lb

P_{DC} = 23,000 lb

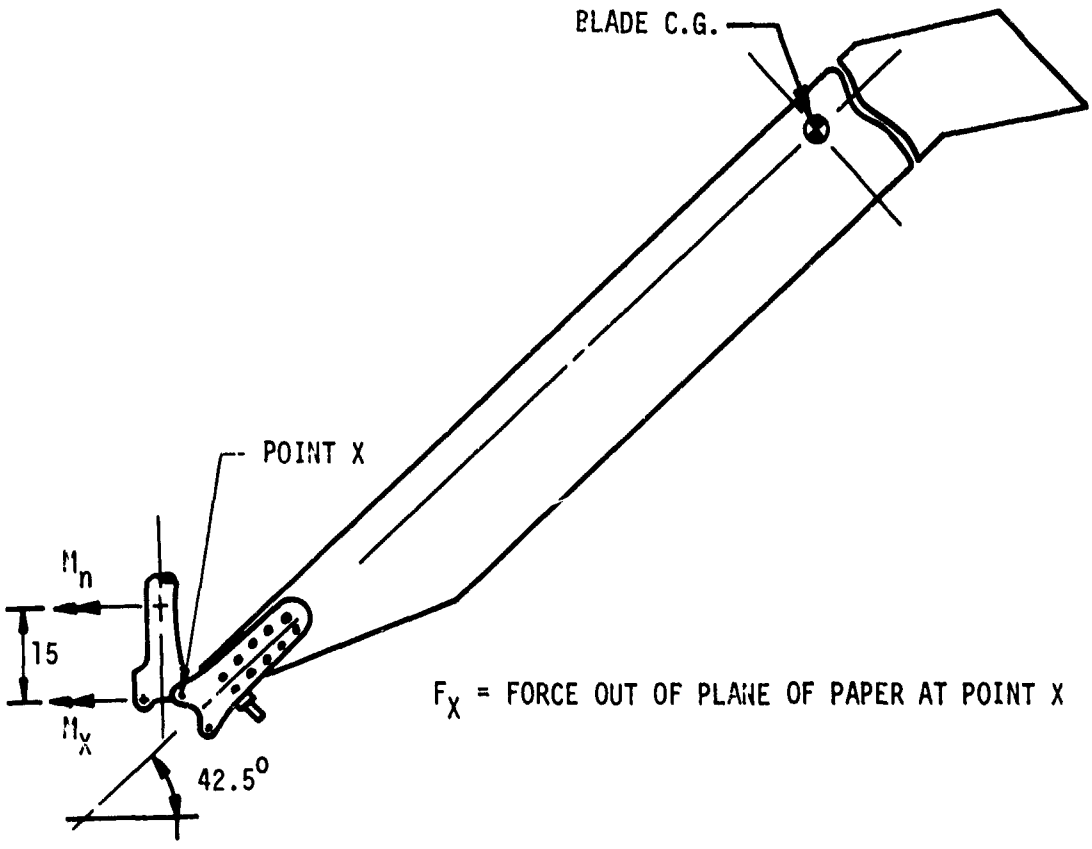

FIGURE 7. BLADE GEOMETRY FOR MAXIMUM LIFTING MOMENT DURING FOLDING

The normal shear is the dead weight of the mass outboard of the flap-lag hinge.

$$Vn = (4/1.5)(-250) = -667 \text{ lb}$$

- Blade Fold Loads

The limit lifting moment, for design of the anti-flapping mechanism, occurs during the blade folding condition with a 45-knot wind. The maximum moment occurs on Blade #1 during the unfold cycle. Figure 7 depicts the geometry for the maximum load condition.

Loads at the blade fold joint are (Reference 1):

$Mx = 24{,}000$ in.-lb

$Fz = 317$ lb

Moment at the flap-lag hinge:

$Mn = Mx + Fz \times d$

$Mn = 24{,}000 - (317)(15) = 19{,}245$ in.-lb

where Mx, Mn, Fz and d are defined by Figure 7.

Starting Conditions

- Static Design Loads

The shaft torque "Q" is 1.5 times the SLS (Sea Level Standard) single engine intermediate power rating at normal operating speed.

$Q = 511{,}000$ in.- lb

Distributing the starting torque to three of the four blades, the torque per arm (T') is as shown below:

$T' = Q/3 = 170{,}330$ in.-lb

Chordwise Shear:

$$P_{HC} = \frac{T}{R}$$

$T = 170{,}330$ in.-lb

$R = 145.3 - 15 = 130.3$ in.

$$P_{HC} = \frac{(170{,}330)}{130.3} = 1307 \text{ lb}$$

Normal Shear:

During the starting condition, the maximum normal shear is the reaction to the deadweight outboard of the flapping axis. Since the weight acts downward, the shear load is negative.

$$V_{Nmax} = -250 \text{ lb}$$

Normal Moment at Flapping Axis:

$$Mn = (145.3 - 15)(250) = 32,575 \text{ in.-lb}$$

This is reacted by the elastomeric bearing, P_{HA}, and the droop stop.

In addition, during startup, the blade "bottoms out" against the lag stop which is built into the damper. These bearing forces, as well as damper loads, are summarized in Table 3.

Table 3
Reaction Forces During Startup

Force	Magnitude (lb)
P_{HA}	17,000
P_{HC}	300
P_{DA}	1,900
P_{DC}	17,000

- Limit Rotor Acceleration Load

The limit shaft torque resulting from 1.5 times the main gearbox power rating at the operating main rotor speed is distributed equally to all four blades. Ninety three and one-half percent of the engine power is applied to the main rotor; the remaining six and one-half percent of the power is used for tail rotor power and gearbox losses.

$$Q = 920,000$$

Torque per blade:

$$T = \frac{Q}{4} = \frac{920,000}{4}$$

$$T = 230,000$$

For this condition the loads are given in Table 4.

Table 4

Reaction Forces During Limit Rotor Acceleration

Force	Magnitude (lb)
P_{HA}	23,000
P_{HC}	406
P_{DA}	2,570
P_{DC}	23,000

Cruise Flight Loads

The flapping angle spectrum is presented in Table 9. The design condition is 6° of flapping which represents a condition exceeded less than 0.2 percent of the flight time.

Flapwise Loads

Flapwise steady shear at flap-lag axis - shaft axis system:

$$P_{HF} = \frac{\text{Gross Weight - Weight Outboard of Flap-Lag Axis}}{\text{Number of Blades}}$$

where

Gross Weight = 16,250 lb

Weight outboard of flap-lag axis = 250 lb

$$P_{HF} = \frac{16,250 - (4)(250)}{4} = 3812 \text{ lb}$$

P_{HF} Pushrod = 960 lb

P_{HF} Total = 4772 lb

Flapwise vibratory shear at flap-lag axis - shaft axis system:

$$P_{HF} = T_C \text{ TAN } \alpha$$

where T_C = centrifugal force = 69,220 lb

$$P_{HF} = 69,220 \text{ TAN } 4.2^{o}$$

$$P_{HF} = \pm 5083 \text{ lb}$$

Flapwise damper component reaction:

$$P_{HF} = \pm 716 \text{ lb}$$

Flapwise pushrod reaction:

$$P_{HF} = \pm 1600 \text{ lb but is zero when other contributions are max.}$$

Total flapwise shear at flap-lag axis:

$$P_{HF} \text{ Total} = 4772 \pm 5083 \pm 716 \pm 0 = 4772 \pm 5799 \text{ lb}$$

Chordwise Loads

The chordwise shear is developed by distributing the shaft torque equally to all four blades at the flap-lag hinge.

$$P_{HC} = \frac{Q}{4e}$$

where

$$Q = 612,037 \text{ in.-lb}$$

$$e = \text{Offset} = 15 \text{ in.}$$

$$P_{HC} = 10,200 \text{ lb}$$

Chordwise vibratory shear at flap-lag hinge:

$$P_{HC} = T_C \sin \alpha$$

where

$$T_C = 69,220 \text{ lb}$$

$$\alpha = \pm 1.5^{o}$$

$$P_{HC} = (69,229)\ (.02618)$$

$$P_{HC} = \pm 1812 \text{ lb}$$

Chordwise damper component reaction:

$$P_{HC} = \pm 38 \text{ lb}$$

Total chordwise shear at flap-lag hinge:

$$P_{HC} = Vc \text{ Total} = 10{,}200 \pm 1812 \pm 38 = 10{,}200 \pm 1850 \text{ lb}$$

Axial Loads

The equations for the variation in centrifugal tension for the design flapping angle have been developed previously in Reference 2 and for 3.3° coning, and 4.2° flapping, the equations reduce to

$$P_{HA} = .9905\ T_C \pm .0095\ T_C$$

where

$$T_C = \text{centrifugal force} = 69{,}220 \text{ lb}$$

$$P_{HA} = 68{,}562 \pm 658 \text{ lb}$$

The axial component of the damper load acting at the flap-lag hinge is

$$P_{DA} = \pm 2980 \text{ lb}$$

Total axial load at flap-lag hinge is

$$P_{HA} = P_{HA} + P_{DA}$$

$$P_{HA} = 68{,}562 \pm 3638 \text{ lb}$$

Limit Flight Loads

Contained in Reference 1 are the limit main rotor head loads and moments with respect to the aircraft x, y and z axes. Those loads and moments are transformed to axes parallel and perpendicular to the main rotor drive shaft. Figure 8 depicts the sign convention for the shaft coordinate system. The relationships between forces and moments in these coordinate systems are

$$F_{sx} = F_x \cos\theta + F_z \sin\theta$$

$$F_{sz} = F_z \cos\theta - F_x \sin\theta$$

---

[2] "Main Rotor Head Loads, CH-53A," SER-65046, Sikorsky Aircraft.

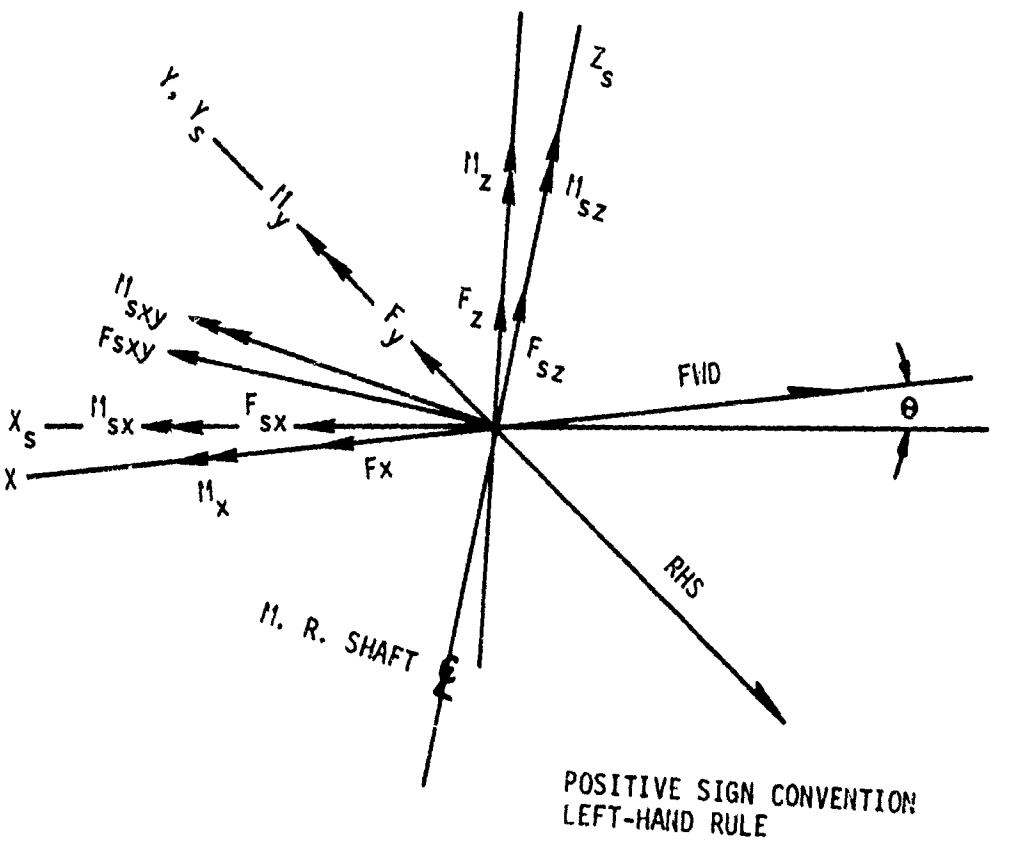

X, Y, Z - Fuselage Reference System

X_s, Y_s, Z_s - Drive Shaft Reference System

FIGURE 8. MAIN ROTOR HEAD LOAD SIGN CONVENTION

$$F_{sxy} = F_{sx} \leftrightarrow F_y$$

$$M_{sx} = M_x \cos \theta + M_z \sin \theta$$

$$M_{sz} = M_z \cos \theta - M_z \sin \theta$$

$$M_{sxy} = M_{sx} \leftrightarrow M_y$$

where

F_x, F_y, F_z = Total applied main rotor head loads

M_x, M_y, M_z = Total applied main rotor head moments

Table 5 contains the resulting head moments and thrusts which are used to calculate the maximum normal shear load per blade at the flap-lag hinge.

The axial, flapwise and edgewise loads at the flap-lag hinge are summarized in Tables 6, 7 and 8.

Centrifugal Tension

The loads at the flap-lag axis at selected speeds are presented in Table 6.

Chordwise Shear

The shaft torque is reacted by the chordwise shear at the flap-lag hinge using the relation $P_{HC} = Q/be$.

The chordwise shear loads were calculated using the above equation with shaft torques from Table 5 and are summarized in Table 7.

Flapwise Shear

The flapwise shear force at the flap hinge causes the pitching and rolling moments which in turn control the helicopter:

$$P_{HF} = \pm \frac{M^1}{2e} + \frac{F_{sz}}{\Lambda} - Tc \text{ Tan } B^1$$

where

B^1 = precone angle = 8^0

e = hinge offset = 15 inches

M^1 = Msx, Msxy, My, whichever is the largest for a given flight condition

TABLE 5. SUMMARY OF MAIN ROTOR LIMIT LOADS AND MOMENTS

KEY	GROSS WEIGHT	SPEED (KTS)	RPM (lbs)	F_Y (lbs)	F_{SX} (lbs)	F_{SZ} (lbs)	M_Y (in-lbs)	M_{SX} (in-lbs)	M_{SZ} (in-lbs)	M_{SXY} (in-lbs)	F_{SXY} (lbs)	Q_{MR} (in-lbs)
A*	16,250	210	329	82	4517	16,565	484,560	-42,155	608,695	486,390	4518	609,235
B*	16,250	175	329	521	1186	985	-519,060	-67,290	471,428	523,405	1295	471,045
C*	19,930	203	329	406	7899	32,036	600,108	16,332	420,781	600,330	7910	420,576
D*	16,250	105	329	810	-5690	42,035	-581,316	-307,163	486,596	657,478	5747	486,667

KEY	NUMBER	CONDITION
A	1-F6-9-021	Yaw Recovery
B	1-F3-40-003	Push Over
C	3-F1-27-002	Pull Up
D	2-F2-5-003	Roll Pullout

Fsz = Vertical Load along the shaft axis

Tc = Centrifugal Force

The limit flapwise loads are summarized in Table 8.

Table 6
Centrifugal Tension Loads at Flap Hinge

90% N_R	100% N_R	110% N_R	125% N_R
56,207 lb	69,220 lb	83,756 lb	108,122 lb

Table 7
Chordwise Shear Loads at Flap Hinge

Condition No.	Q (in.-lb)	P_{HC} (lb)
1-F6-9-021	609,235	10,156
1-F3-40-002	471,045	7,852
3-F1-27-002	420,576	7,011
2-F2-5-001	486,667	8,113

Table 8
Flapwise Shear Loads at Flap Hinge

Condition No.	M^1	$\frac{M^1}{2e}$	$\frac{Fsz}{4}$	Tc Tan B^1	P_{HF}
1-F6-9-021	486,390	16,213	4,141	15,195	27,267
1-F3-40-003	523,405	17,446	246	15,195	32,395
3-F1-27-002	600,330	20,011	8,009	15,195	27,197
2-F2-5-001	657,478	21,915	10,508	15,195	26,602

- Limit Pushrod Loads

The control system limit loads were developed for the in-flight jam condition. The pushrod loads are less than P_{HF} in Table 8 and therefore do not affect the design of the hub.

Fatigue Spectrum

The fatigue spectrum includes both high- and low-cycle occurrences and can be presented in a variety of ways. The most convenient for high-cycle fatigue is the flapping angle (B) vs. the percent time as given in Table 9.

Table 9

Flapping Angle Spectrum

Flapping Angle (B)	% Time	Head Moment (In.-Lb)
±13	.0001	396,240
±12	.0002	365,760
±11	.0003	335,280
±10	.0014	304,800
± 9	.0025	274,320
± 8	.0125	243,840
± 7	.0280	213,360
± 6	.0950	182,880
± 5	.410	152,400
± 4	1.95	121,920
± 3	97.50	91,440

- Low Cycle Fatigue (LCF) Loads

Low cycle fatigue loads are those loads that occur only a limited number of cycles per flight hour and are developed from the maximum and minimum loads in the load spectrum.

ON/OFF Cycle

The ON/OFF cycle consists of all the load conditions imposed on the aircraft during one complete flight mission*. From these loads, the maximum and minimum stresses are combined for each component to give one LCF cycle per each flight hour of the aircraft.

*During a flight mission the peak stress reached is that which is not exceeded more than 0.5% of the design life of the aircraft.

Ground Idle/Lift-Off Cycle

For each complete mission, there are three times when the aircraft lands and the main rotor speed is allowed to decay to 40 percent N_R. The main rotor is then accelerated to its normal rotor speed, takes off, and experiences in-flight loads. As in the ON/OFF cycle, the maximum and minimum stresses for these conditions are combined for each component to obtain three cycles per each flight hour of the aircraft.

Start Cycle

During one mission of the aircraft, the main rotor is accelerated from rest to its operating rotor speed. Based on experience, the LCF load developed during the start condition is taken to be twice the normal in-flight damper load. At the same time, a 1G static droop blade load is applied to the main rotor head.

Droop Stop Pounding

To account for the loads imposed on the aircraft due to droop stop pounding, the following LCF spectrum is used:

Four contacts per flight hour @ 2G deadweight moment.

One contact per flight hour @ 2.67G deadweight moment.

C. Reliability Goals

One of the driving forces behind the increased use of composites is the increase in reliability, i.e., the decrease in failure rate. Hub failures can be classified according to severity and cause.

Severity of failures is categorized as minor, major and critical. Minor failures merely require maintenance and generally are termed discrepancies. Major failures represent a threat to personnel and equipment and result in a degradation in performance. Critical failures result in loss of control of the aircraft.

Classification by cause divides failures into inherent or induced modes. Induced failures generally include any damage caused by external influences such as by foreign objects, by certain environmental factors or by conditions outside the design envelope such as overload conditions. Inherent failures include anything that is not induced such as fretting, cracking, etc.,which occur at load levels within the design envelope. Examples are given in Table 10.

TABLE 10

Examples of Hub Failures

Inherent Failures

Minor

- fretting
- delaminations
- change on bolt preload

Major

- formation of a small crack
- loss of primary fastener

Critical

- loss of multiple primary fastener
- growth of large crack

Induced Failures

Minor

- scratch, gouge
- delamination (composite only)
- lightning (composite only)

Major

- gouge
- small ballistic perforation

Critical

- large ballistic perforations

Inherent Failures

General design requirements related to inherent modes of failure are taken from the Prime Item Development Specification (PIDS), Reference 3, and are summarized on page 39. For many items the inherent modes are the same for either a metal or a composite hub. Examples of these are cracking, fretting, loosening of inserts, corrosion of certain components, and debonding of liners. There are, however, some inherent modes which are unique to composites. They include items such as surface crazing and delamination.

In order to quantify the inherent reliability goals of the composite hub it was necessary to look at the titanium hub data as a baseline.

Titanium hubs exist on the UH-60A, the CH-53E and the CH-53D. A summary of available data is presented in Table 11. These "failures" are all minor and are termed discrepancies and have been used to estimate a MTBM.

It is important to realize that both the UH-60A and the CH-53E are development aircraft and the fully "matured" versions will have greater MTBM's. The data on the BLACK HAWK (UH-60A) indicates that the hub assembly, excluding the elastomeric bearings, has a relatively high MTBM. The requirement for a fully matured UH-60A hub is as follows:

Hub	=	2,173 hours
Shaft Extension	=	16,666 hours
Bifilar	=	380 hours
Pressure Plate	=	33,333 hours

Based on the CH-53D data, which is a more complex but fully matured titanium hub, these goals for the BLACK HAWK appear to be reasonable. As a result of fatigue substantiation tests the crack initiation time has been determined to be approximately 23,800 hours. Therefore, it has, relative to its 20,000-hour requirement, an unlimited life. In summary, the composite hub should have an unlimited life and a system MTBM of at least 2,173 hours.

---

[3] UH-60A Prime Item Development Specification, November 1, 1976, Contract No. DAAJ01-77-C-000L (P6A).

Table 11

Review of Existing Titanium Hub Reliablity and Maintainability Data

Aircraft	Discrepancy	No. of Events	MTBM
UH-60A	1936 Flight Hours		
	Elastomeric Bearing	7	277
	Hub Assembly (Brkt., pin, bolt)	3	645
CH-53E	1075 Flight Hours		
	Unbalance	3	358
	Fretting	2	537
CH-53D	17,498 Flight Hours		
	Scored	3	5832
	Unbalance	8	2187
	Distorted	5	3499

Induced Failure Modes

Induced failures result from external forces. They fall under the general headings of environmental damage, foreign object damage, and overload damage. The Prime Item Development Specification (PIDS) provides the requirements for the current titanium hub. Because of differences due to the use of composites, the requirements have been expanded somewhat. Overload damage is that which is outside of our design requirements and is not covered by any specification.

Environmental hazards include lightning strikes, corrosion, salt spray, ice, etc. The PIDS design requirements for environmental effects are summarized on page 40. Lightning strikes present no particular hazard to the titanium hub. They should be included in the design requirements for a composite hub, and a conservative strike is a 200K amp initial surge followed by a 200 amp current for a duration of two seconds.

The design approach that was used to maximize the reliability of the hub is summarized below.

- Choose a material layup with high strength and good resistance to crack formation and propagation.
- Minimize the tendency for delamination by careful attention to design details.
- Use redundant load paths.
- Design for low operating stresses.
- Use conservative design allowables.
- Good quality control - readily inspectable.
    - Individual components
    - Completed assembly on the aircraft
- Choose designs and manufacturing techniques which provide reproducibility from part to part.
- Eliminate, if possible, regions on the present hub which have a low MTBM.

Design Requirements Related to Inherent Modes of Failure

Safe-life design shall be employed as the primary means of satisfying the useful life requirements.

Whenever practicable, "fail-safe" design principles shall be employed to permit use of "on-condition" replacement rather than mandatory component retirement times. These principles shall include slow crack growth, crack arrestment, alternate load paths, and the establishment of adequate inspection intervals and procedures.

Resistance of materials to fracture (both static-fracture toughness and fatigue-crack propagation) will be one of the primary considerations in material choice as dictated by the end-product application of the material. Factors that shall be considered both in choice of materials and processing of materials include, but shall not be limited to:

Inclusions introduced during manufacturing.

Ply layup.

Stress risers through design or fabrication.

Where it is necessary to develop data and properties for materials and composites, the test materials, processes and composites shall be those intended for use in production aircraft. Minimum properties obtained from the foregoing sources shall be used for design purposes. In MIL-HDBK-5 "A" values shall be used in the design of structural components except that "B" allowables can be used for the fail safe or multiredundant structures which are designed to carry full limit loads after failure of one member.

Design Requirements for Environmental Hazards

The selection of allowable stresses used for design shall include consideration of reduction of material strength due to environmental effects. Allowable stresses shall be selected on the basis of creep, thermal expansion, joint-fastener re[illegible]ation, and fracture toughness. Temperature extremes range from + 18[illegible] to -65°F.

All system parts shall be suitably treated or finished to provide protection from corrosion.

The aircraft and its subsystems shall be capable of operating during and after exposure to salt spray conditions. No degradation in performance or life shall be in evidence for an exposure up to 10 percent of the component design service life.

The aircraft and its subsystems shall be capable of being subjected to radiant energy at the rate of 100 to 400 watts per square foot. Fifty to 84 watts per square foot shall be assumed to be in wave lengths above 7,800 angstrom units and four to eight watts per square foot shall be assumed to be in wave lengths below 3,800 angstrom units. The duration of the sunlight exposure shall be assumed to be 48 continuous hours.

The aircraft shall operate with no adverse effects while being subjected to blowing snow of a crystal size range of 0.02 to 0.4 mm with a median of 0.1 mm to a wind speed of 35 knots.

Foreign Object Damage (FOD) results from ballistic impacts, bird strikes, hail, and tool drops or other handling damage. Specific requirements exist only for ballistic impacts and are presented in Table 12. For the composite hub it is necessary to define limits for other types of FOD. Bird strikes on the hub, while potentially high in impact energy (1/2-lb bird impacting on aircraft traveling at 145 knots can transfer approximately 200 foot-pounds of energy), are extremely rare and hence can be ignored. Hail up to 1/2 inch in diameter impacting at 145 knots should not result in damage to any of the structural composite. Tool droop damage varies depending upon total impact energy and energy intensity (i.e., whether a point or a blunt portion hits the hub). A reasonable design criterion is that no damage to structural material occur for impacts resulting from a 2" diameter steel ball dropped from 10 feet.

Table 12

Ballistic Requirements

Essential components listed below shall accept damage from impact by a projectile of the type and striking velocity specified and still be capable of supporting limit load without failure (yielding is allowed for this condition) and continued safe flight for at least 30 minutes at normal operating loads.

Flight Essential Component	Projectile	Striking Velocity	Fusing
Main Rotor Shaft	23 mm API or 23 mm HEI	1600 FPS	Most critical with superquick or time-delay
Main Rotor Hub and Elastomeric Bearing Assembly	23 mm API or 23 mm HEI	1600 FPS	Most critical with superquick or time-delay

D. Maintainability and Repairability Goals

Inspection Requirements

The present titanium hub assembly requires a minimum of inspection. A visual inspection is performed prior to each flight and after every 10 flight hours. After 500 flight hours the hub is subjected to a more thorough visual inspection and a check of all bolt torques There are no scheduled overhaul requirements. These inspection intervals are appropriate for a matured composite hub; however, at the 500-hour interval, a coin tap inspection should be included. This would be followed up by an ultrasonic pulse echo inspection of any questionable areas. Such inspections may require removal of certain coatings such as the radar-absorbing films. Therefore, the inspection intervals are similar for the metal and composite hub, but the composite hub requires a more complex inspection procedure.

Maintenance Requirements

Maintenance frequencies for several major subassemblies are given in Table 13 (Reference 3). Removal times of the elastomeric bearings, of the entire hub-shaft extension bifilar system from the aircraft, of the hub-bifilar from the shaft extension, and the time required for lowering the hub for air transport should not be increased as a result of utilizing a composite hub.

Table 13

Maintenance Frequency of the Titanium Hub

	Maintenance Frequency Per 1000 Flight Hours		
	On A/C Removal Frequency	On A/C Repair Frequency	Total Maintenance Frequency
Hub	0.45	0.01	0.46
Bifilar Assy.	0.20	2.43	2.63
Pressure Plate	0.01	0.02	0.03

Repair Requirements

Scratches, gouges, and nicks in the hub up to 0.040 inch in depth and 2 inches long can be repaired on the aircraft in the field. On the bifilar, scratches up to 0.020 inch are field repairable. These repairs are performed by blending with a suitable abrasive wheel followed by a dye penetrant inspection. The repaired area is cleaned and subsequently painted. The bifilar bushings are pressed into the bifilar support. These bushings are actually exposed bearings and are subject to rapid wear. They require frequent replacement but because of the press fit, they are not field replaceable.

Restoration Time

In general, the composite components will require more time to repair than will the metal components. For example, repair of a scratch in the composite consists of blending out the scratch, coin tap inspection of the area, cleaning, bonding on a patch, removing excess resin, coin tap inspection of the repair, cleaning and painting. The repair times for various components for the metal hub are presented in Table 14 and represent design goals for the composite hub. However, because the repair procedures are more complex for a composite structure, it is anticipated that these goals may not be achieved.

Table 14

Restoration Time for the Titanium Hub

A - On Aircraft (Elapsed Time)

	REMOVALS			REPAIRS		
	Mean Removal Time	Max. Removal Time	Removal Crew Size	Mean Repair Time	Max. Repair Time	Repair Crew Size
Hub	2.30	2.50	2	0.20	0.30	1
Bifilar Assembly	.60	.80	2	0.60	0.80	1
Pressure Plate	2.30	2.50	2	0.20	0.30	1

B - Off Aircraft (Man-hours)

	Intermediate Level	Depot Level
Hub	6.0	240
Bifilar Assembly	*	*
Pressure Plate	*	*

* No data

III. COMPOSITE HUB CONCEPTS

A. Design Approach

Structural Configuration

The design [illegible] were presented in Section II. They can be summarized as:

- Meet the structural and ballistic requirements of the existing hub.
- Achieve a substantial cost and weight savings over the existing hub.
- Retain as many of the other existing components as practical.

Changes to elastomeric bearings were ruled out because of the relatively long development time required to achieve a suitable replacement. Changes to the horn, pushrod, and other control components were prohibited because changes in pitch-flap coupling, etc., would affect handling qualities. Changes in the damper-accumulator system were also ruled out to help meet the goal of utilizing a maximum number of existing components. Alteration to the shaft extension was permitted. There are several reasons for this: first, it is not an expensive component (approx. $4,000); second, without alteration it can greatly increase the complexity of the composite hub; and third, because the existing extension has an unlimited fatigue life, the number of spares produced is not large and therefore the introduction of a new extension into the inventory will not greatly penalize the life-cycle cost of the composite hub system.

In order to achieve the desired cost and weight reductions, efforts were made to simplify and integrate parts wherever possible. For example, the modified shaft extension was designed to eliminate the need for an upper pressure plate and its associated cones. Another area for integration was to eliminate the need for a separate bifilar support by incorporating it into the top plate of the hub. This integration is given in more detail in the discussion of the various hub configurations.

Structural Sizing

Accurate structural sizing was necessary for the subsequent cost and weight trade-off studies. Preliminary sizing was performed using NASTRAN models to determine load paths and stress levels for a variety of loading conditions.

These include the following:

(1) 4 X CF

(2) Limit Rotor Acceleration

(3) Limit Flight Load

(4) Fatigue Design Loads

(5) Static Droop

The analyses relied upon superposition of independent load cases to compute the actual stress state for any specific load combination. The actual models are presented, along with a description of each configuration analyzed, on page 55.

The design allowables for the composite are consistent with those of $(0^{\circ}_2 \pm 45^{\circ})_{sym}$ type A-S graphite/epoxy laminates. Other layouts and reinforcements were considered but, as will become clear in the next few paragraphs, this was the preferred material.

Static allowables are presented in Table 15. Both room temperature dry (R.T.D.) and reduced data for 180°F is presented for the graphite/epoxy. The reductions account for the effects of temperature and moisture on the composite.

Table 15

Static Strength of Titanium, Stainless Steel and Graphite/Epoxy	
Titanium - 6Al-4V*	17-7 PH Stainless Steel**
F_{bru} = 197,000 psi	F_{bru} = 288,000 psi
F_{so} = 79,000 psi	F_{so} = 134,000 psi
F_{tu} = 130,000 psi	F_{tu} = 222,000 psi

Table 15 (Cont.)

$0^{\circ}_{2} \pm 45^{\circ}$ AS Graphite/Epoxy**	R.T.D.	Reduced
F_{bru} =	130,000 psi	100,000 psi
F_{nt} =	33,000 psi	30,000 psi
F_{tu} =	93,000 psi	87,500 psi

F_{bru} = bearing ultimate

F_{so} = shear out ultimate

F_{tu} = tension ultimate

F_{nt} = net tension ultimate - with a hole

* Reference 4 ** Reference 5

The appropriate fatigue allowables (Reference 6) for the titanium and the stainless steel are given in Figures 9 and 10.

The R.T.D. fatigue allowables (Reference 5) for $0^{\circ}_{2} \pm 45^{\circ}$ graphite/epoxy are presented in Figures 11 thru 13. The environmental reductions at 10^{7} cycles are 6% for tensile strength and 30% for bearing strength. Figure 13 describes the lap shear strength of graphite/epoxy of a R.T.D. laminate. A 20% reduction is used to account for environmental effects.

. Material Selection

The choice of materials was greatly influenced by the ballistic requirements. Carrying limit load or flying safely for 1/2 hour after a 23 mm HEI strike requires that the hub have redundant load paths and that the material be capable of carrying shear as well as tension after a ballistic strike. For equivalent ballistic hit

---

[4] Sikorsky Aircraft Structures Manual.

[5] "Advanced Composites Design Guide," Rockwell International-Los Angeles Aircraft Division, Contract No. F33615-71-C-1362, January 1973.

[6] "Fatigue Properties and Analysis," SER-50586, Sikorsky Aircraft, April 196[illegible]

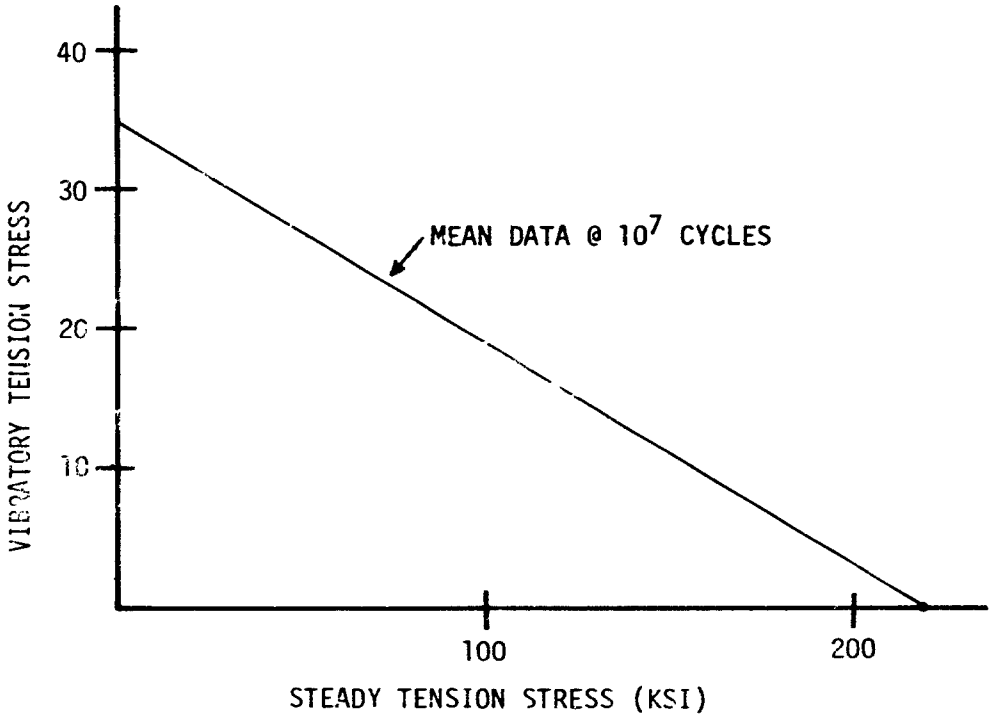

FIGURE 9. GOODMAN DIAGRAM FOR 17-7 PH STAINLESS STEEL SHIMS

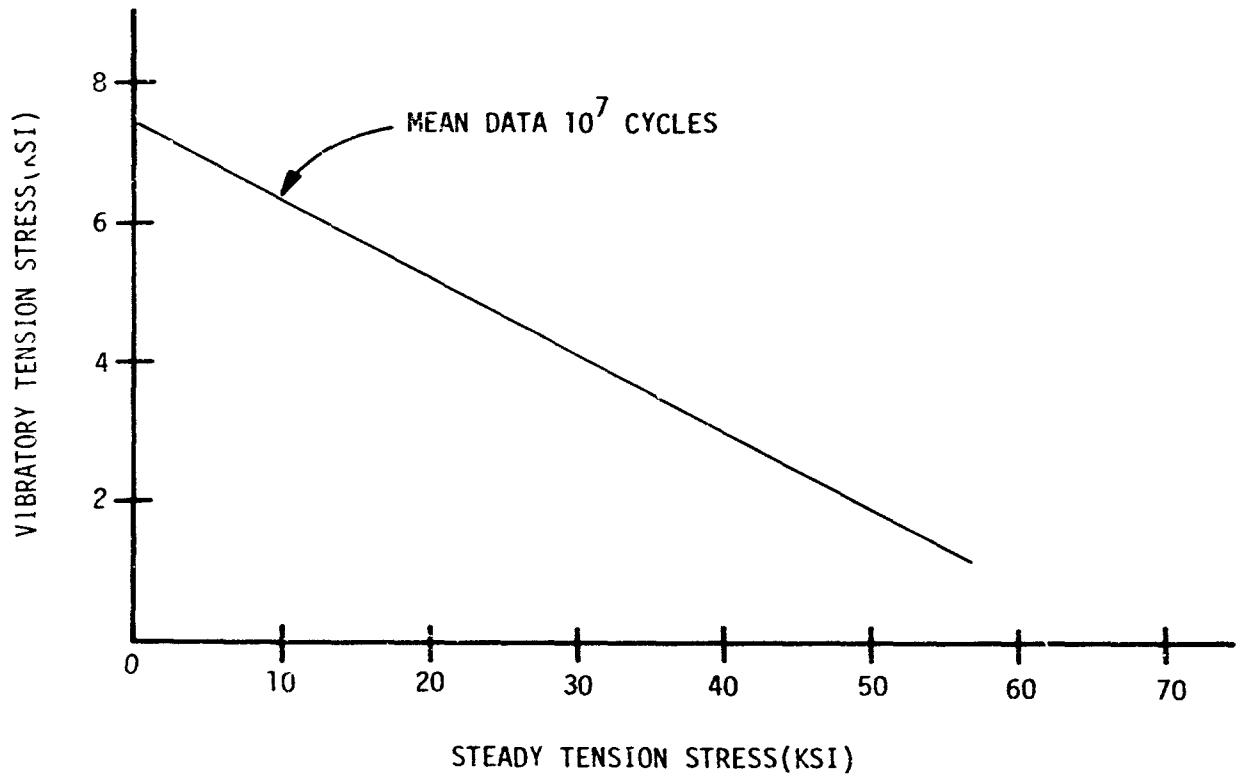

FIGURE 10. GOODMAN DIAGRAM FOR TITANIUM WITH CHAFING, NON-LUBRICATED FROM TEM-K3-3865

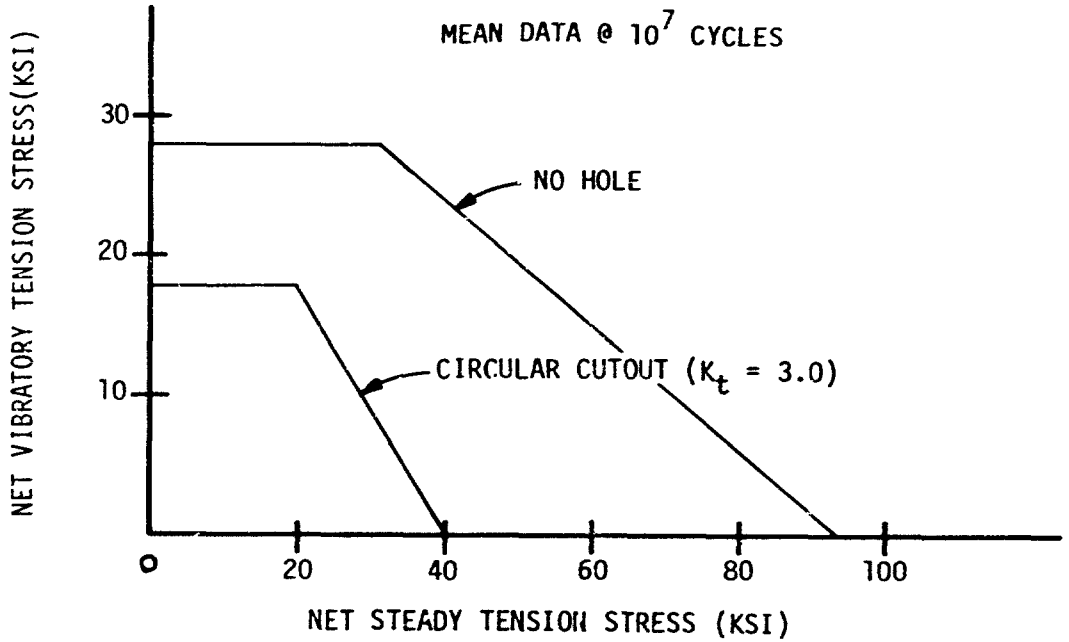

FIGURE 11. GOODMAN DIAGRAM FOR $0^\circ_2 \pm 45^\circ$ A.S. GRAPHITE/EPOXY - TENSION STRENGTH

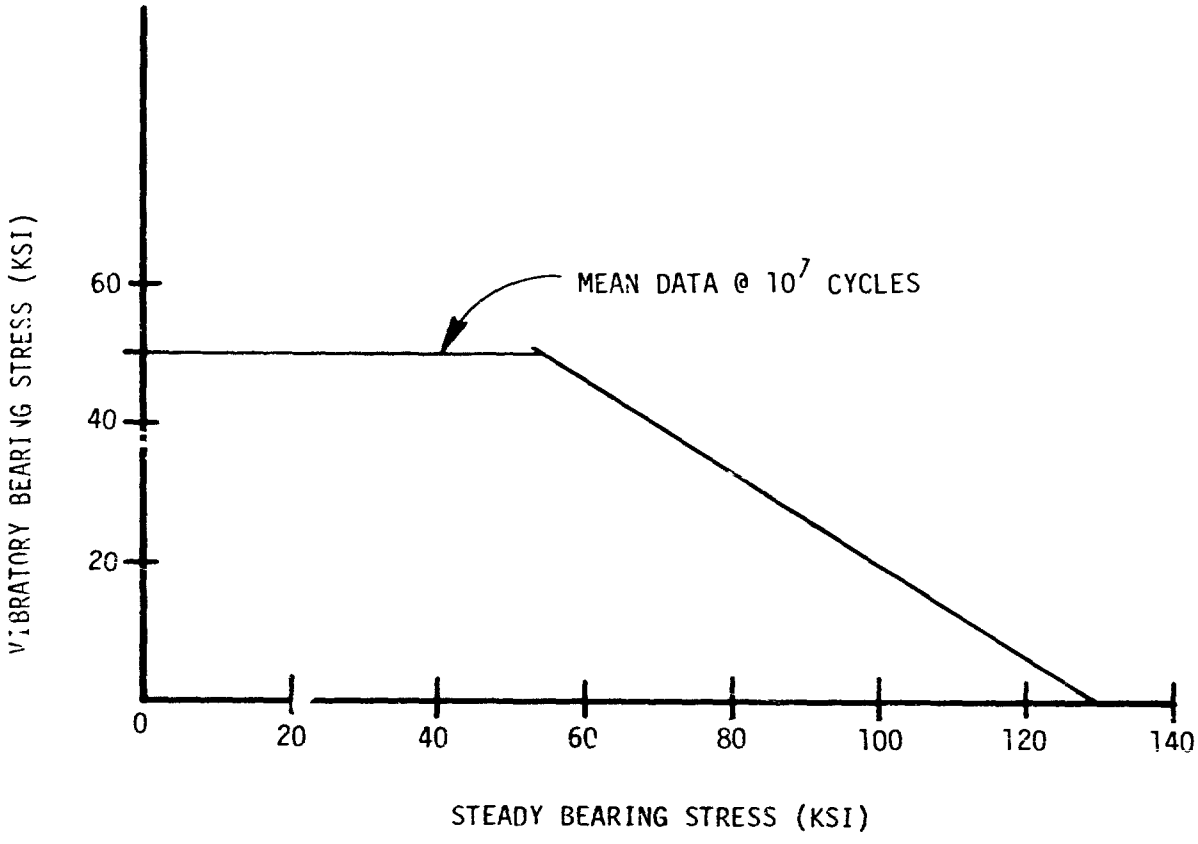

FIGURE 12. GOODMAN DIAGRAM FOR $(0_2^o \pm 45^o)$ A.S. GRAPHITE/EPOXY - BEARING STRENGTH

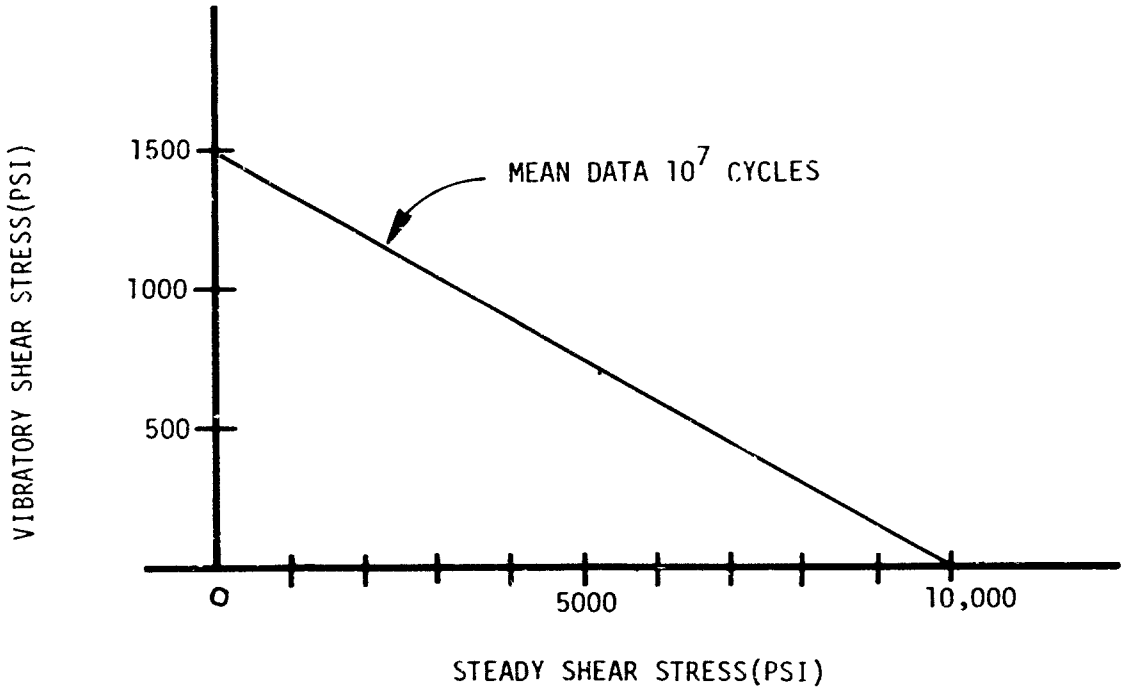

FIGURE 13. GOODMAN DIAGRAM FOR A.S. GRAPHITE/EPOXY - LAP SHEAR STRENGTH

fiberglass has more massive damage than graphite. Even with this damage it carries tensile loads well, but does not carry shear loads nearly as well as the damaged graphite. The limit load requirement results in a high shear force, and therefore fiberglass was eliminated.

Boron/epoxy behaves ballistically in approximately the same way as graphite/epoxy (Reference 7). They both experience very localized damage zones and have good tension, shear and compression load-carrying capability during, and after, impact. Boron/epoxy is more expensive, heavier, and more difficult to machine and for these reasons was also eliminated. Graphite/epoxy had the best combination of properties and was chosen for all of the composite components.

The ballistic requirements also had an effect upon the type of joints used between metal (titanium) and graphite/epoxy. Bonded joints are generally more desirable in composites than bolted joints. They are structurally efficient, which denotes a lighter weight joint than a bolted one designed to carry the same load. Where the load density in a joint is low, as is the case in blades, bonded joints are preferable. However, where the load density is high, bolted joints tend to become more preferred. For the case of the relatively small, highly loaded hub which must sustain ballistic damage, the bolted joint becomes a strong choice. This was demonstrated by a series of tests on bolted and bonded joints. A bolted joint test specimen is shown in Figure 14. The composite is $(0^0_2 + 45^0)$ AS graphite/epoxy. A .30 cal. projectile was fired through the tab on the side of the test specimen shown in Figure 14. As can be seen, the damage was localized, which was the expected behavior, and hence the specimen was felt to be representative. An aligned and a tumbled round were shot through the bolt pattern at each end of the specimen (see Figure 15). The projectile penetrated the metal first and then the composite. This type of penetration is more severe because of petaling of the titanium and the more intense interface shock, which results in a larger zone of delamination within the composite. The bolted joint specimen experienced damage over a region somewhat larger than the projectile due primarily to petaling. The specimen was subsequently loaded to 21,000 lb, at which point the titanium end plates failed (see Figure 14). The residual strength could not be determined but warrants additional investigation in the near future.

---

[7] "Tolerance of Advanced Composites to Ballistic Damage," E.F. Olster and P. A. Roy, ASTM STP 546, American Society for Testing and Materials, Philadelphia, Pa., 1973.

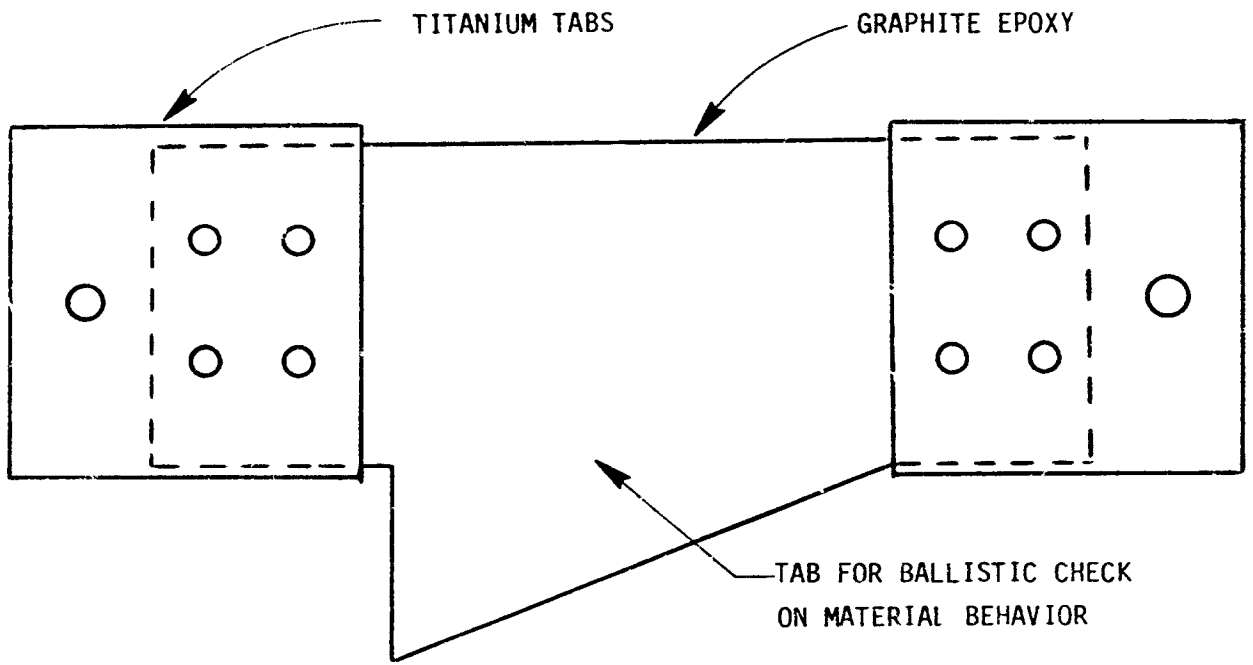

FIGURE 14. BOLTED JOINT - BALLISTIC TEST SPECIMEN

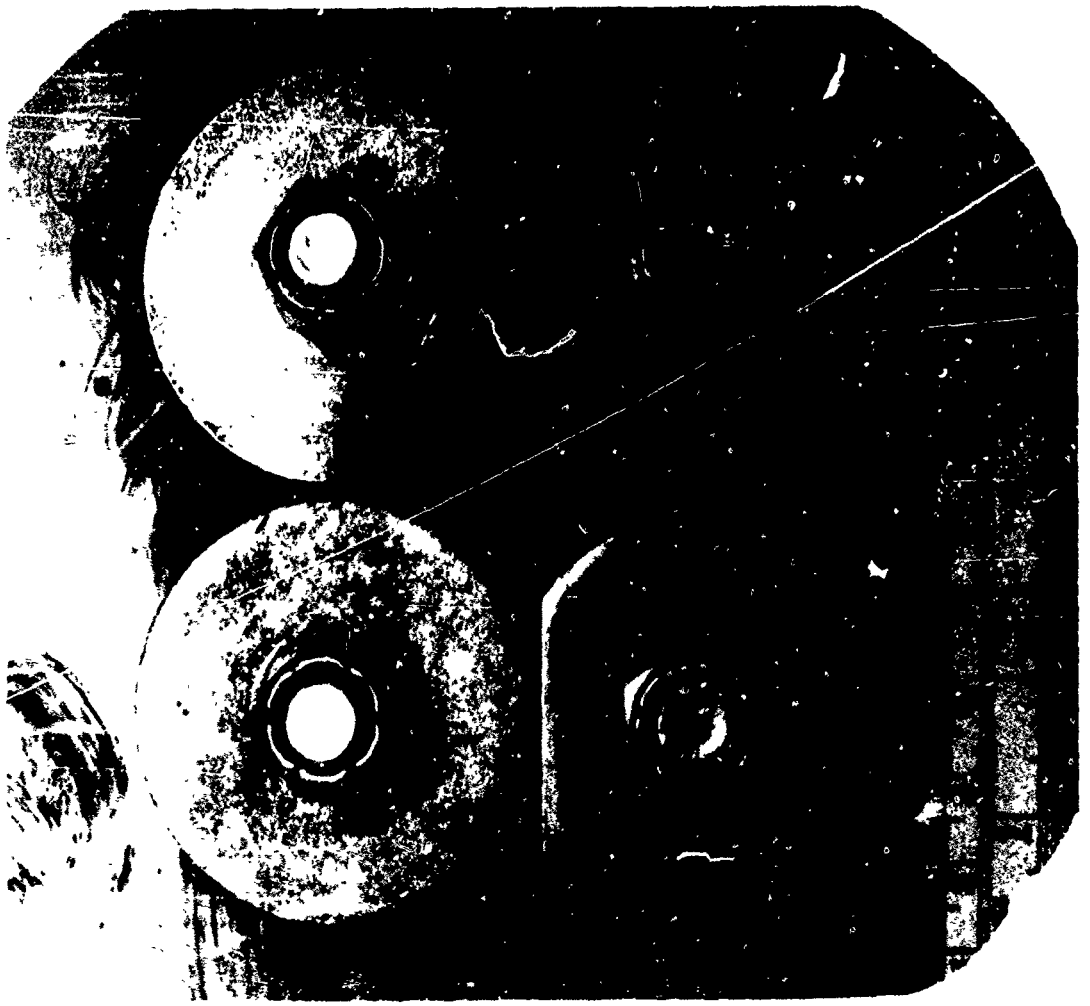

FIGURE 15. BALLISTIC TEST OF BOLTED JOINT

A similar size bonded joint specimen failed completely at the bond line and exhibited massive delamination of the composite itself (see Figure 16). It is clear that, on a comparative basis, a bolted joint is ballistically safer than a bonded one, and hence all primary joints between metal and composite were bolted.

B. Hub Concepts

A series of six composite hub configurations were evaluated. A NASTRAN was performed on each concept for structural sizing of the subcomponents. Each concept is discussed below.

. Concept A

Concept A is shown in Figure 17. It consists of a filament-wound torus over-wrapped with a second filament-wound shell shaped like an automobile tire. The entire structure is bolted to a redesigned titanium shaft extension. The torus was chosen as a simple means of providing a shear web. The torus is wound around a salt mandrel containing the four metal inserts to which the elastomeric bearings are bolted. These inserts also serve a second function: they restore some of the shear stiffness lost by cutting large openings in the wall for the elastomeric bearing, the damper, and the control horn. If a bifilar were to be incorporated it would remove even more of this vertical surface (see Figure 17), and thereby "reduce" the system to basically two flat plates. The basic structural model used for analyzing the concept is shown in Figure 18. The basic design of the hub was determined by the geometric requirements outlined in Section II. The results of the preliminary analyses were used to "size" the structural components. This hub concept is very easy to manufacture and results in a 44 percent cost save as compared to the present titanium hub. The weight estimates indicated that this hub is 20 percent lighter than its titanium counterpart. It has some drawbacks, however. The primary one is the indirect vertical shear path which, after a ballistic strike, may be almost totally ineffective. Another drawback relating to a ballistic strike is the lack of redundancy with respect to elastomeric bearing retention. The bearing is retained by the insert which is attached to only the upper and lower portion of the torus. The additional restraint offered by composite material wrapping around the inserts is minimal because there are few continuous fibers. Additional drawbacks are the requirement for a separate bifilar and a damper attachment which is "hidden" and not easily accessible.

. Concept B

Concepts B and C are similar to the three-plate concept used by Kaman for the CH-54B. Concept B consists of three separate plates that are bolted to a shaft adapter (see Figure 19). The heavy

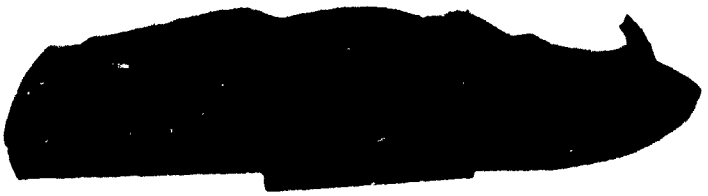

FIGURE 16. BALLISTIC TEST OF THE BONDED JOINT

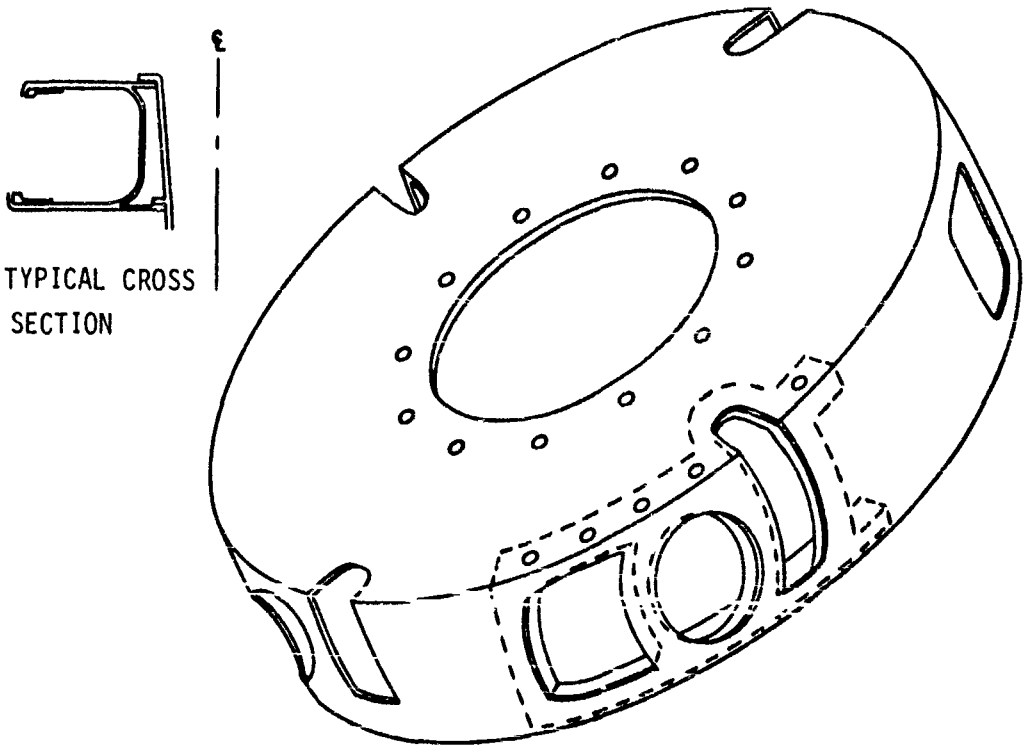

ADVANTAGES

EASY TO MAUFACTURE

MODERATE WEIGHT SAVINGS

LARGE COST SAVINGS

DRAWBACKS

HEAVY BEARING ADAPTER

ADD-ON BIFILAR

INDIRECT SHEAR PATH

HIDDEN DAMPER ATTACHMENT

FIGURE 17. COMPOSITE HUB CONCEPT A

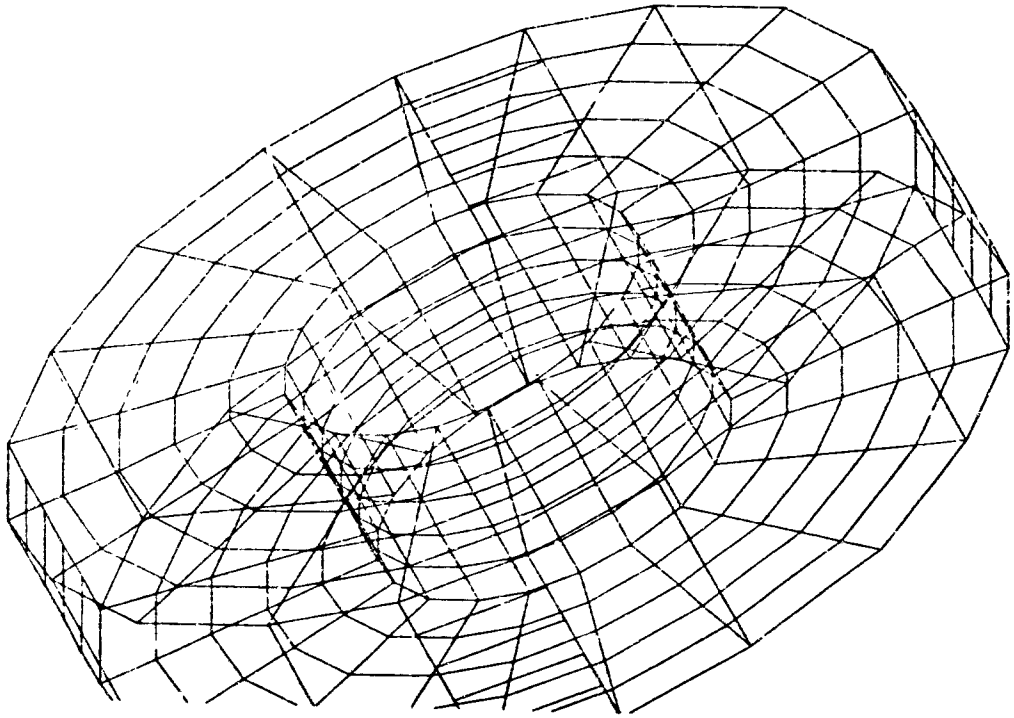

FIGURE 18. STRUCTURAL MODEL OF CONCEPT A

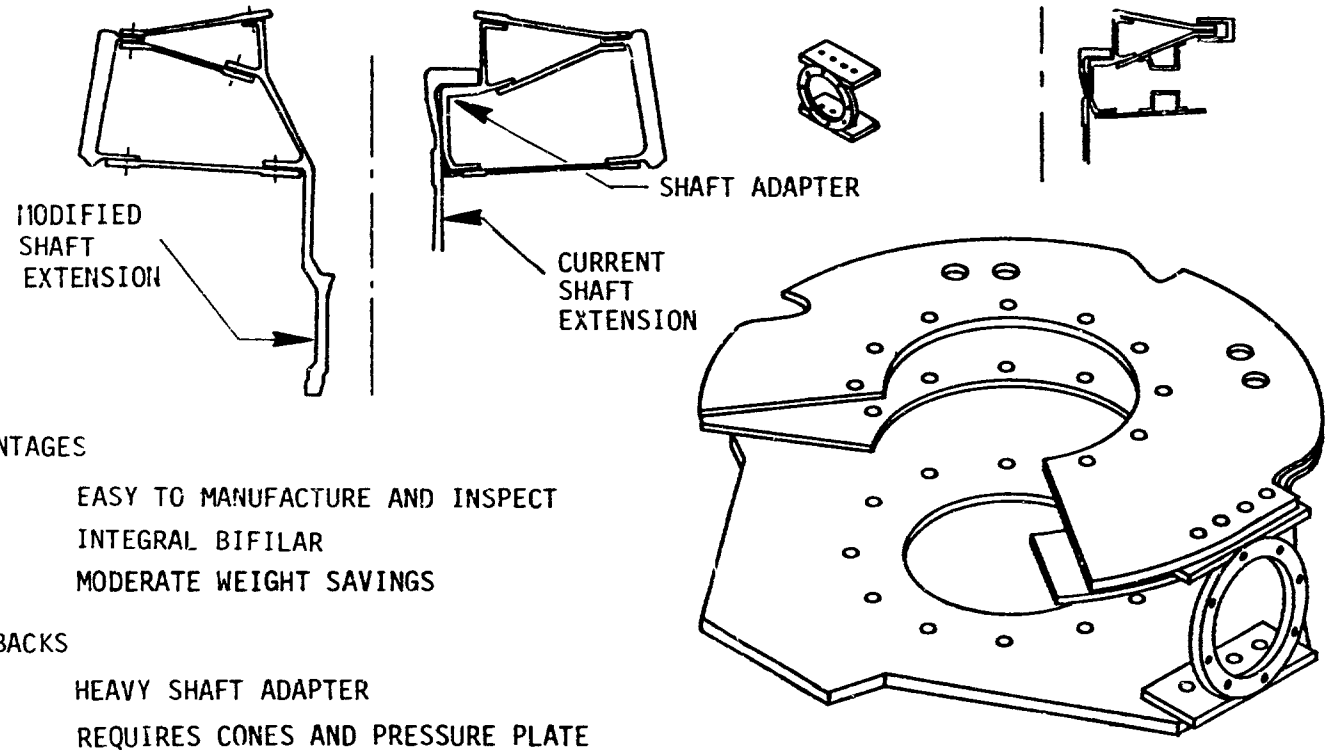

ADVANTAGES

- EASY TO MANUFACTURE AND INSPECT
- INTEGRAL BIFILAR
- MODERATE WEIGHT SAVINGS

DRAWBACKS

- HEAVY SHAFT ADAPTER
- REQUIRES CONES AND PRESSURE PLATE
- SMALL ANGLE BETWEEN PLATES - HIGH VERTICAL SHEAR LOADS
- MINIMAL REDUNDANCY AT BEARING ATTACHMENT POINTS
- SMALL COST SAVINGS

FIGURE 19. COMPOSITE HUB CONCEPT B

shaft adapter cannot be eliminated without a major disassembly being required for air transport. For example, to lower the hub, the top plate has to be completely removed, which requires removal of the bolts holding the top lug of the bearing adapter. This provides access to the bolts attaching the middle plate to the shaft, but it introduces the possibility of in-flight vibration due to lack of alignment upon reassembly. Hence, the best approach is to use a shaft adapter, which permits the hub to remain intact. The NASTRAN model used for structural sizing is shown in Figure 20. As a result of the small angle between the two upper plates necessitated by the spacing requirement for the elastomeric bearings, shear loads generate high forces in the plates and at the bolted joints.

This concept is easy to manufacture and inspect. It is easy to incorporate the bifilar support into the two upper plates and thereby eliminate the need for an additional 30-pound component. The shaft adapter is heavy and reduces the weight savings to 16 percent; however, this shaft adapter uses the same shaft extension, cones and pressure plate as exist on the present hub. There is a cost savings of 9 percent compared to the titanium hub. Ballistically, this hub has minimal redundancy since, if the lower portion of the bearing adapter is hit, the bearing and blade can be lost.

Concept C

This three-plate hub (see Figure 21) is attached to a modified shaft extension at two locations, an upper ring and a lower ring. In comparison to Concept B, the angle or orientation of the middle plate results in higher structural efficiency. The middle plate has four cutouts to accommodate and permit movement of the elastomeric bearings; but these cutouts and the high curvature makes it less easy to manufacture than the flatter plates of the previous concept.

The NASTRAN model is shown in Figure 22. The weight savings is 32 percent and the cost savings is 19 percent for this concept. It has the same general attributes as Concept B, which are an integral bifilar and a lack of redundancy for retaining the bearing end plate given a ballistic strike in the lower plate.

Concept D

Concept D, shown in Figure 23, consists of a flat upper plate and a molded lower one. These plates are bolted and bonded together. The system bolts to a titanium shaft extension. At the end of each arm is a titanium bearing adapter which is bolted to both the upper and lower plate. The NASTRAN model is shown in Figure 24. The tubular arms provide a direct shear path between the bearing

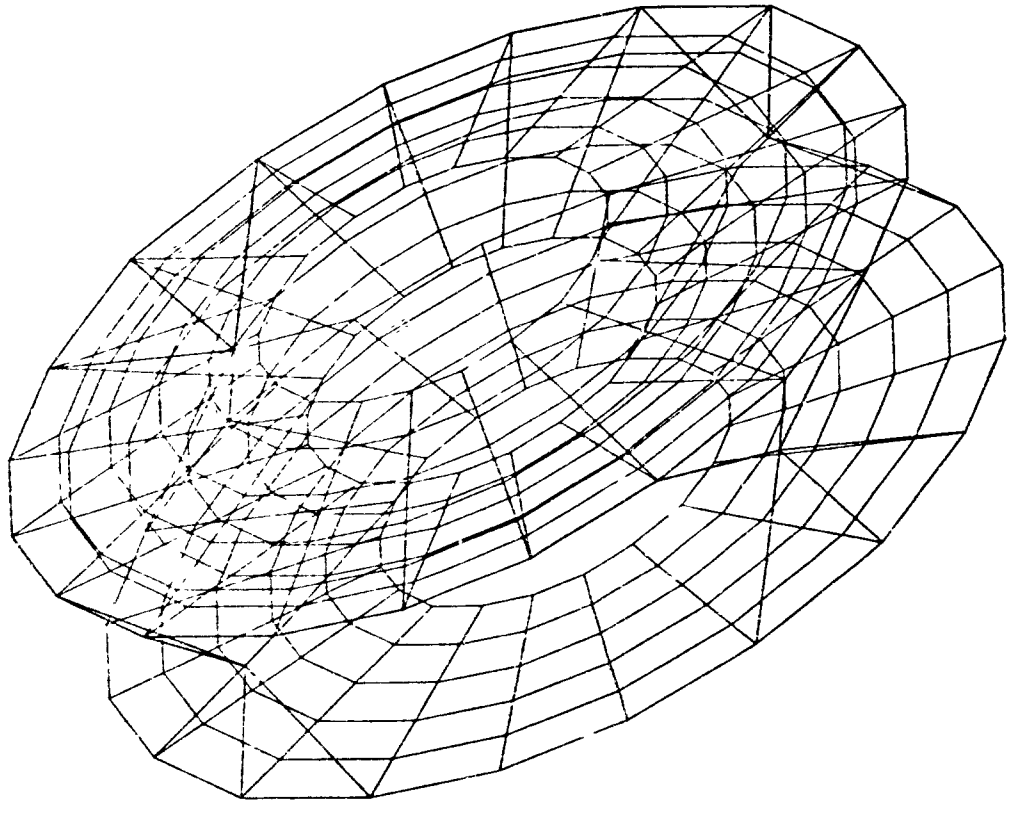

FIGURE 20. STRUCTURAL MODEL OF CONCEPT B

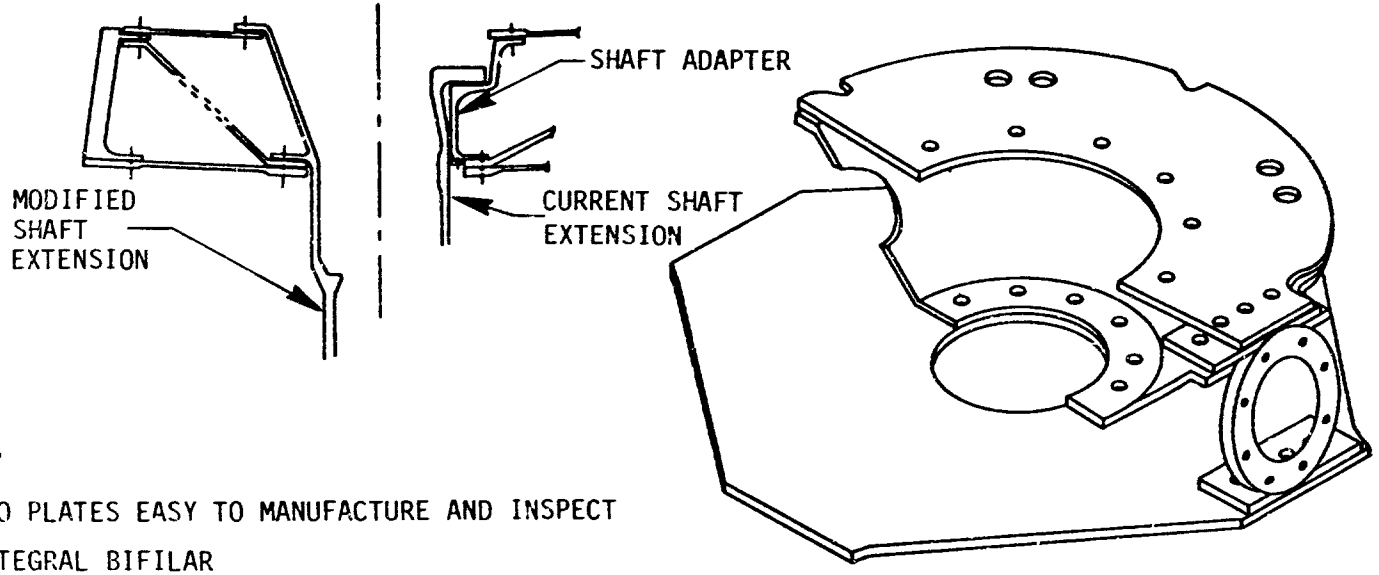

ADVANTAGES

TWO PLATES EASY TO MANUFACTURE AND INSPECT

INTEGRAL BIFILAR

LARGE WEIGHT SAVINGS

DRAWBACKS

SHARP CURVATURE OF PAN PLATE - MANUFACTURING, INSPECTION

EFFICIENCY OF PAN PLATE - HOLE, ORIENTATION

REDUNDANCY AT BEARING IS MINIMAL

COST PENALTY

FIGURE 21. COMPOSITE HUB CONCEPT C

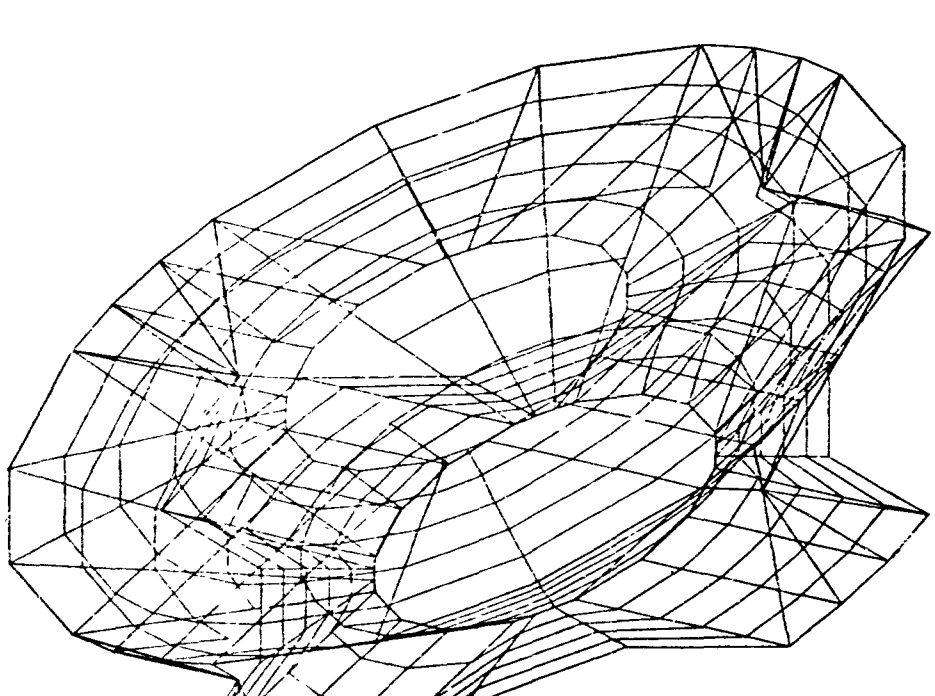

FIGURE 22. STRUCTURAL MODEL OF CONCEPT C

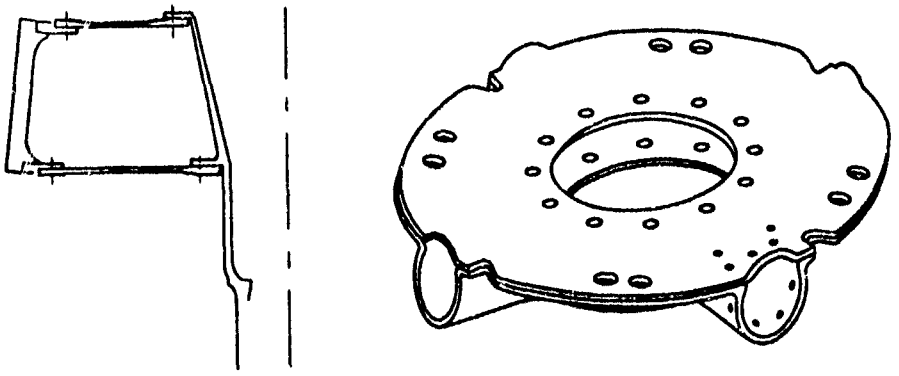

ADVANTAGES

- TOP PLATE EASY TO MANUFACTURE AND INSPECT
- DIRECT SHEAR PATH
- REDUNDANCY AT BEARING
- INTEGRAL BIFILAR
- MODERATE WEIGHT SAVINGS

DRAWBACKS

- COST PENALTY
- BOTTOM PLATE DIFFICULT TO MAKE AND INSPECT
- LITTLE AXIAL REDUNDANCY IN LOWER PLATE

FIGURE 23. COMPOSITE HUB CONCEPT D

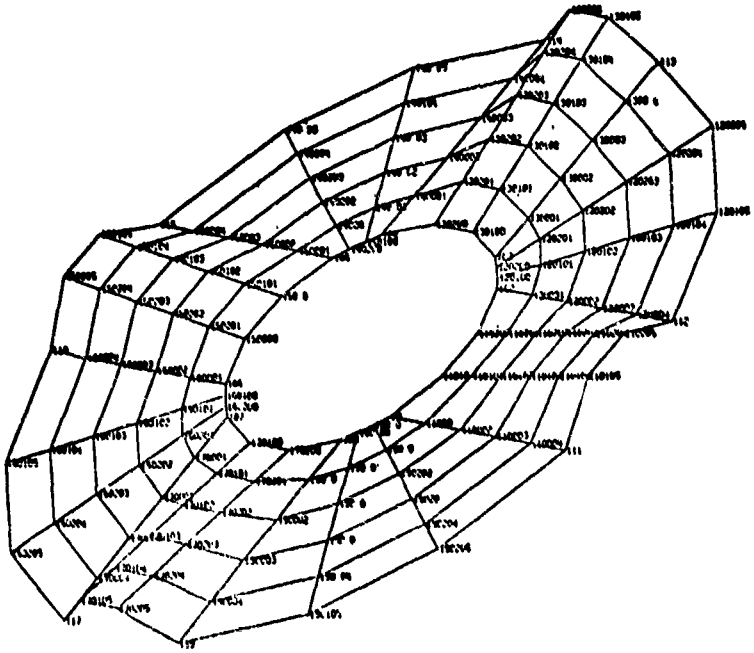

EXPLODED VIEW

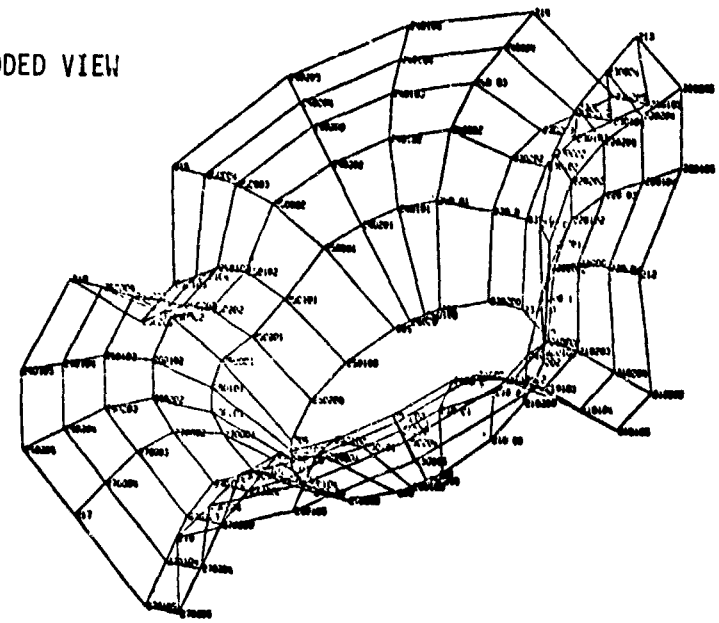

FIGURE 24. STRUCTURAL MODEL OF CONCEPT D

end plates and the shaft. The top plate is easy to manufacture and inspect whereas the opposite is true for the lower molded plate. The bifilar support can be made integral with the top plate, which results in a net weight savings and provides material for structural redundancy in the top plate in the form of a four-bar self-equilibrating system between adjacent arms (see Figure 23). This configuration results in a weight savings of 27 percent and a cost savings of 11 percent as compared to the baseline hub. This hub has redundant attachments for the bearing adapter; however, it lacks redundant load path for a ballistic hit in the lower portion of any tube.

Concept E

Concept E, shown in Figure 25, consists of four filament-wound tubes sandwiched between two flat plates. The tubes are bolted and bonded to the plates and the entire assembly is bolted to a redesigned titanium shaft extension. The elastomeric bearings are attached by means of titanium bearing adapters which are bolted to the filament-wound tubes.

A NASTRAN model is shown in Figure 26. The plates and tubes are all approximately 0.4 inch thick and have a $(0_2^0 \pm 45^0)$ fiber orientation. The bifilar support is integral with the top plate. The tubular arms provide a direct shear path as well as a redundant axial path for elastomeric bearing loads.

The positive attributes of this configuration are numerous. The $(0_2^0 \pm 45^0)$ layup in the upper and lower plate provides a direct load path for normal operation. The load is transferred from the elastomeric bearing to the bearing adapter to the composite plate and finally into the titanium shaft extension. The $\pm 45^0$ plies also form a self-equilibrating four-bar system, which is efficient in reacting radial loads in the event of damage due to a ballistic strike. The bearing adapter is attached to the tube by eight equally spaced bolts which also overcome the drawbacks of Concepts A-C, which are attached only at the upper and lower surfaces. Additional redundancy is obtained by the attachment of the tubes, as well as the plates, to the titanium shaft. All components are essentially flat which makes layup fast, and the tubes can be filament-wound over expandable mandrels. This concept resulted in an estimated 27 percent weight savings and a 37 percent cost savings. Its primary drawback is that it consists of many parts. An alternate was considered which required molding the tubes in pairs (see Figure 25). This "Lincoln log" approach has inherent redundancy in that the load path is continuous between opposing arms. This alternative was not pursued because it was felt that a rather lengthy effort was required to develop successful molding techniques for these complex parts.

"LINCOLN LOG" APPROACH IS AN
ALTERNATIVE TO FOUR SEPARATE TUBES

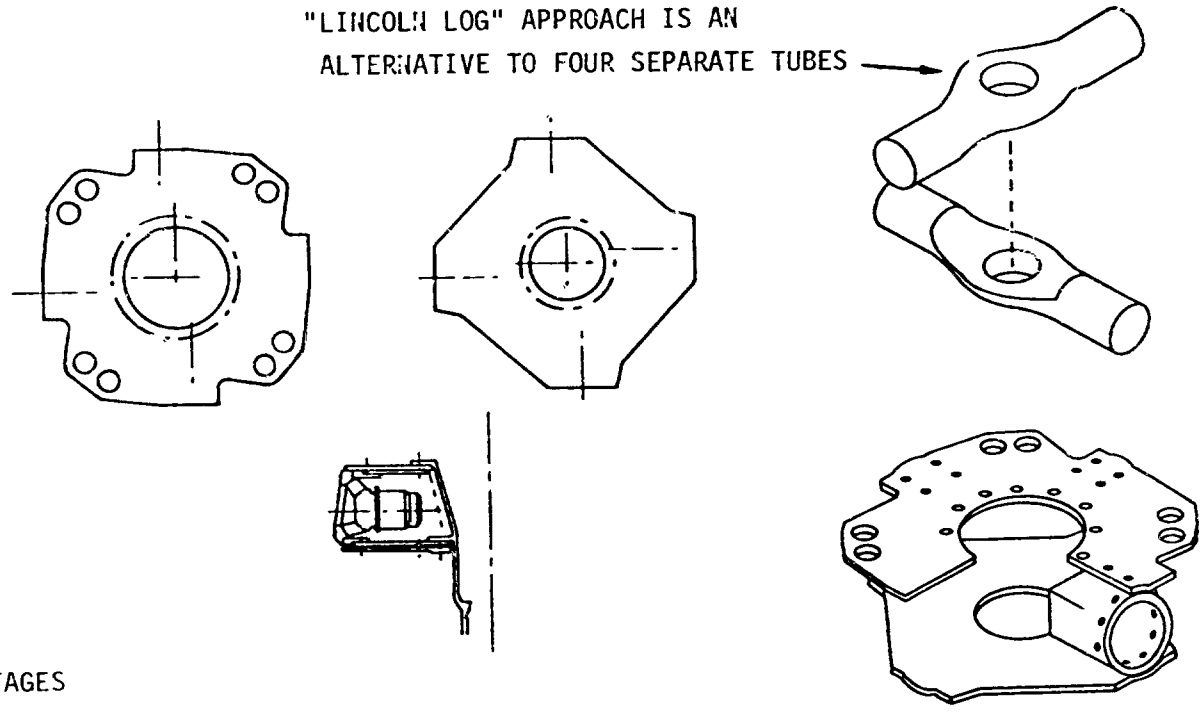

ADVANTAGES

- TOP & BOTTOM PLATE ARE EASY TO FABRICATE AND INSPECT
- FILAMENT-WOUND TUBES ARE EASY TO FABRICATE
- HIGHLY REDUNDANT
- INTEGRAL BIFILAR
- SIGNIFICANT COST SAVINGS
- SIGNIFICANT WEIGHT SAVINGS
- DIRECT SHEAR PATH

DRAWBACKS

- MANY PARTS

FIGURE 25. COMPOSITE HUB - CONCEPT E

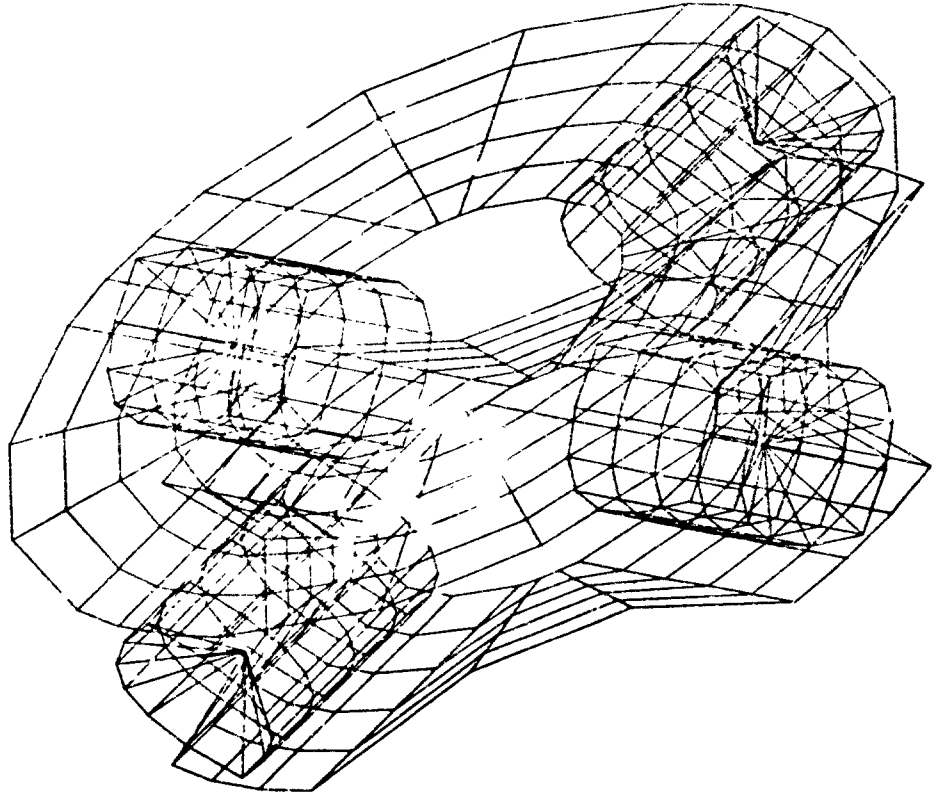

FIGURE 26. STRUCTURAL MODEL OF CONCEPT E

"LINCOLN LOG" APPROACH IS AN
ALTERNATIVE TO FOUR SEPARATE TUBES

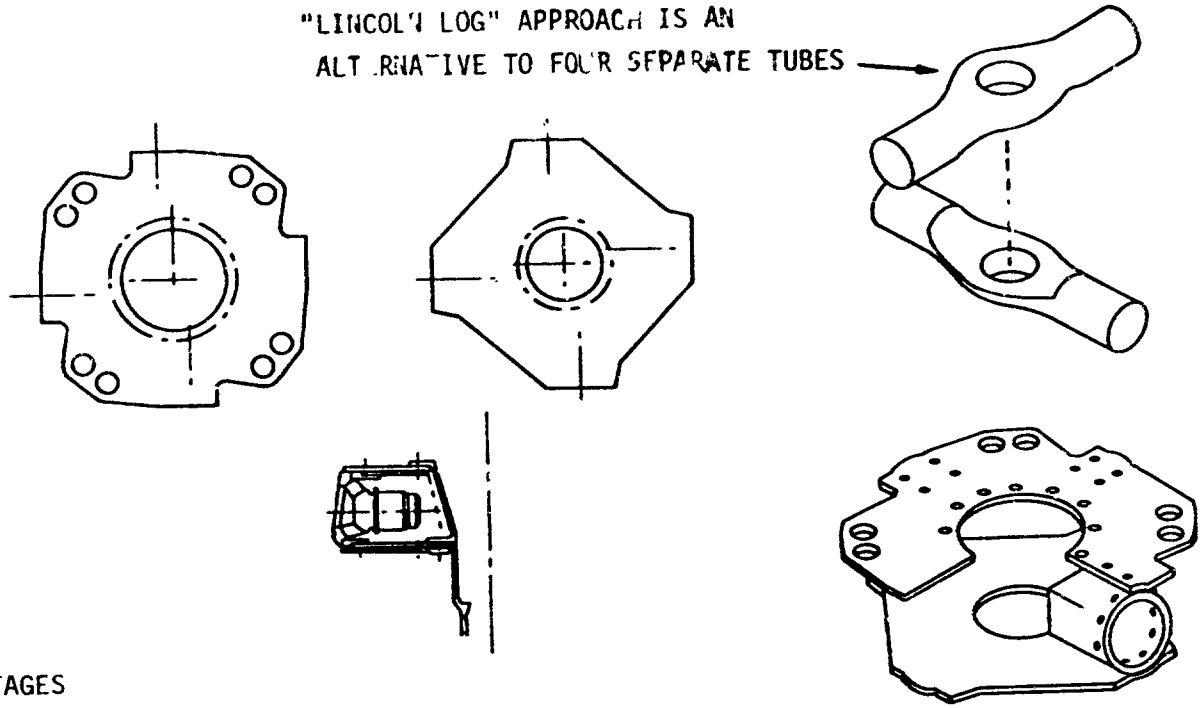

ADVANTAGES

- TOP & BOTTOM PLATE ARE EASY TO FABRICATE AND INSPECT
- FILAMENT-WOUND TUBES ARE EASY TO FABRICATE
- HIGHLY REDUNDANT
- INTEGRAL BIFILAR
- SIGNIFICANT COST SAVINGS
- SIGNIFICANT WEIGHT SAVINGS
- DIRECT SHEAR PATH

DRAWBACKS

- MANY PARTS

FIGURE 25. COMPOSITE HUB - CONCEPT E

Concept F

Concept F is shown in Figure 27. It is similar to the previous composite hub in that it consists of two plates and four filament-wound arms. The difference lies in the fact that it uses the current shaft extension. To do this, the plates are dished as shown and an adapter is required for the cones and pressure plate. In comparison to Concept E the plates are somewhat more complex since they are no longer essentially flat. The upper plate requires metal shims at the attachment to the shaft because of the short edge distance. The filament-wound tubes are slightly more difficult to manufacture because of the more extreme changes in curvature and more complex shape. Modified bearing end plates and bearing adapters (Table 19) are used in the weight and cost estimates for this concept. This increases the weight and cost savings over that for Concept E. The resultant weight savings is 29 percent and the resultant cost savings is 39 percent.

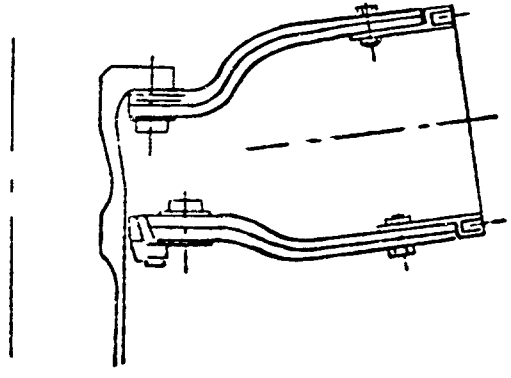

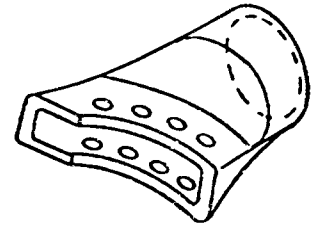

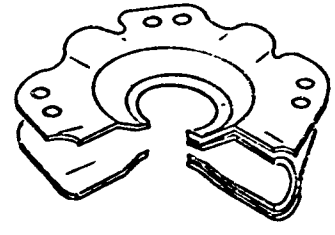

ADVANTAGES

- HIGHLY REDUNDANT
- DIRECT SHEAR PATH
- INTEGRAL BIFILAR
- FILAMENT-WOUND TUBES EASY TO MANUFACTURE
- SIZEABLE WEIGHT SAVINGS
- USES CURRENT SHAFT EXTENSION
- USES CURRENT CONES AND PRESSURE PLATE

DRAWBACKS

- MANY PARTS
- REQUIRES LAMINATED SHIMS IN UPPER PLATE

FIGURE 27. COMPOSITE HUB CONCEPT F

C. Trade-Off Study

Concepts A through F were evaluated by means of a trade-off study, which included the following items:

(1) Reliability Estimate
(2) Cost Estimate
(3) Ballistic Tolerance
(4) Producibility Estimate
(5) Repairability Estimate
(6) Lightning Protection
(7) Weight Estimate
(8) Maintainability Estimate
(9) Radar Cross Section

The approach taken was to evaluate each parameter separately to determine a base score. This base was adjusted by a ranking factor to obtain the final weighted score. The ranking factors were chosen in a manner which reflected the relative importance of the various parameters. For example, ballistic vulnerability is a very important factor and was given a ranking factor of 10, whereas ease of obtaining adequate lightning protection was assigned a ranking factor of 3 (although the requirement itself was not compromised).

. Reliability Estimate

The reliability trade-off results are presented in Table 16. Nine items were evaluated. Item 1 is a ranking based upon the number of major parts. Reliability is generally inversely proportional to a parts count. The base score was chosen as 140/N, where N is the parts count. There is some redundancy here since a parts count is also used in the producibility estimate.

Item 2 is a ranking based upon the ease of layup. The assumption here is that complexity in layup leads to inherent failures. Concept A is filament-wound in two separate steps. The technique is simple and reproducible and was given the highest score, 10. Concept B consists of three relatively flat plates which can easily be laid up from prepreg sheets cut from broadgoods, and hence the high score. Concepts E and F consist of basically two flat plates and four filament-wound tubes. These also are easily manufactured and were given a score of 10. The middle plate of Concept C is quite difficult to lay up due to the sharp curvatures involved and as a result was penalized. Concept D requires very careful hand layup of many pieces for each layer of the lower plate. This complexity resulted in a substantial penalty which is reflected in the score.

Reliability is affected by the quality or uniformity of components. This fact was evaluated by comparing the ease of ir-

TABLE 16. TRADE-OFF STUDY - RELIABILITY ESTIMATE

CONSIDERATION

ITEM	DESCRIPTION
	INHERENT
1.	Number of Major Parts
2.	Ease of Layup
3.	Ease of Inspection - Components
4.	Ease & Criticality of Visual Inspection - Assembly
5.	Structural Redundancy
	INDUCED
6.	Potential for Handling Damage (Raise & Lower Hub)
7.	Potential for Damage by Bearing
8.	Potential for Damage by Damper
9.	Ease & Accessibility for Maintenance

EVALUATION

CONCEPT	ITEM										SCORE
		1 140/N	2	3	4	5	6	7	8	9	
A	(9)	15.5	10	7	5	14	8	10	3	7.8	80.3
B	(12)	11.6	10	10	9	10	10	10	8	10	88.6
C	(11)	12.7	8	9	9	8	6	10	9	9.7	81.4
D	(10)	14	4	7	10	14	8	8	10	8.7	83.7
E	(14)	10	10	10	9	20	8	8	10	9.4	94.4
F	(15)	9.33	10	7	9	20	9	8	10	9.0	91.3

specting individual components prior to assembly. Concepts B and E received scores of 10 because the relatively flat plates pose no problems and the constant thickness filament-wound tubes are easily inspected. Inspection of Concept A is hampered slightly by the fact that the metal bearing retention inserts affect ultrasonic response and the fact that the thickness of the outer winding, the "tire" shaped shell, varies linearly with radius. For these reasons, Concept A was given a score of 7. Concept C is similar to B, but because of the increased curvature and cutouts in the middle plate, it was penalized. Concept D received a low score because of the complexity in curvature that would require numerically controlled inspection equipment. Concept F was given a penalty because of the laminated shims in the tubes and upper plate.

Another factor contributing to reliability is the ease of inspection in critical areas of the hub. Concept D received the highest score because cracks in both the composite and metal could be readily seen. Concepts B and C are similar, with inspection generally being easy except for the lug of the bearing adapter, which is hidden between the two upper plates. Concepts E and F are also similar and are penalized slightly because the attachment of the tube to the shaft extension is not readily accessible. Concept A was penalized because the metal bearing adapter which forms a major shear web is hidden from view and the internal shear web, the inner wall of the torus, is not clearly visible.

Structural redundancy is very important and for that reason was given a peak score of 20 points. Concepts E and F received this score because of the redundancy in both plates arising from the $(0^{\circ}_2 \pm 45^{\circ})$ layup which forms a direct load path as well as a diffuse, four-bar load path. Both the plates and the tubes are attached to the shaft extension, and the bearing adapters are tied to both the plates and the tubes, thereby providing alternate load paths. Concept D is similar to E except for the lack of a second axial load path provided by the lower plate given a ballistic strike in the lower portion of any arm. For that reason, it was penalized. Concept A lacks a very effective shear path for vertical loads, and a ballistic strike in any shear member could severely affect the stiffness and overall behavior. Concept B was penalized because of the lack of redundancy at the bearing adapter. This is especially critical at the lower plate where a ballistic strike can result in loss of a blade. Concept C is similar, but because of the more severe local curvature and reduced area in the middle plate, this concept was penalized more than B.

Another factor contributing to reliability is the potential for handling damage induced by raising or lowering the hub. Concept B was given the highest score due to the fact that the present

metal shaft extension is used and the procedure for raising or lowering the hub is similar to that for the present metal hub. Concept F is similar to the present hub design, except that the possibility exists for damage in the attachment to the upper flange due to bushing debonding or delamination. Concepts A, D and E received modest scores because a large number of bolts are inserted through thick laminates and the potential exists for delamination upon removal of these close tolerance bolts. Concept C received a low score because of the complexity in the area of the lower region where two plates come together. This raises the potential for misalignment and delamination.

The elastomeric bearings can, if not aligned properly, scrape or scratch the inside of the tubes. Because there is plenty of clearance in Concepts A, B and C they were given a score of 10. All other concepts require more careful alignment and, therefore, received a lower score.

In addition to the bearings, the dampers require attention. Again, the determining factor is accessibility and clearance. Concepts D, E and F were given the top score because of the relatively free access to the damper and damper bearing.

Concepts B and C were penalized slightly because the middle plate encroaches on the work space, and Concept A was severely penalized because the damper and damper bearing are hidden.

The last item considered was the ease and accessibility for maintenance. This reflects overall complexity of the hub. The approach taken was to use the results of the maintainability scores and factor them so that the highest one equals 10.

- Cost Estimate

The production costs of each hub concept were estimated using 1978 dollars and labor rates. Composite material costs were estimated to be $70/pound for type AS graphite/epoxy prepreg. The breakdown is self-explanatory and is given in Table 17. The score was computed in such a way that if the cost of the hub equaled the target value, the score equaled 1. Because of the ease of manufacture, the filament-wound hub is least expensive.

- Ballistic Tolerance

The results of the ballistic evaluation are presented in Table 18. Eight regions have been chosen for evaluation regarding behavior after a 23 mm HEI strike. For a projectile traveling vertically

TABLE 17. TRADE-OFF STUDY - COST ESTIMATE - 1978 DOLLARS, 400th UNIT

CONCEPT	BASIC HUB	BEARING END PLATES	BEARING ADAPTERS	BIFILAR SUPPORT	SHAFT EXTENSION	CONES & PRESSURE PLATE	DAMPER BRACKETS	TOTAL C	RANK $\frac{T-C}{T}+1$
A	5400	5040	6500	980	3850	-	1500	23270	1.19
B	16500	5040	3300	150	5800*	1300	1500	33590	.84
C	16500	5040	3300	150	4200	-	1500	30690	.94
D	19950	5040	2500	150	3800	-	1500	32990	.86
E	12000	5040	2000	150	3850	-	1500	24540	1.15
F	12000	3000**	1800	150	3850	1300	1500	23600	1.19
TITANIUM	24780	5040	-	980	3850	1300	2800	38750	
T=TARGET	(75%)							29062	

* Adapter

** Modified Bearing

TABLE 18. TRADE-OFF STUDY - BALLISTIC TOLERANCE

CONSIDERATION

ITEM	DESCRIPTION
1.	Vertical Hit at Bearing Retention Area.
2.	Lateral Hit at Bearing Retention Area, Between Plates.
3.	Lateral Hit at Bearing Retention Area, Upper Plates.
4.	Lateral Hit at Bearing Retention Area, Lower Plates.
5.	Vertical Hit at Hub, Radial Station 9.
6.	Lateral Hit at Hub, Radial Station 9, Between Plates.
7.	Lateral Hit at Hub, Radial Station 9, Upper Plates.
8.	Lateral Hit at Hub, Radial Station 9, Lower Plates.

EVALUATION

CONCEPT	ITEM								SCORE
	1	2	3	4	5	6	7	8	
A	10	10	7	7	10	4	9	9	66
B	7	9	7	7	10	10	8	9	67
C	7	9	6	7	10	7	8	9	63
D	10	10	7	7	8	10	9	8	69
E	10	10	10	10	10	10	10	10	80
F	10	10	10	10	7	10	10	10	77

and striking the bearing adapter area all concepts except B and C are adequate. Concepts B and C could fail at the lower plate in such a way that the entire blade is lost.

For a lateral hit at the bearing adapter region between both plates all concepts except B and C are redundant. Concepts B and C were penalized slightly because of the exposed support for the bearing. Only Concepts E and F received a score of 10 if the lateral hit is at the level of the upper plate because the loads can be transferred into the shaft through the filament-wound tubes. All other concepts were penalized because of the much less efficient load path. In fact, a properly directed hit could result in complete severence and loss of a blade. The same arguments apply to strikes directed at the lower plate.

For a vertical hit between the shaft and the bearing (approximately at radial station 9) all hub concepts are good except D and F. Concept D was penalized because a strike could remove a major tension and bending region, namely the lower portion of an arm. Concept F was penalized because loss of the cone seat insert or its support completely removes the capability for carrying head moment.

For a lateral hit at radial station 9 and midway between the upper and lower surfaces of the hub, only Concepts A and C received a score of less than 10. Concept A received a low score because this type of hit removes most of the shear web. Concept C was penalized because the middle plate, its shear member, has a large cutout and therefore loss of material is critical in this design. For a lateral hit, at radial station 9 in the upper plates, only Concepts E and F are completely redundant and can transfer load around the damage either in the top plate or in the tube. All other concepts are acceptable due to the large plate area and have received high scores. The same arguments are true for a lateral hit directed at radial station 9 in the bottom portion of the hub except for Concept D, which has no alternative load path and was therefore penalized more severely.

The final score is the sum for each of the eight items considered. It is given in Table 18 and, as is evident, the best is Concept E.

Producibility Estimate

Seven items were considered in the producibility trade-off study. The results are shown in Table 19. Points were awarded based upon the various considerations and then "adjusted" to obtain a score of unity. For example, Concepts A and E received a top score for ease of layup; Concept A, because it is totally filament-wound,

TABLE 19. TRADE-OFF STUDY - PRODUCIBILITY ESTIMATE

CONSIDERATION

ITEM	DESCRIPTION
1.	Ease of Layup
2.	Ease of Inspection
3.	Ease of Assembly
4.	Major Bonding Operations
5.	Drilling/Reaming Operations
6.	Major Machining Operation
7.	Number of Major Parts

EVALUATION

CONCEPT	ITEM														SCORE
	1	N/30	2	N/30	3	N/30	4	4/N	5	88/N	6	11/N	7	15/N	
A	(30)	1.0	(20)	.66	(30)	1.0	2	2.0	48	1.83	6	1.83	9	1.66	9.98
B	(25)	.83	(25)	.83	(25)	.83	3	1.33	84	1.04	9	1.22	12	1.25	7.33
C	(22)	.73	(22)	.73	(25)	.83	3	1.33	84	1.04	8	1.37	11	1.36	7.39
D	(12)	.40	(12)	.40	(25)	.83	3	1.33	56	1.57	8	1.37	10	1.50	7.40
E	(30)	1.0	(25)	.83	(30)	1.0	4	1.0	88	1.0	11	1.0	14	1.07	6.90
F	(20)	.66	(20)	.66	(30)	1.0	4	1.0	48	1.83	11	1.0	15	1.0	7.15

and concept E, because the components are easily fabricated flat plates and filament-wound tubes. Concept D received the lowest score because of the complexity of laying up the lower plate. The dishing out of plane contour of plates in Concepts B, C and F adds complexity and resulted in lower scores.

Ease of inspection affects the overall producibility and Concepts B and E received top scores. Again, the complex curvature of the lower plate in Concept D resulted in a substantial penalty.

The ease of assembly of the components is an important factor in producibility and the filament-wound hub, Concept A, received a full score. The assembly of Concepts E and F is easy, and tolerances are taken up in the adhesive layer. Concepts B, C and D are less forgiving and were lightly penalized.

The number of major bonding operations was included in the consideration and here an inverse relationship was used. The assumption for Concepts E and F was that all four arms or tubes would be cured at one time and result in one bonding (curing) operation for the arms alone. The highest score was given to Concept A, the filament-wound hub.

From a producibility standpoint, Concept A is by far the best, as reflected by the final score.

Repairability Estimate

Three items were considered with respect to repairability of the hub. The first two pertain to accessibility to components which require frequent maintenance. The third relates to the ease of repair of exterior surface and is highly influenced by the curvature of the surface.

Access to, and repair of, the damper lug area is relatively easy for all concepts except the filament-wound hub, as reflected by the scores in Table 20.

In the vicinity of the elastomeric bearing all of the concepts which have tubes around the bearing are more likely to be damaged and, due to the curvature, are less easily repaired, as reflected in the reduced scores of Concepts D, E and F.

Repair to the exterior surface was judged to be very easy for only one three-plate hub concept. All other hubs are more difficult to repair due to their curvature and the most difficult is Concept D because of its complex lower plate.

The final scores indicate that the most repairable hub concepts are those consisting of three plates.

TABLE 20. TRADE-OFF STUDY - REPAIRABILITY

CONSIDERATION

ITEM	DESCRIPTION
1.	Accessibility to Damper Lug
2.	Accessibility to Bearing Area (Maintenance Induced)
3.	Exterior Surface Repair

EVALUATION

CONCEPT	ITEM			SCORE
	1	2	3	
A	3	10	6	19
B	8	10	10	28
C	9	10	9	28
D	10	7	5	22
E	10	7	6	23
F	9	7	6	22

- Lightning Protection

A requirement of any composite hub is that it have adequate protection against a specified lightning strike. This protection can be obtained by providing an aluminum mesh over the top surface and by providing a path for current flow from the blade spindle to the shaft. Top surface protection is easy to install in all the hub concepts, as indicated by the scores in Table 21. Current flow between the spindle and the shaft is provided by a contact plate (see Figure 28). This plate is easily installed in all hub concepts except Concept A, where a hole must be cut through the inner wall of the forms and the work area is restricted. The complexity of the contact plate is reflected in the third series of scores. For concepts where tubular arms are used, the plate can be a lightweight, simple metal stamping; where the plate is exposed to air loads as in Concepts B and C, it must be heavier. Concept A was given a low score because of the relative inaccessibility of this plate. Concepts D, E and F received the highest total scores.

- Weight Estimates

The weight estimates are self-explanatory and are summarized in Table 22. Of all the hubs, the lightest, as well as the heaviest, are the three-piece concepts. Concept B incurred a substantial weight penalty as the result of its shaft adapter. Concept C is the lightest solution which utilizes a maximum number of existing rotor head components.

- Maintainability Estimate

Seven items were considered in the maintainability trade-off and the results are presented in Table 23. Inspection of the hub concepts while on the aircraft is similar in all instances except for Concept D which, because of its curvature, is more difficult. The elastomeric bearing is completely exposed in Concepts B and C and relatively exposed in Concept A; hence the higher scores. The damper and damper bearing are hidden with the hub in Concept A, whereas for all other hubs these components are easy to inspect, as reflected in the ranking.

The difficulty involved with removing the hub from the shaft extension is nearly the same for all concepts considered. Hub "C" received the lowest score because additional care must be taken to prevent binding of the bolts in the lower plate. This is a potential problem because, during removal, the lower plate is attached to the rest of the hub only by four bearing adapters at the periphery of the plate. Since the elastomeric bearing attaches in a similar manner for all hubs, they were all given an identical

TABLE 21. TRADE-OFF STUDY - LIGHTNING PROTECTION

CONSIDERATION

ITEM	DESCRIPTION
1.	Ease of Installing Top Surface Protection
2.	Ease of Installing Spindle Protection
3.	Complexity of Spindle Protection

EVALUATION

CONCEPT	ITEM			SCORE
	1	2	3	
A	10	3	3	16
B	10	9	5	24
C	10	9	5	24
D	10	10	10	30
E	10	10	10	30
F	10	10	10	30

TABLE 22. WEIGHT ESTIMATE (DEVIATION FROM TARGET WT.*)

CONCEPT	MODIFY SHAFT EXTENSION ONLY	SCORE = 1/DEVIATION
A	-5%	1.05
B	+10%**	.91
C	-17%	1.23
D	-12%	1.14
E	-12%	1.14
F	-14%**	1.16

* DEVIATION = $\frac{\text{NEW WT.} - \text{TARGET WT.}}{\text{TARGET WT.}}$

** RETAIN SAME SHAFT AND BEARING END PLATE

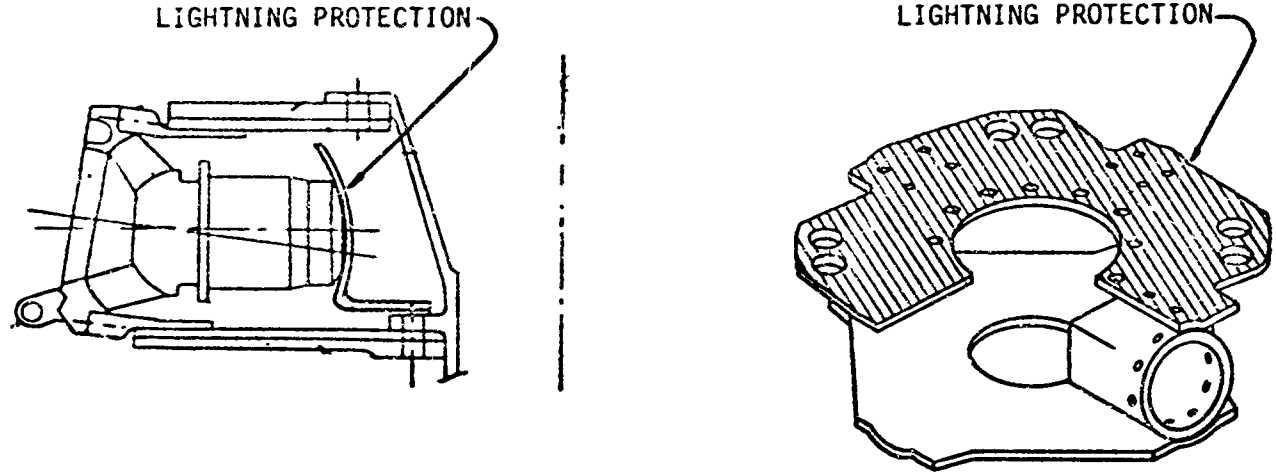

FIGURE 28. LIGHTNING PROTECTION

TABLE 23. TRADE-OFF STUDY - MAINTAINABILITY ESTIMATE

CONSIDERATION

ITEM	DESCRIPTION
1.	Inspection of Hub } On Aircraft
2.	Inspection of Bearing } On Aircraft
3.	Inspection of Damper } On Aircraft
4.	Simplicity of Installation/Removal of Hub Assembly
5.	Simplicity of Installation/Removal of Bearing Ass'y
6.	Simplicity of Installation/Removal of Damper Ass'y
7.	Ease of Repair of Surface Damage

EVALUATION

CONCEPT	ITEM							SCORE
	1	2	3	4	5	6	7	
A	8	7	5	7	10	5	6.7	48.7
B	8	10	9	7	10	9	10	63
C	7	10	9	6	10	9	10	61
D	4	5	10	8	10	10	7.8	54.8
E	8	5	10	8	10	10	8.2	59.2
F	8	5	10	7	10	9	7.8	56.8

score for ease of installation and removal of that component. The damper assembly is readily accessible in all but Concept A, as reflected in the scores.

The scores for the last item, ease of repair of surface damage, were taken from the repairability estimate (see Table 20) and factored to give a maximum of 10. The highest score was given to Concept B, a three-plate hub system.

Radar Cross Section

Since graphite/epoxy behaves like metal with respect to radar energy, two basic approaches were considered for providing a substantial reduction in radar cross section.

These were: (1) a radar absorbing rotor head fairing, and (2) a radar absorbing film applied, where required, to the surface of the composite. The differences between the hub concepts were considered to be slight and for that reason they were given the same score (see Table 24).

Final Trade-off Results

The final results of the trade-off studies are presented in Table 24. For each parameter a weighting factor was determined as shown below:

$$R_{weighting} = \frac{\text{Ranking Factor}}{\text{Highest Base Score}}$$

By multiplying $R_{weighting}$ times the base scores, a weighted score for each parameter was determined. The sum of the weighted scores is given in Table 24. The trade-off study was performed to determine which composite hub concept should be chosen for further refinement; based upon the results, Concept E was chosen.

TABLE 24. FINAL TRADE-OFF SUMMARY

CONCEPT	COST R = 7		WEIGHT R = 8		PRODUCI-BILITY R = 7		RELIABILITY R = 10		MAINTAIN-ABILITY R = 10		REPAIR-ABILITY R = 6		RADAR R = 3		LIGHTNING R = 3		BALLISTIC R = 10		SCORE
	Base Score	Wt. Score	Base Score	Wt. Score	Base Score	Wt. Score	Base Score	Wt. Score	Base Score	Wt. Score	Base Score	Wt. Score	Base Score	Wt. Score	Base Score	Wt. Score	Base Score	Wt. Score	
A	1.19	7.00	1.05	6.83	9.98	7.00	80.3	8.51	49	7.78	19	4.07	10	3	16	1.6	66	8.25	54.04
B	.84	4.94	.91	5.91	7.33	5.14	88.6	9.39	63	10.00	28	6.00	10	3	24	2.4	67	8.37	55.15
C	.94	5.53	1.23	8.00	7.39	5.18	81.4	8.62	61	9.68	28	6.00	10	3	24	2.4	63	7.87	56.28
D	.86	5.06	1.14	7.44	7.40	5.19	83.7	8.87	55	8.73	22	4.71	10	3	30	3.0	69	8.62	54.59
E	1.15	6.76	1.14	7.41	6.90	4.84	94.4	10.00	59	9.37	23	4.93	10	3	30	3.0	80	10.00	59.31
F	1.19	7.00	1.16	7.54	7.15	5.02	91.3	9.67	57	9.05	22	4.71	10	3	30	3.0	77	9.62	58.61

IV. REFINEMENT OF THE SELECTED CONCEPT

A. Physical Description

The final configuration is shown in Figure 29. It consists basically of four filament-wound tubes bolted and bonded to two flat plates. Both the plates and the tubes have molded-in stainless-steel shims in the shaft attachment region. The stainless-steel shims were used to obtain adequate bearing strength without increasing laminate thickness. The tubes are filament-wound around a slightly expandable mandrel. The windings are expanded into a cavity to obtain good dimensional control of the outer surface. The elastomeric bearings are attached to a titanium bearing adapter which is located between the circular tube and the flat plates. This provides the redundant attachment to both the tube and the plate as well as an easy means of transitioning from a flat to a curved surface.

The bifilar bushings are field replaceable, and are actually large-diameter, hollow, stainless-steel bolts. They thread into a titanium plate on the upper surface of the top plate and thereby provide a compressive force transverse to the composite plate which prevents delamination in this region. The damper bracket consists of an aluminum forging which supports a large titanium bolt running from the top to the bottom plate. The titanium bolt was used for purposes of weight savings. The flange of the damper bracket forging is bolted to the vertical wall of the adjacent filament-wound tube. Phenolic shims isolate the aluminum from the graphite/epoxy. Bonded-in bushings are used for the removable bolts,which include shaft attachment bolts and the damper bearing bolts.

The type AS graphite/epoxy system is oriented parallel to and at $\pm 45^{o}$ to each arm. This provides a direct load path for normal operation and a four-bar self-equilibrating, redundant load path in the event of a loss of the primary path.

Protection from foreign object damage is provided by a 0.030-inch-thick layer of woven fiberglass on exposed surfaces. Protection from a direct lightning strike is provided by an aluminum mesh bonded to the fiberglass over the entire upper surface of the top plate. Protection from an indirect lightning strike that can enter the hub from the spindle is provided by a "contact plate", which is attached to the nut plates.

A significant reduction in radar return is achieved by coating the edges and interior regions (see Figure 30) with a radar absorbing film (NR-95 manufactured by the Tulsa Division, North American Rockwell). The top surface is not coated due to the fact that this flat surface would reflect radar energy away from ground or air-borne receivers.

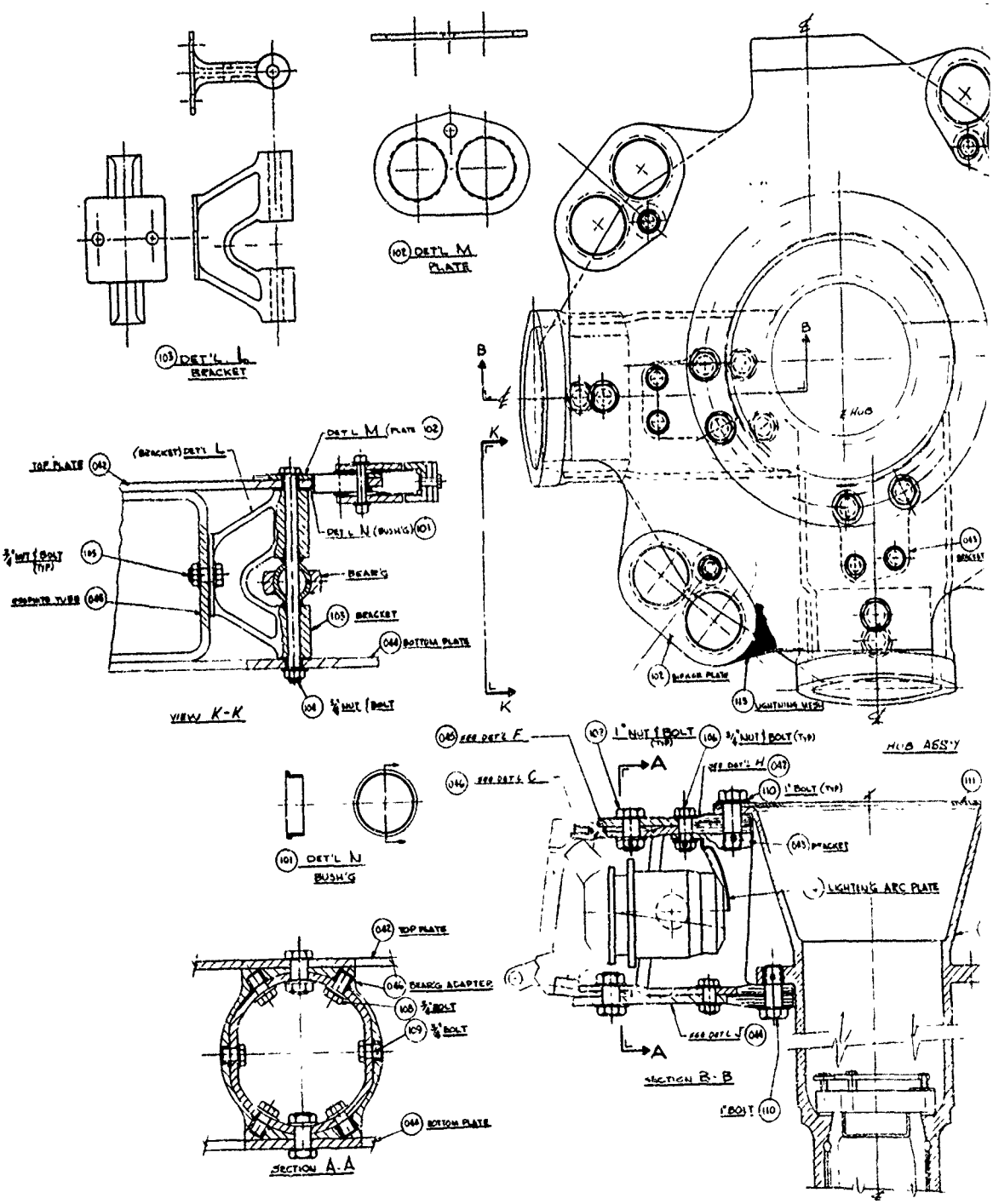

FIGURE 29

FINAL CONFIGURATION OF CONCEPT E

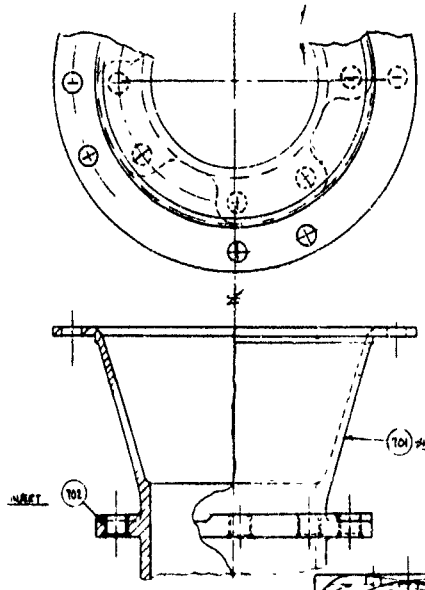

(047) SHAFT DET'L G

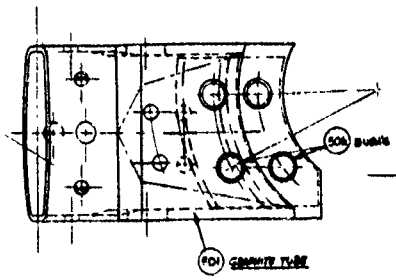

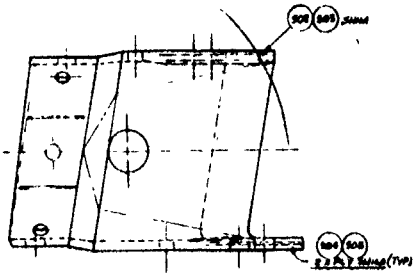

(045) DET'L F (COMPOSITE)
(SEE SECTION B-B)

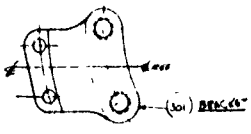

(043) DET'L D BRACKET (4) REQD
(SEE SECTION B-B)

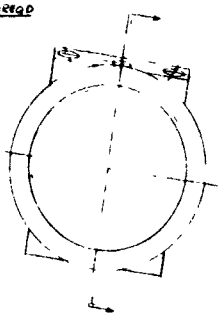

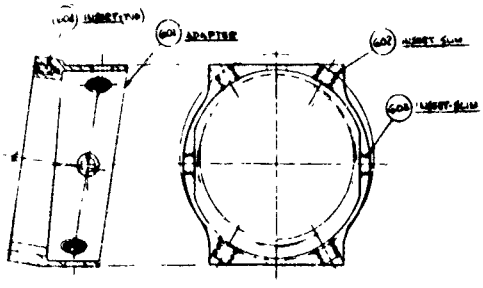

(046) DET'L C BEAR'S RING
SEE SECTION B-B)

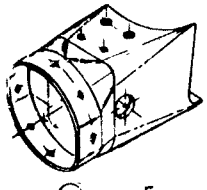

(048) DET'L E
(SEE SECTION B-B)

(114) LIGHTENING

2

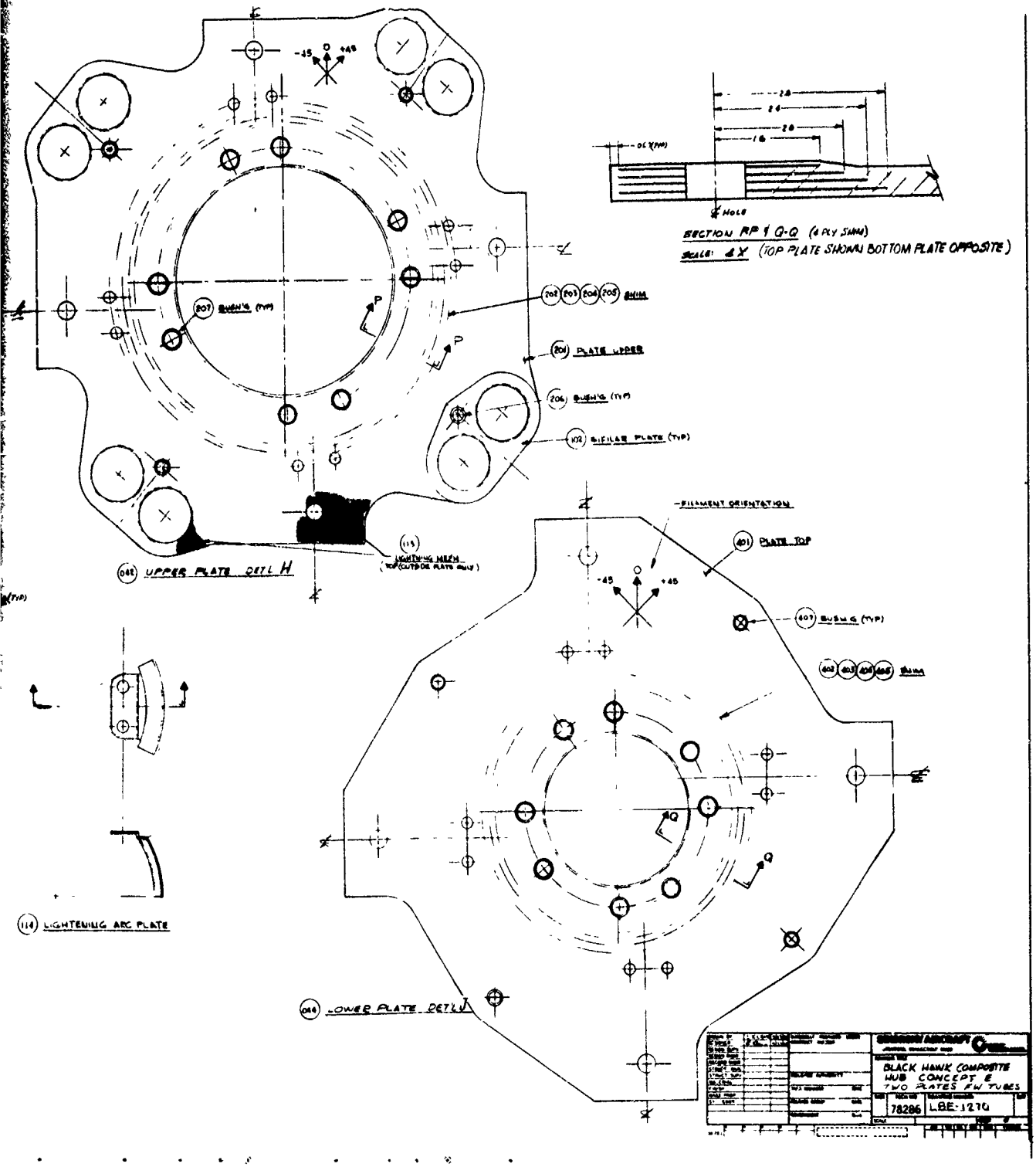

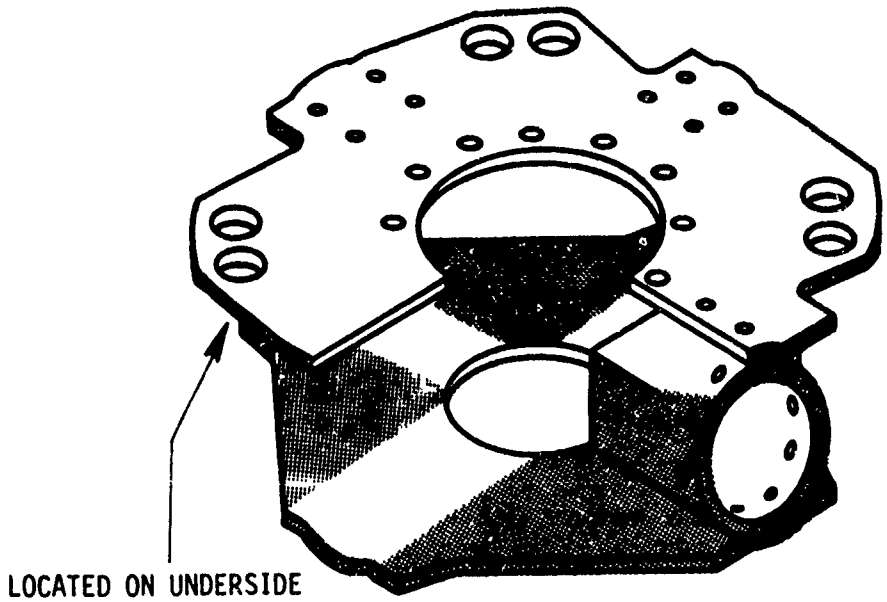

FIGURE 30. LOCATION OF RADAR ABSORBING FILM (SHOWN BY SHADING)

The film is approximately 0.040 inches thick and has a layer of peel ply between it and the composite hub. This peel ply permits removal of the film for inspection and/or repair.

B. Discussion of the Attributes

. Structural Integrity

Structural analyses of the hub were conducted for the limit load and the fatigue design load conditions. The NASTRAN model is shown in Figure 31. This figure features cutouts in the upper plate which are present to permit control horn movement. This coarse grid model was appropriate for determining load paths, deflected shapes and the so-called "far field stresses". Detailed stresses around a hole, for example, were estimated using the appropriate orthotropic stress concentration factor times the far field stress. This model was made up of QUAD1 and TRIA1 plate elements. Loads were introduced by a series of rods connected from the theoretical hinge location to the periphery of the hub arm where the bearing adapter is located. The model was stiffened at this location to more accurately simulate end plate stiffness; this prevents large radial stresses and displacements from developing in the tubes. This restraint is provided in the actual hub by the elastomeric bearing end plate and by the bearing adapter.

Along the cutouts in the top and bottom plate, which represent the regions that are attached to the shaft extension, the model was restrained from all displacements. This represents a stiffer situation than actually exists and provides higher, and hence conservative, design loads for the bolts as well as the composite in this region.

The details of the analysis are lengthy and are presented in Appendix A. A summary of the margins of safety for each major area of each component is presented in Table 25. The positive margins indicate adequate structural design at the design conditions.

. Ballistic Vulnerability Analysis

The ballistic design requirements specify that the hub support flight loads for 30 minutes and sustain the limit loads after a 23 mm HEI strike. This includes strikes at all obliquities, all regions (not masked), and for all fuzings, within the entire lower hemisphere and up to 15^{0} above a horizontal plane passing through the hub. Masking is complex and depends upon the azimuthal position, as is shown in Figure 32. A 23 mm HEI projectile was

TABLE 25. MARGIN OF SAFETY - SUMMARY

	MS_{Static}	$MS_{Fatigue}$
Top Plate		
Attachment to Shaft	.63	.25
Attachment to Tubes	.09	.39
Bifilar	+HIGH	1.03
Shims	1.73	1.07
Bottom Plate		
Attachment to Shaft	.53	1.27
Attachment to Tubes	.14	.84
Shims	.85	1.52
Tubular Arms		
Attachment to Shaft		
Top Ring	1.33	.35
Lower Ring	.41	.84
Attachment to Plates	.43	1.46
Attachment to Bearing Adapters	.32	+HIGH
Shaft Extension		
Upper Bolt Ring	.36	.11
Lower Bolt Ring	.35	.33
Bearing Adapter	.34	+HIGH
Damper Lug	+HIGH	+HIGH
Bolts		
Main to Shaft	.64	.57
Bearing Adapter to Tube	.48	+HIGH
Damper	2.28	2.68

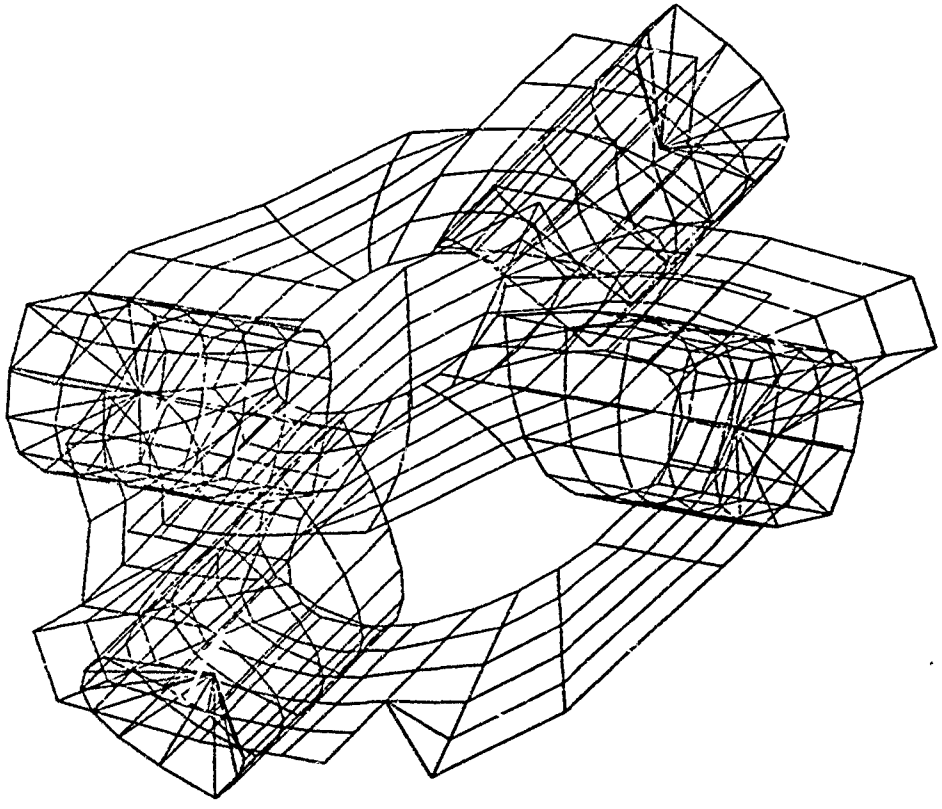

FIGURE 31. COARSE GRID NASTRAN MODEL OF THE FINAL CONFIGURATION OF CONCEPT E

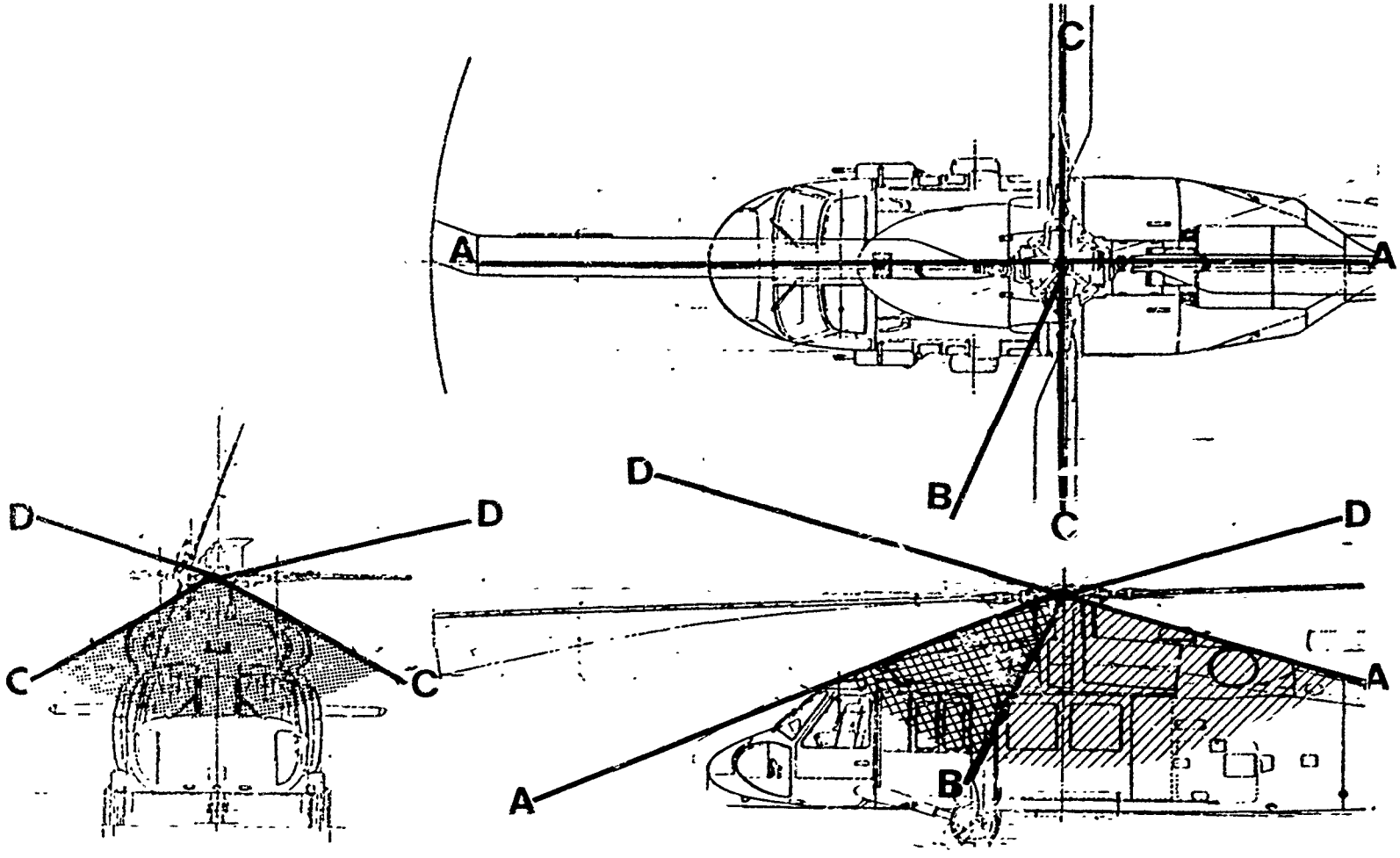

FIGURE 32. BALLISTIC MASKING OF THE HUB-MASKING IS SHOWN BY CROSS HATCHING AND IS A FUNCTION OF AZIMUTHAL POSITION AS INDICATED BY LETTERED RAYS.

estimated to be capable of severing a region approximately six inches in diameter in the hub, either upon entering or exiting depending on the fuzing.

The region close to the shaft in the lower plate is the most highly loaded region; therefore, a hub with a 6-inch-diameter hole in the critical region was analyzed using NASTRAN.

Stress contour plots indicated that only load paths in the lower plate were substantially affected. The results of the analysis, presented in Appendix B, indicate that the limit load can be carried. For this analysis the 1.5 safety factor was not applied to the allowables. Similarly, for the 30-minute flight requirement, a head moment associated with 3^0 of flapping was used in the analysis. In 30 minutes the ballistically damaged hub is subjected to approximately 9000 cycles. Again, the analysis indicated a positive margin; thus the composite hub meets the basic ballistic requirement.

A mission abort possibility exists for all ballistic threats considered. The 7.62 mm and the 12.7 mm API projectiles can damage the bifilar, and the 23 mm HEI can completely sever the bifilar from the rest of the hub. A vibration analysis was performed to determine the effect of this mass loss. The analysis indicated that the 4P and 1P responses are the dominant harmonics of the airframe. The magnitudes are summarized in Table 26. The BLACK HAWK A/C has been flown with 1P unbalance of magnitudes over 50 percent greater than those predicted for the loss of bifilar mass, and no destructive vibration resulted. The conclusions from this analysis are that the BLACK HAWK A/C may be operated after the loss of a bifilar mass; the vibration will be severe but will not result in an immediate safety-of-flight risk to the A/C or crew. Another area of concern relates to a comparison of vulnerable area between the composite hub and its titanium counterpart. The vulnerable area of the masked hub and the probability of mission abort for the composite hub are presented below.

(1) For 7.62 and 12.7 mm API threats the vulnerable region is in the vicinity of the bifilar. For the front, rear, left and right view the projected area, Ap, and the vulnerable area, Av, are given below (see Figure 33).

$$Ap = 36" \times .5" = 18 \text{ in.}^2$$

$$Av = 5" \times .5" \times 3 = 7.5 \text{ in.}^2$$

$$P^*ma = \frac{Av}{Ap} = .42$$

* probability of mission abort

Table 26

Airframe Response Resulting from the Loss of One Bifilar Mass

	4P + g's	1P + g's
Pilot Vertical	.15	.09
Pilot Longitudinal	.02	.02
Pilot Lateral	.27	.05

For the bottom view the projected area is zero due to masking. Therefore the 5-view average vulnerable area is

$$Av, 5\text{-view} = \frac{A_{right} + A_{left} + A_{front} + A_{rear} + A_{bottom}}{5}$$

$$Av, 5\text{-view} = \frac{7.5\ in^2 \times 4 + 0 \times 1}{5}$$

$$Av, 5\text{-view} = 6\ in^2 = .04\ ft^2$$

(2) For 23 mm HEI threats all regions are threatened. For the front, rear, left and right view

$$A_p = Av = 9" \times 36" = 324\ in^2$$

$$P_{ma} = \frac{Av}{Ap} = 1.00$$

As before, the projected area for the bottom view is zero and the 5-view average vulnerable area is

$$Av, 5\text{-view} = \frac{4 \times 324\ in^2 + 1 \times 0\ in^2}{5}$$

$$Av, 5\text{-view} = 259\ in^2 = 1.80\ ft^2$$

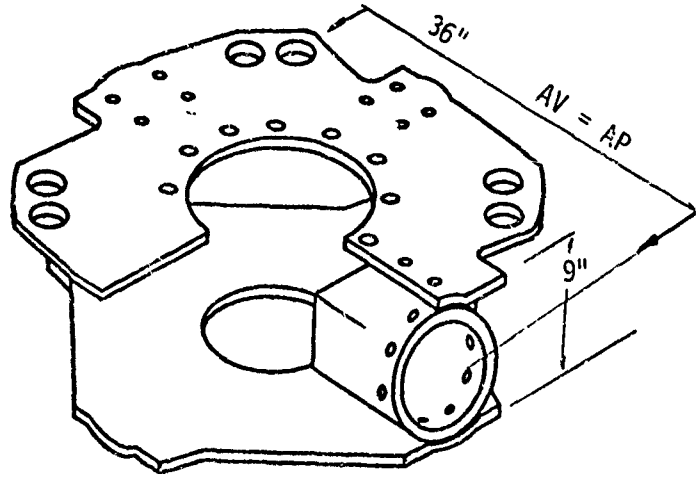

a

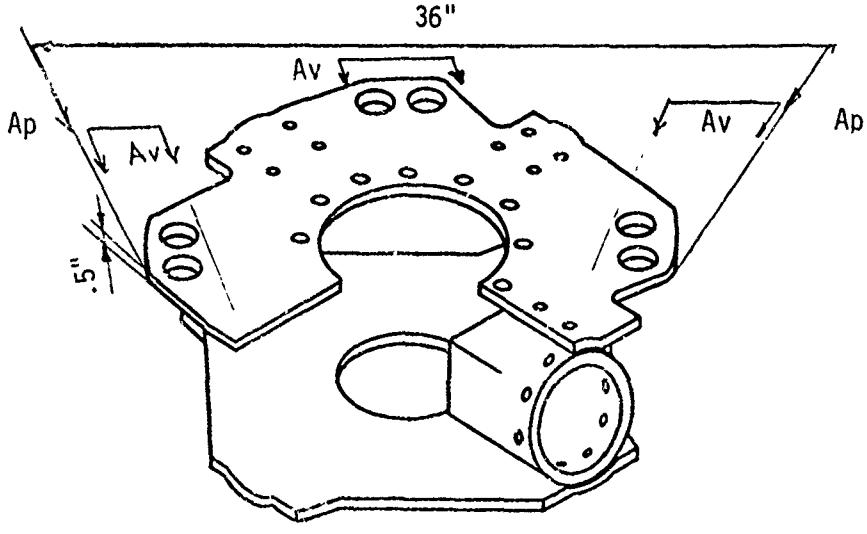

b

FIGURE 33. VULNERABLE AREAS OF THE HUB

a = 23 mm HEI

b = 7.62 AND 12.7 mm API

The analysis for the BLACK HAWK hub was conducted in an identical manner. The aluminum bifilar support was included with the titanium hub to obtain a comparable system. Within the accuracy of these estimates, the vulnerable area is the same for both the titanium and the composite hub.

Damage Tolerance Assessment

In Section II, induced failures were classified according to severity and to types, i.e., environmental damage, handling damage, and ballistic damage. Some kinds of environmental hazards such as temperature and moisture degrade the material properties and are accounted for by reduced allowables. This discussion relates to induced damage from impact. The factors considered include hail, small stones, tool drops, ballistic impacts, etc.

There are three major parameters governing damage tolerance of the commonly used types of graphite/epoxy composite: (1) the thickness of the composite, (2) the type and thickness of protective coatings, and (3) the impact energy.

The thickness of the composite in the hub is of the order of 1/2 inch. A lot of data exists on thin laminates because they are commonly used (Reference 8). The behavior of thick panels differs significantly, and little published data is available at this time. For example, a thin panel subjected to a 1-pound wrench dropped from a height of 4 feet might experience a perforation or a very localized deformation such that cracking and crazing occur. The same drop test performed on a 1/2-inch-thick panel would result in minimal damage; perhaps a slight gouge if the tool was sharp, i.e., a high local energy intensity or possibly a slight permanent indentation if the tool was blunt, i.e., low local energy intensity.

Because of the scarcity of data a series of tests were performed by dropping tools on representative thickness of graphite/epoxy and titanium. Different size wrenches were dropped on these simply supported specimens of titanium and graphite/epoxy. The wrenches ranged in weight from .25 pound to 1.5 pound and were dropped from a constant height of 3 feet. The results were surprising. The unprotected graphite/epoxy responded in much the same way as did the titanium. With blunt objects at impact energies of 1.1 foot-pounds, a small "dent" formed in both specimens. At higher impact energies, up to 4.5 foot-pounds, a larger "dent" was formed, and in the composite there were some signs of very localized crazing. The amount of blending required to eliminate the damaged zone was the same in both cases and therefore

[8] "Foreign Object Impact Damage to Composites," STP 568, American Society for Testing and Materials, January 1975.

for this study the damage was estimated to be similar. When the energy intensity was increased, as was done by orienting the wrench such that a pointed area hit the specimen, the damage was again the same. Small gouges, similar in size, were formed in both materials. The result of this study was that for low levels of impact energy and relatively low velocity strikes, unprotected graphite/epoxy is as damage tolerant as titanium.

Some recent work by J. Labor (Reference 9) indicates that thin panels of graphite/epoxy withstand 145-knot hail and small stone impact with a minimal amount of damage. Thick panels are expected to behave even better. The rationale is that the thin panels behave like a beam on a soft elastic foundation and can deform locally, whereas the thick plate behaves like a beam on a stiff elastic foundation and the stiff support spreads out the load and distributes it over a larger region.

Various investigators have found a significant improvement in damage tolerance by using protective coatings. Data exists on thin coatings applied to thin panels (Reference 8). It is expected that significant improvements in damage tolerance can be achieved in thick panels also. The coatings that were considered included fiberglass/epoxy, kevlar/epoxy, ballistic nylon/epoxy, and urethane films. Urethane is effective but greatly inhibits inspection of the underlying graphite/epoxy. Kevlar and nylon attenuate ultrasonic energy more than a similar thickness of fiberglass and hence they too have an adverse effect on inspectability. Another advantage of fiberglass is that it absorbs less moisture than either Kevlar or nylon and is easily machined or abraded away for repairs. The 0.030-inch-thick woven fiberglass cover used over the entire hub does not severely impede coin tap or ultrasonic inspection. Further, since for low-energy impacts, which are the most common for a hub, unprotected graphite/epoxy is as damage resistant as titanium, the protection added by the fiberglass may render the composite hub more damage tolerant than its titanium counterpart.

The composite hub has one other advantage. Scratches and gouges in the metal hub up to 0.040 inch deep and in the bifilar up to 0.020 inch deep can be field repaired. However, these scratches, if not repaired in time, can turn into a thumbnail crack and eventually into a thrucrack. Since the formation of any crack requires a replacement hub, scratches and gouges are significant forms of damage. Larger and deeper scratches and gouges up to 0.080 inch deep can be repaired in the composite hub. The "repair" replaces the damaged material and the gouge propagates,

---

[9]"Service/Maintainability of Advanced Composite Structures," J.D. Labor, Northrup Corp., Contract No. F 33615-76-C-3142.

not in the thickness direction as a thumbnail crack, but along the plies in an interlaminar mode. This mode results in a delamination that is not critical and which can be repaired at a later time.

High energy impacts include bird strikes and ballistic strikes. Bird strikes on the hub are so rare that they need not be addressed. Ballistic strikes can be severe to both hubs. A direct 23 mm HEI strike will result in significant damage, although not a forced landing, of either hub. Damage from a 7.62 or 12.7 mm API, in general, will not be fully repairable. Temporary repairs can be made at the field level to permit either hub to fly, but a complete restoration to former status is unlikely in either hub. At ballistic velocities, small fragments or a glancing strike can cause a major delamination in the composite. However, the likelihood of this type of strike with an impact angle of about 1^{0} to 5^{0} is remote. The same impact on titanium would result in minor damage. Therefore, for high energy impacts, the composite is not as damage tolerant as the titanium hub.

Reliability and Maintainability Assessment

A preliminary analysis of the composite hub design indicates that the use of composite materials has, potentially, both positive and negative effects on the R&M characteristics of the hub, relative to conventional metal designs now in service. Qualitative and quantitative R&M assessments were made by comparing design features of the proposed hub with those of the existing Black Hawk titanium hub. The quantitative analysis is based on the Black Hawk values for the titanium hub stated in References (3) and (10), and a damage tolerance analysis developed from Reference (11). The results of the quantitative assessment were incorporated into a preliminary life-cycle cost analysis which compares the composite hub with the current titanium hub.

A preliminary reliability assessment of the composite hub was performed to estimate failure rates and to assess qualitative reliability characteristics. As presented in Table 27, a parts comparison with the current hub provides the basis used for estimating the failure rate of the composite hub. Table 28 reviews the probable inherent and induced failure modes of the hub. A damage-tolerant assessment is also presented in Table 28.

The composite hub inherent failure rate assessment is based on a parts comparison with the Black Hawk titanium hub. The existing titanium hub consists of four major components; the proposed

---

[10] UH-60A Maintainability Prediction Report, SER-70597, June 10, 1977.
[11] Navy 3M, SH-3D data, January through December, 1975.

TABLE 27.

COMPOSITE HUB FAILURE RATE ASSESSMENT
TITANIUM VERSUS COMPOSITE HUB PARTS COMPARISON

COMPONENT/PARTS		BLACK HAWK TITANIUM FAILURE RATE λ/10-3 HRS	COMPONENT PARTS		ASSESSED COMPOSITE FAILURE RATE λ/10-3 HRS
Titanium Hub		λ = .46	Composite Hub		λ = .58
Hub	(1)		Upper composite plate	(1)	
Inserts, mount to extender	(16)		Lower composite plate	(1)	
Cone inserts	(8)		Composite spindle tube	(4)	
Cone seat (cone face)	(1)		Titanium spindle adapter	(4)	
Damper bracket	(4)		Damper bracket	(4)	
Bolts/inserts	(32)		Bifilar plate	(4)	
Spindle inserts	(48)		Bifilar bushing	(8)	
			Damper bracket mount bolt/nut/ washer	(12)	
			Bolting plates	(48)	
			Tube/plate attachment bolt/nut/ washer	(16)	
			Tube/plate/adapter attachment bolt/ nut/washer	(8)	
			Tube/adapter attachment bolt/insert	(24)	
TOTAL:	110		TOTAL:	138	

TABLE 27. (Cont'd)

COMPOSITE HUB FAILURE RATE ASSESSMENT
TITANIUM VERSUS COMPOSITE HUB PARTS COMPARISON

COMPONENT/PARTS		BLACK HAWK TITANIUM FAILURE RATE λ/10-3 HRS	COMPONENT PARTS		ASSESSED COMPOSITE FAILURE RATE λ/10-3 HRS
Extender		λ = .06	Extender		λ = .07
Titanium extender	(1)		Titanium extender	(1)	
Bolts	(12)		Bolts	(16)	
Expandable pins	(4)		Inserts	(8)	
Lower cone inserts	(18)		Lower cone inserts	(18)	
Cone face	(1)		Cone face	(1)	
Spline	(1)		Spline	(1)	
TOTAL:	37		TOTAL:	45	
Bifilar		λ = .20	* Incorporated into composite hub upper plate.		-
Upper Pressure Plate		λ = .015	* Eliminated by design.		-
		.735			.65

TABLE 28.

BLACK HAWK COMPOSITE HUB
FAILURE MODES AND DAMAGE TOLERANCE ASSESSMENT

COMPONENT/PROBABLE FAILURE MODE	INHERENT	INDUCED	DAMAGE TOLERANCE ASSESSMENT
Upper Composite Plate			
(a) Cracks or delamination around center hole	X		(h) FOD
(b) Cracks or delamination around hub retention holes	X		The upper plate is susceptible to high-energy impact damage on the upper surface and edges. This type of damage will require removal of the hub for repairs.
(c) Cracks or delamination around spindle tube attachment holes	X		
(d) Cracks or delamination around damper or bifilar mount holes	X		(i) Maintenance-induced damage
(e) Surface cracks, distortion	X		Tool damage of the upper plate results in small scratches or dents to the surface. Edge tool strikes may induce delamination. Due to the high location of the hub on the aircraft, the probability of high energy tool drops are small.
(f) Edge delamination	X		
(g) Fracture	X		
(h) FOD		X	
(i) Maintenance-induced damage		X	
(j) Ballistic damage		X	(j) Ballistic Damage
			This type of damage will require removal of the hub for analysis and repair or scrap.

TABLE 28. (Continued)

BLACK HAWK COMPOSITE HUB
FAILURE MODES AND DAMAGE TOLERANCE ASSESSMENT

COMPONENT/PROBABLE FAILURE MODE	INHERENT	INDUCED	DAMAGE TOLERANCE ASSESSMENT
Lower Composite Plate			
(a) Cracks or delamination around center hole	X		(h) FOD
(b) Cracks or delamination around hub retention holes	X		The lower plate is most susceptible to high-energy impact damage along the plate edge. Damage of the plate edge will require hub removal for repairs.
(c) Cracks or delamination around spindle tube attachment holes	X		(i) Maintenance-induced damage
(d) Cracks or delamination around damper mount holes	X		Tool damage of the lower plate results in small scratches or dents to the surface. Edge tool strikes may induce delamination. Due to the high location of the hub on the aircraft, the probability of high energy tool drops is small.
(e) Surface cracks, distortion	X		
(f) Edge delamination	X		
(g) Fracture	X		
(h) FOD		X	(j) Ballistic damage
(i) Maintenance-induced damage		X	This type of damage will require removal of the hub for analysis and repair or scrap.
(j) Ballistic damage		X	

TABLE 28. (Continued)

BLACK HAWK COMPOSITE HUB
FAILURE MODES AND DAMAGE TOLERANCE ASSESSMENT

COMPONENT/PROBABLE FAILURE MODE	INHERENT	INDUCED	DAMAGE TOLERANCE ASSESSMENT
Composite Spindle Tubes			
(a) Cracks or delamination around tube opening	X		(h) FOD The spindle tube is most susceptible to high-energy side wall impact. This area is partially protected by the upper plate, blade damper and horn. Damage in this area will require hub removal for repairs. (i) Maintenance-induced damage Tool damage of the spindle tube results in small scratches or dents to the surface. Edge damage during installation may cause delamination. Tool drops on this component are unlikely. (j) Ballistic damage This type of damage would require removal of the hub for analysis and repair or scrap.
(b) Cracks or delamination around tube mount holes	X		
(c) Cracks or delamination around damper mount holes	X		
(d) Surface cracks, distortion	X		
(e) Edge delamination	X		
(f) Fracture	X		
(g) Tube/plate bond separation	X		
(h) FOD		X	
(i) Maintenance-induced damage		X	
(j) Ballistic damage		X	

TABLE 28. (Continued)

BLACK HAWK COMPOSITE HUB
FAILURE MODES AND DAMAGE TOLERANCE ASSESSMENT

COMPONENT/PROBABLE FAILURE MODE	INHERENT	INDUCED	DAMAGE TOLERANCE ASSESSMENT
Titanium Spindle Adapter			
(a) Cracking	X		
(b) Stripped inserts	X		
(c) Fretting	X		(g) Ballistic damage
(d) Bond separation	X		Damage tolerance of the spindle adapters is similar to the existing titanium hub in this area. Titanium is less susceptible to high-energy FOD impacts and maintenance-induced damage. Titanium is more susceptible than composite to crack propagation after ballistic damage.
(e) FOD		X	
(f) Maintenance-induced damage		X	
(g) Ballistic damage		X	

TABLE 28. (Continued)

BLACK HAWK COMPOSITE HUB
FAILURE MODES AND DAMAGE TOLERANCE ASSESSMENT

COMPONENT/PROBABLE FAILURE MODE	INHERENT	INDUCED	DAMAGE TOLERANCE ASSESSMENT
Damper Bracket			
(a) Cracking	X		
(b) Corrosion	X		
(c) Fretting	X		(h) Ballistic damage
(d) Fracture	X		Aluminum is relatively damage resistant but is susceptible to crack propagation when notch damaged. The bracket is partially protected by the upper plate, blade damper and horn. Repair or replacement of the bracket may be done at field level.
(e) Worn bushing	X		
(f) FOD		X	
(g) Maintenance-induced damage		X	
(h) Ballistic damage		X	

TABLE 28. (Continued)

BLACK HAWK COMPOSITE HUB
FAILURE MODES AND DAMAGE TOLERANCE ASSESSMENT

COMPONENT/PROBABLE FAILURE MODE	INHERENT	INDUCED	DAMAGE TOLERANCE ASSESSMENT
Bifilar Plates			
(a) Cracking	X		Damage tolerance of the bifilar plate is similar to the existing bifilar attachment. Repair or replacement of the plate may be done in the field.
(b) Fretting	X		
(c) Worn	X		
(d) FOD		X	
(e) Maintenance-induced damage		X	
(f) Ballistic damage		X	

TABLE 28. (Continued)

BLACK HAWK COMPOSITE HUB
FAILURE MODES AND DAMAGE TOLERANCE ASSESSMENT

COMPONENT/PROBABLE FAILURE MODE	INHERENT	INDUCED	DAMAGE TOLERANCE ASSESSMENT
Bifilar Bushings			
(a) Cracking	X		Damage tolerance of the bifilar bushing is similar to the existing bifilar bushing. Repair or replacement of the bushing may be done in the field.
(b) Fretting	X		
(c) Worn	X		
(d) FOD		X	
(e) Maintenance-induced damage		X	
(f) Ballistic damage		X	

TABLE 28. (Continued)

BLACK HAWK COMPOSITE HUB
FAILURE MODES AND DAMAGE TOLERANCE ASSESSMENT

COMPONENT/PROBABLE FAILURE MODE	INHERENT	INDUCED	DAMAGE TOLERANCE ASSESSMENT
Titanium Extender			
(a) Fretting, cone face	X		Damage tolerance of the extender is identical to the existing titanium extender.
(b) Fretting, hub face	X		
(c) Spline wear	X		
(d) Worn insert	X		
(e) Stripped insert		X	
(f) Fracture	X		
(g) Cracking	X		
(h) FOD		X	
(i) Maintenance-induced damage		X	
(j) Ballistic damage		X	

TABLE 28. (Continued)

BLACK HAWK COMPOSITE HUB
FAILURE MODES AND DAMAGE TOLERANCE ASSESSMENT

COMPONENT/PROBABLE FAILURE MODE	INHERENT	INDUCED	DAMAGE TOLERANCE ASSESSMENT
Attaching Hardware			
(a) Bolt fretting	X		Damage tolerance is the same as for the production BLACK HAWK hub.
(b) Bolt fracture	X		
(c) Stripped threads		X	
(c) Loose bolt	X		
(e) Worn bolt	X		
(f) Nut fretting	X		
(g) Nut cracking	X	X	
(h) Nut loose		X	
(i) Stripped insert		X	
(j) Unable to hold torque nut, insert	X		
(k) Liner fretting	X		
(l) Worn liner	X		

TABLE 28. (Continued)

BLACK HAWK COMPOSITE HUB
FAILURE MODES AND DAMAGE TOLERANCE ASSESSMENT

COMPONENT/PROBABLE FAILURE MODE	INHERENT	INDUCED	DAMAGE TOLERANCE ASSESSMENT
Attaching Hardware (Continued)			
(m) Loose liner	X	X	
(n) Maintenance-induced damage		X	

composite hub is comprised of two. Table 27 presents, for the major components of each hub, a listing of detail parts and quantity of each per assembly. The failure rate estimates are based on a ratio of the number of parts for each component. Based on this parts count comparison, the estimated failure rate for the basic composite hub is higher than that of the titanium hub. The same is true for the hub extender. The two remaining titanium hub components do not have counterparts in the composite hub design which eliminates the failure rates associated with those items from the composite hub. The resulting overall composite hub/extender failure rate (λ_C) is predicted to be smaller than the titanium hub/extender rate (λ_T).

(λ_C = .65/1000 vs. λ_T = .735/1000).

Table 28 lists, for each of the generic components of the composite hub, the probable failure modes, both inherent and induced. This preliminary analysis indicates an increased number of inherent failure modes for the composite hub over the titanium design due to the introduction of modes peculiar to the composite materials. The large quantity of attaching hardware present in the composite design also increases the number of inherent failure modes. The damage tolerance characteristics were evaluated in the previous section and are summarized in Table 28. The damage tolerance analysis indicated that the composite hub is as tolerant of low-energy impact as the titanium hub, but less tolerant of high-energy impacts. This initial assessment was based on small tests. Full scale testing would be required to establish, quantitatively, the damage tolerance of the hub.

Table 29 summarizes the significant maintenance tasks, estimated repair and replacement times, and maintenance related design characteristics of the composite hub. A discussion of important maintainability considerations follows. The composite hub/extender installation is common to the existing Black Hawk titanium hub. Installation of the extender includes the pressure plate, cones, and main mast nut. The four spindle assemblies and blades attach to the hub with 48 spindle bolts. The remove/replace time is an estimated 5.8 man-hours as documented in Reference 10. The teardown of the composite hub from the extender achieves a minor savings in maintenance time over the titanium hub. The number of composite hub attachment bolts is equivalent to the titanium hub installation, but the composite design does not require an upper cone and pressure plate. Therefore, the teardown of the composite hub, estimated to be 1.7 man-hours, is .3 man-hour less than that of the titanium hub. The total remove/replace time for the

TABLE 29.

COMPOSITE HUB MAINTAINABILITY ASSESSMENT

COMPONENT	MAINTENANCE ACTION	PROPOSED MAINT. LEVEL			ESTIMATED MAN-HOURS	MAINTENANCE CHARACTERISTICS
		AVUM	AVIM	DEPOT		
Composite Hub	Remove and replace	X			7.5	Composite vs. Titanium Hub - Common spindle mount - Common aircraft installation - Slight reduction in hub/ extender teardown workload
Upper plate	Repair	X	X		TBD	
Lower plate	Repair	X	X		TBD	- Composite has potential for lower maintenance level repair
Spindle tube	Repair			X	310	AVUM - surface repair AVIM - composite surface repair
Spindle adapter	Repair	X	X			- Composite repair requires more man-hours than titanium
Damper bracket	Remove and replace	X			.9	- Field-removable damper bracket
	Repair	X	X		.6	- Reduced mounting hardware

TABLE 29. (Continued)

COMPOSITE HUB MAINTAINABILITY ASSESSMENT

COMPONENT	MAINTENANCE ACTION	PROPOSED MAINT. LEVEL			ESTIMATED MAN-HOURS	MAINTENANCE CHARACTERISTICS
		AVUM	AVIM	DEPOT		
Composite Hub (Continued)						
Bifilar plate	Remove and replace	X			.9	- Integral bifilar design reduces potential maintenance time
	Repair	X	X		.6	- Composite design allows replacement of single component instead of large support
Bifilar bushing	Remove and replace	X			.3	- Composite design provides field-replaceable bushings
Mounting hardware	Remove and replace	X		X	.1 - .7	- Common attachment hardware - Poor access to nuts and bolts may increase inspection and repair time
Extender	Remove and replace	X			7.5	- Composite hub extender very similar to current BLACK HAWK design - Common BLACK HAWK installation to aircraft

TABLE 29.(Continued)

COMPOSITE HUB MAINTAINABILITY ASSESSMENT

COMPONENT	MAINTENANCE ACTION	PROPOSED MAINT. LEVEL			ESTIMATED MAN-HOURS	MAINTENANCE CHARACTERISTICS
		AVUM	AVIM	DEPOT		
Extender (Continued)	Repair	X		X	14	- Titanium repair identical to current BLACK HAWK design

composite hub is an estimated 7.5 man-hours compared to 7.8 man-hours for the titanium hub.

Repair procedures and level of repair for the composite hub were assessed and compared to the titanium hub. Reference 2 indicates that most failures of the Black Hawk titanium hub cause hub removals; only .01 failure per thousand hours involves repairs on the aircraft. On-aircraft repairs usually cover blending of small nicks and scratches. The remaining hub repairs are performed at depot. On-aircraft repair of composite material is anticipated to be more extensive but also more complex and time-consuming than titanium repairs. It is expected that this will involve primarily the repair of minor damage in the surface layers of the hub. Such repairs will involve removing paint and dirt, preparation of the surface, and the application of bonded patches. It may be practical to perform more extensive repairs of the composite hub on the aircraft. This would tend to reduce the removal frequency and might produce positive benefits in terms of aircraft availability and maintenance cost. Further work will be needed to investigate this possibility, and for the current study no such benefits were assumed. All off-aircraft repairs of the titanium hub are performed at depot because factory-type measuring and repair equipment is required. Two hundred and forty man-hours are allocated, Reference 9, for depot repair on the titanium hub. Using the parts comparison analysis of Table 27, depot repair of the composite hub is estimated to require an average of 310 man-hours. Due to the nature of composite repairs, it may be possible to perform some major hub repairs at the intermediate maintenance level rather than depot. An extensive maintenance repair study would be required to assess these factors.

Composite structure introduces additional inherent failure modes not displayed by titanium, such as bond separation, edge and interlaminar delamination. The current design philosophy of the composite hub indicates that bond separations are not critical since mechanical fasteners are used for primary load path elements; their secondary function is to clamp the separate hub composite components. This hardware provides compressive loads in the bond area which minimizes tendencies for bond separation. Interlaminar separations are not expected to be critical because the multidirectional buildup of the composite components carries loads around fault areas without critical consequences. Propagation of surface delamination will eventually appear as surface buckling or cracking, which is visually evident and detected by inspection, although this could be masked slightly by the radar/lightning coatings. Based on this qualitative analysis, it is anticipated that no special inspection of the mature composite hub will be required in the field other than the standard preflight, 10-hour,

and 500-hour visual inspection except for a 500-hour coin tap inspection followed by an ultrasonic pulse echo inspection of any questionable areas. Further stress analysis and full-scale tests would be required to confirm this tentative conclusion. To verify the integrity of major structural repairs made at depot, nondestructive inspection techniques will be required. This would include ultrasonic and/or radiographic equipment, both of which are generally available at the depot level.

The results of the R&M assessment are summarized below:

Reliability Assessment

- The composite hub/extender installation improves overall aircraft reliability.
- Low-energy damage tolerance of the composite hub is expected to be equivalent to that of the titanium hub.
- The composite hub is projected to be less tolerant of high-energy impacts than the titanium hub.

Maintainability Assessment

- The on-aircraft remove and replace time of the composite hub/extender installation is equivalent to that of the titanium hub/extender installation.
- Time required to separate hub from the extender is estimated to be slightly less for the composite hub design.
- Composite materials require longer maintenance repair times on the average than does titanium.
- It is anticipated that the composite hub will require no inspections in the field beyond the visual types of checks made at the same scheduled intervals as the existing titanium hub, except for a 500-hour coin tap inspection.
- The composite hub is expected to be more repairable in the field than the titanium hub.

Radar Cross Section

In many respects the bare, uncoated, composite hub is similar, from a radar cross section standpoint, to the production UH-60A titanium hub. A majority of the components on the hub are similar or identical to those on the BLACK HAWK. These are the shaft extension, blade dampers, control horn, pushrods, and bifilar weights. These components are mounted at the same location on the hub and at the same relative location with respect to one another. Therefore the direct specular energy returned from these components will be the same.

Although there is a great deal of similarity between the composite and the titanium hub designs there are differences also. One substantial difference is the addition of the top and bottom composite plates. The edges of the plates are curved to minimize the energy return. This avoids the specular energy return of high peak values associated with flat surfaces as exist on the edge of the current bifilar. These surfaces are important because they are essentially perpendicular to incident radar energy radiated close to the horizontal plane, which is the major threat for a low-flying helicopter. The avoidance of these peak spikes by shaping is important at the high frequencies of typical hostile fire control radars. By changing shape from a flat surface to a curved one, the returned energy is significantly reduced.

Areas of concern relative to low-level spiked specular reflection are the cavity type reflectors created by the damper bracket and the corner reflector created by the juncture of the top and bottom plates and the tubes. While these radar return sources are masked to perhaps 40 to 60 percent by other components such as the main rotor damper and pitch control horn, the multiple reflective surfaces need a radar absorptive material (RAM) to reduce the total reflected radar energy from these surfaces.

It is recognized that a second order traveling (or creeping) wave will be generated by the irregular planform shape of the top and bottom plates and travel along the surface. The manner in which these surface currents, resulting from the creeping or traveling wave components, interact with the contributions from the other regular (largely cylindrical) shaped contributions is difficult to predict and therefore is generally evaluated experimentally.

The areas requiring the RAM are shown in Figure 30.

Since the RAM is not easily removed if bonded directly to the hub it is applied with a "peel-ply" layer between it and the hub. This permits easy removal for inspection and repair purposes. Peel ply is acceptable here because of the relatively low strains which exist in the hub. For each hub the RAM is estimated to cost $100 and weigh 7 pounds.

Lightning Protection

The design requirement for lightning is that the hub be capable of withstanding a 200,000 amp surge followed by a 200 amp flow for a 2-second duration. Direct strikes to the hub can hit any portion of the top plate. An aluminum wire fabric, 200 x 200 mesh, covering the upper surface and edges provides adequate protection. This mesh is bonded over the fiberglass which provides protection to the graphite/epoxy (see Figure 28). Film adhesive is used to bond the mesh to the hub. A layer of cured adhesive 0.010 inch thick is permitted on the outer surface of the mesh. At the edges of the top plate, the mesh is sandwiched between the fiberglass and the 0.040-inch-thick radar absorbing film.

Current flows from the mesh to the shaft by arcing between the mesh and the upper bolt ring of the shaft extension. An alternate path exists through the bolts. Current can also enter the hub from a blade. For this current path, a lightning arc plate is provided (see Figures 28 and 29). This plate is bolted to a bracket that is connected to the shaft via the main bolts. The arc plate is located at the inboard end of the elastomeric bearing. The lightning arc plate is basically a bracket consisting of a portion of a sphere which remains in contact with, or close to, the upper portion of the spindle nut. Attributes of this system are not only low cost and weight but it is maintenance free and does not impede inspection or removal of the elastomeric bearing.

Weight Summary

The weight of each item making up an assembly is summarized on Sheet 2 of the hub drawings. This parts list is duplicated in Table 30. The data is categorized in Table 31 in a manner which permits a direct comparison with the metal hub. A comparison of the basic hub weights above is not meaningful since they do not represent similar systems. The smallest comparable system includes the basic hub, the bolts, and the bifilar assembly. On this type of a basis, the composite hub results in a 33.8-pound or 17-percent weight savings. A comparison of the total system shows that there is a reduction of 52.1 pounds or 17 percent as compared to the

TABLE 30. PARTS LIST FOR THE COMPOSITE HUB

PART NO.	DESCRIPTION	NUMBER REQ'D		MAT'L	WEIGHT (LB)
		PER ASS'Y.	PER HUB		
041	Hub Ass'y.	-	1		254.42
042	Top Plate	1	1		21.51
201	Graphite Plate	1	-	Graphite	17.49
202	Shims	1	-	Stainless	
203	"	1	-	"	
204	"	1	-	"	3.66
205	"	1	-	"	
206	Bushing	4	-	"	.12
207	"	8	-	"	.23
043	Bracket Ass'y.	-	4	-	6.62
301	Bracket	1	-	Titanium	6.33
302	Insert	2	-	Stainless	.29
044	Bottom Plate	-	1	-	22.91
401	Graphite Plate	1	-	Graphite	19.76
402	Shims	1	-	Stainless	
403	"	1	-	"	
404	"	1	-	"	2.78
405	"	1	-	"	
406	Bushing	8	-	"	.24
407	"	4	-	"	.12
045	Tube	-	4	-	38.41
501	Graphite Tube	1	-	Graphite	34.04
502	Shims	1	-	Stainless	
503	"	1	-	"	
504	"	1	-	"	3.89
505	"	1	-	"	
506	Bushing	4	-	"	.48
046	Bearing Adapter	-	4	-	39.36
601	Adapter	1	-	Ti	37.68
602	Insert	4	-	Stainless	.48
603	"	2	-	"	.24
604	"	8	-	"	.96

TABLE 30. PARTS LIST FOR THE COMPOSITE HUB (Cont'd)

PART NO.	DESCRIPTION	NUMBER REQ'D		MAT'L	WEIGHT (LB)
		PER ASS'Y.	PER HUB		
101	Bifilar Bushing	2	4	Stainless	3.84
102	Bifilar Plate	1	4	Titanium	6.51
103	Damper Bracket	1	4	Aluminum	14.64
104	3/4" Nut & Bolt	1	4	Titanium	3.54
105	3/4" Nut & Bolt	-	8	"	.50
106	3/4" Nut & Bolt	-	16	"	3.15
107	1" Nut & Bolt	-	8	"	3.01
108	3/4" Bolt	-	16	"	2.58
109	3/4" Bolt	-	8	"	1.06
110	1" Bolt	-	16	Stainless	13.14
111	Cover Plate	-	1	Aluminum	.24
112	1/4" Screws - Cover Plate	-	8	Stainless	.10
113	Lightning Mesh	1	1	Aluminum	.02
114	Arc Plate	1	4	"	.28
047	Shaft Extension	-	1	-	73.00
701	Shaft	-	1	Titanium	72.75
702	Inserts	-	8	Stainless	.25

TABLE 31. WEIGHT SUMMARY

	WEIGHT (LB) TITANIUM	COMPOSITE
Basic Hub	148.	128.8
Misc. Inserts & Bolts & Cover Plate	18.6	24.8
Shaft Extension	75.	73.
Cone & Pressure Plate	13.	-
Damper Bracket & Bolts	21.5	18.2
Bifilar Assembly	31.2	10.4
TOTAL:	307.3	255.2

Target 15% Reduction

Target Weight = 261.2#

metal hub. Sizeable reductions in weight were achieved by integrating the bifilar support with the upper plate and by simplifying the shaft extension and eliminating the cone and pressure plate. If weight of the radar-absorbing film is included, the weight saved is reduced to 46.1 pounds, which meets the 15 percent weight reduction goal.

Cost and Producibility Estimates

This section includes a discussion of production costs, development costs, acquisition costs, and finally the 20-year life-cycle cost.

Production Costs

The average cost of the 400th titanium hub was presented in Table 17. The elastomeric bearing end plates were excluded from the present comparison since they were not altered. Therefore, the cost of the titanium hub is \$38,750 -\$5,040 = \$33,710. Assembly of these components and the cost of fasteners increase the cost to \$34,500. This production cost is reflected on the learning curve shown in Figure 34. There is little learning on this type of metal hub after the 150th unit; hence, the nearly flat curve shape. Projecting backwards from the 150th unit, using a 92 percent learning curve, the cost of any lesser quantity can be obtained.

A similar approach is used for the composite hub. The learning is assumed to continue up to the 400th unit and it follows an 85 percent learning curve. A detailed labor-material breakdown is presented in Table 32. This shows that the average cost on a full production basis is \$23,500. This represents a 10 percent profit added to the manufacturing cost which was burdened by 18 percent for G & A. Expressing this mathematically, the cost is

$$C = (H \times LR + M)\ (1.18)\ (1.10)$$

where

C = fully burdened cost

H = labor hours

LR= labor rate = \$23.90/hour

M = material costs

TABLE 32. PRODUCTION COST BREAKDOWN FOR THE COMPOSITE HUB

STAGE 1: COMPONENT COSTS

ITEM	LABOR (HOURS)	MATL. (DOLLARS)
Top Plate -042		
-201 cut prepreg 25 lbs @ $50/lb	1	1250
-202 -205 shims	4	100
Laminate- 12 hrs layup, 4 hrs preparation	16	100
Press mold	4	
Rough machine	2	
Install bushings	2	30
Subtotal/Hub (1 required)	29	1480
Bottom Plate -044		
Same as-042		
Subtotal/Hub (1 required)	29	1480
Tubular Arms -045		
-401 - filament wind 13 lbs @ $35/lb	2	455
-502 -505 shims	1	25
Rough machine	2	
Subtotal/Arm	5	480
Subtotal/Hub (4 required)	20	1920
Attachment Bracket - 043		
-301 Cut	0.4	15
-302 Install inserts	0.1	5
Subtotal/Bracket	0.5	20
Subtotal/Hub (4 required)	2.0	80

ITEM	LABOR (HOURS)	MATL. (DOLLARS)
Bearing Adapter -046		
-601 Titanium, machining	4.5	200
-602 inserts	.5	25
Subtotal/Adapter	5.0	225
Subtotal/Hub (4 required)	20.0	900
Shaft Extension -047		
-701 Titanium, machining	29.0	1625
-702 inserts	1.0	25
Subtotal/Hub (1 required)	30.0	1650
Bifilar Bushing -101		
-101 stainless steel, machining	1.0	5
Subtotal/Hub (8 required)	8.0	40
Bifilar Plate -102		
-102 Titanium, machining	1.5	5
Subtotal/Hub (4 required)	6.0	20
Damper Bracket -103		
-103 Aluminum, machining	3.0	30
Subtotal/Hub (4 required)	12.0	120
Fasteners		
Mostly Titanium 20.9 lbs @ $70/lb	-	1461
Inspection of Components	40	-
Subtotal - Stage 1	196	9151

STAGE 2: ASSEMBLY COSTS

ITEM	LABOR (HOURS)	MATL. (DOLLARS)
Assemble S-048		
Bond 113, 101, 102 to 042 Bonding, preparation and cleanup	4	50
Assemble S-049		
Attach 045's to 046's Bond and bolt	36	100
Assemble S-050		
Bond S-049's to S-048 and 044	27	100
Machine S-050		
Face-off, drill and top the 046 adapters, inspect	40	-
Assemble S-051		
Mount 103 dampers & shims	12	80
Attach to Shaft		
Mount S-051 on 047	10	100
Subtotal Stage 2	129	430
Total - Stage 1 & Stage 2	325	9581

Cost = $\left[(325 \times 23.90) + 9581\right]$ (1.18) (1.10) = $22,518

The crossover point (see Figure 34) occurs at the 40th hub, and from then on the composite hub is less expensive to produce. The production cost for any quantity of hubs can be read directly from Figure 34. The cost in 1978 dollars for several specific quantities is given in Table 33. As is evident from the data there is a substantial reduction in production cost for a composite hub as compared to a titanium one for large quantities.

Development Costs

The nonrecurring costs fall into two categories: tooling and general engineering development costs. The tooling costs amount to $266,500. The details are presented in Table 34. The development costs in 1978 dollars are approximately 3.8×10^6 and span a four-year time period.

A detailed breakdown of each phase is given in Table 35. $1,000K is allocated in Phase I over a 2-year period for engineering development which includes detailed design, a static test of a prototype hub and a development program aimed at improving the damage tolerance without degrading inspectability. Phase II is basically directed toward risk reduction. It covers ballistic tests and fatigue tests, and includes a 25-hour flight test program. Phase II is scheduled for 1981 and requires the expenditure of approximately $2,163K. The third phase consists of a one-year service evaluation and is primarily concerned with obtaining R & M data. Finally, in 1983 production can begin. This development timeframe is felt to be somewhat optimistic because no time was allotted for contingencies. This development cost data was used in the following sections which discuss the acquisition costs and the life-cycle costs.

Acquisition Costs

The acquisition costs are the average production cost plus the amortized development cost. According to the BLACK HAWK production schedule, as of the beginning of 1983, 613 A/C remain to be produced. From the learning curve estimates, the average production cost of a co[illegible] hub is $22,300. The amortized development costs are $\frac{\$3,[illegible]}{613 \text{ hubs}}$ = $6,247/hub. Therefore, the total acquisition costs are $6,247 + $22,300 = $28,547. This represents a cost savings of 17 percent or approximately $5,900 as compared to the titanium hub.

TABLE 33. PRODUCTION COST COMPARISONS FOR THE TITANIUM AND COMPOSITE HUBS

NUMBER OF HUBS	1978 DOLLARS	
	COMPOSITE	TITANIUM
50	38K	39K
100	32	36
500	22	34
1000	21	33
5000	20	32

TABLE 34.

Tooling Costs for the Composite Hub

	$ Fabr./Mat'l.
Upper Plate Mold (Matched Die) including templates, models, etc.	60,000
Upper Plate Lay-Up Tooling	6,000
Lower Plate Lay-Up Tooling	60,000
Coke Bottle Mandrels (20 pcs.)	15,000
Coke Bottle Winding Tools	-
Dies for Shims	3,000
Tooling for Detail Sheet Metal Parts - Bifilar Shims + Damper Bracket	5,000
Assembly Bonding Fixture (including templates, models, etc.)	50,000
Transportation Dollies	4,500
Machining Tools	57,000
TOTAL	$266,500

Capital Equipment

(1)	Plates Press 5 ft. X 10 ft. Heated Platen at 400 psi = 1500	= $600K
(2)	Bottle Winding Machine	= $ 50K

TABLE 35. DEVELOPMENT COST BREAKDOWN

PHASE	COST $1000	YEAR 79	80	81	82	83 - 87
I. Eng. Development		▬	▬			
A. Detail Design	400	—				
B. Prototype Hub	400		—			
C. Inspection Development	200		—			
II. Risk Reduction				▬		
A. Ballistic Test	60			-		
B. Head & Shaft Tests	400			—		
C. Whirl Stand	300			—		
D. 25 Hr. Flight	600			—		
E. Fatigue Substantiation	800			—		
F. Cost Verification	3				-	
G. Order Tooling	270				-	
III. Service Evaluation					▬	
A. Obtain R & M Data	400				—	
B. Cost Verification	3					-
IV. Production						▬

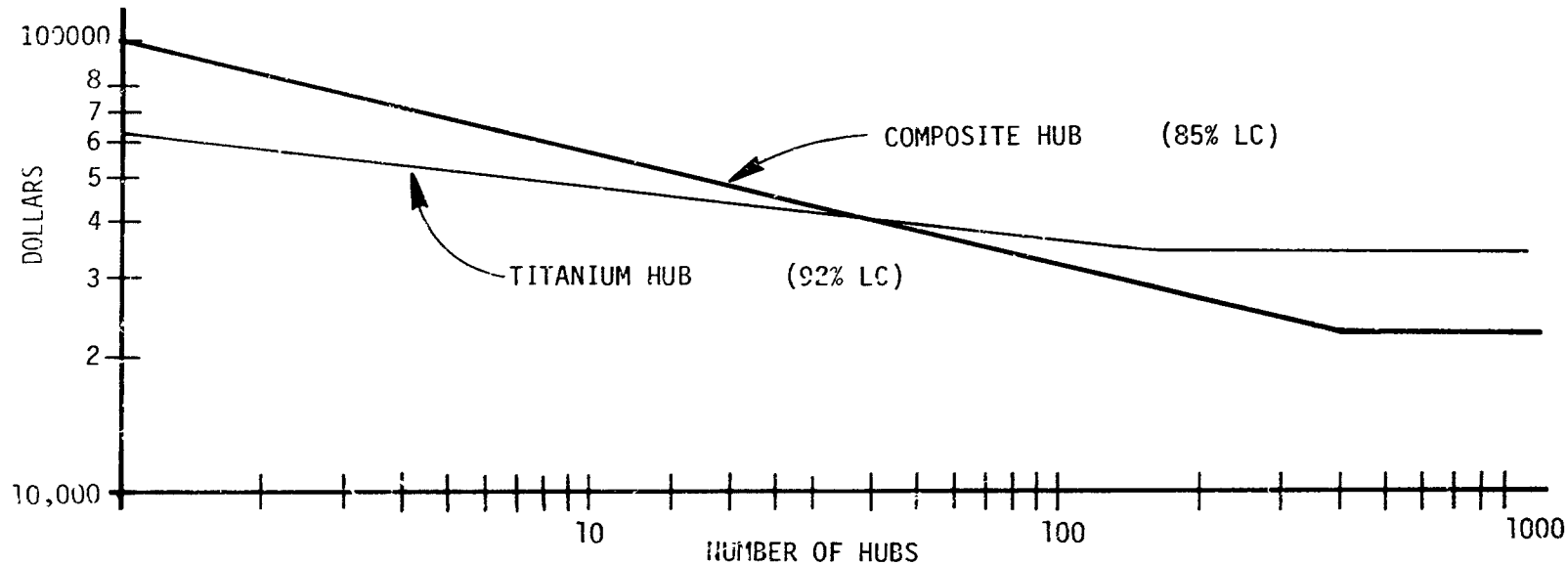

FIGURE 34. AVERAGE CUMULATIVE COSTS FOR A UH-60A ROTOR HUB

Life-Cycle Costs

A differential life-cycle cost between the composite hub and the titanium hub was estimated for a 20-year time span starting October 1977. The development costs presented earlier were spread out as an average monthly cost for each phase of the development program. Field and depot labor rates were assumed to be $15/hour and $24/hour respectively. It was assumed that the composite hub would be fully developed and incorporated into production in January 1983, which is consistent with the development plan described earlier. It was also assumed that none of the A/C produced prior to January 1983 would be retrofitted with a composite hub. This decision was made because it would have been costly to replace the titanium hubs, which have an unlimited life and lower overall maintenance costs, with composite hubs. The hub costs were taken from the learning curve estimated (in 1978 dollars) and were adjusted to reflect a 6 percent/year inflation rate. Aside from these basic costs, the primary differences between the hubs are mean time between repairs, cost of material for repair, and man-hours to repair. The rationale used to achieve these estimates was presented in the R & M section. The data used is presented below:

Item	Titanium Hub	Composite Hub
MTBR (hr)	1,370	1,515
Man-hours to Repair (hr)	155	278
Cost of Materials to Repair ($)	36	148
Man-hours to Replace in Field (hr)	6	7.5

The analysis indicated that over a 20-year life cycle, the cost saved by utilizing a composite hub was $691K In addition, a sensitivity analysis was performed varying the hub introduction time. This data is presented in Figure 35 and indicates that small delays in the introduction time could quickly eliminate the cost savings.

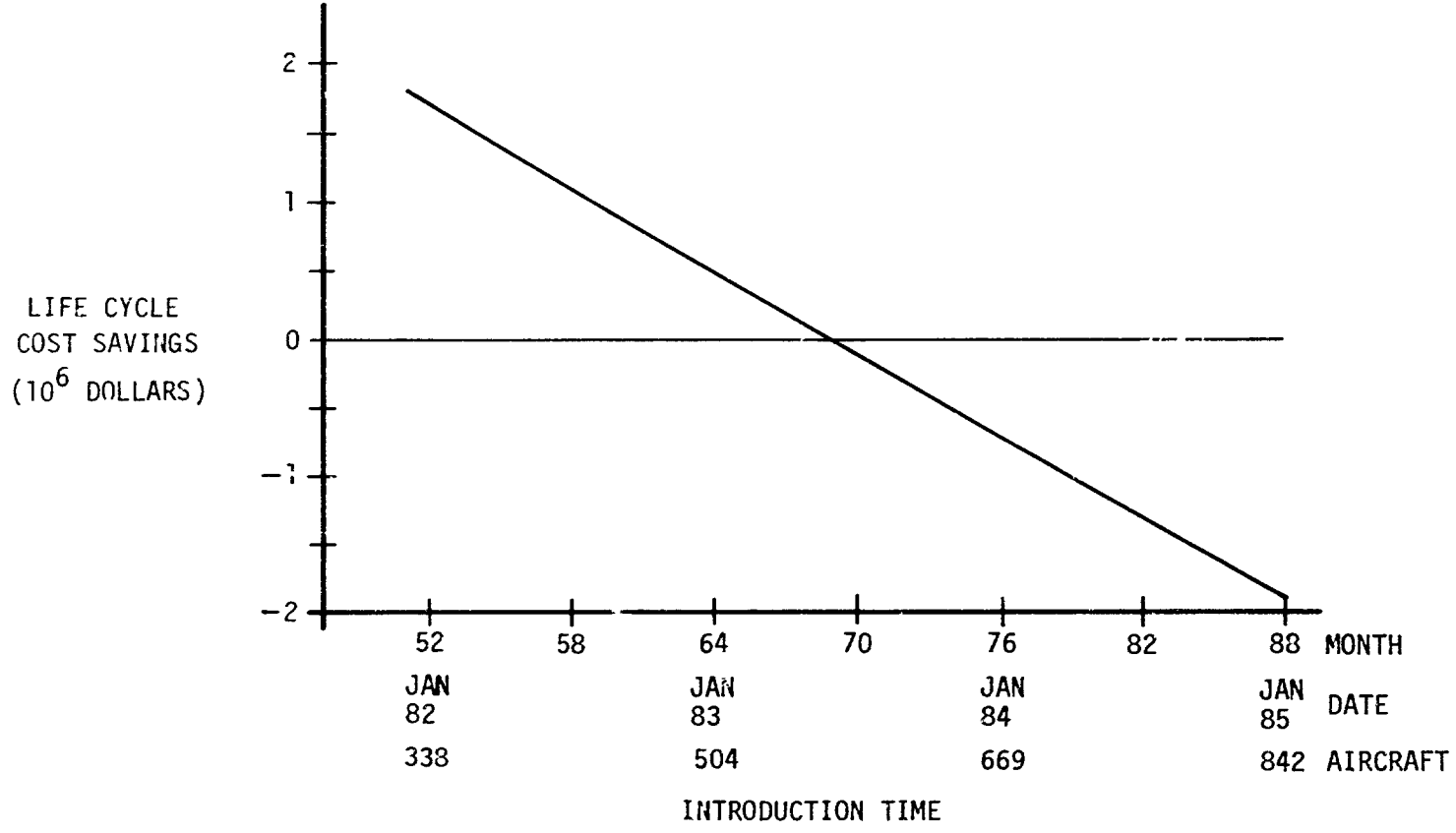

FIGURE 35. LIFE CYCLE COST VERSUS INTRODUCTION TIME

V. CONCLUSIONS AND RECOMMENTATIONS

The attributes of the composite hub are qualitatively summarized in Table 36. The table indicates that there are two fundamental advantages, cost and weight. Structural adequacy, ballistic survivability, and adequate lightning protection are basic requirements of the hub and since the composite hub meets these but offers no substantial improvement in these areas, they cannot be listed as advantages.

Reduced radar cross section would be classified as an advantage if it were not for the fact that it was achieved by using a radar absorbing film which would provide similar benefits if applied to the present metal hub. The reliability, maintainability, and damage tolerance characteristics of the hub are reflected in life-cycle costs so they are not independent advantages.

The 45-pound weight reduction in the rotating system is significant and can be reflected in increased payload, speed, range, etc., or conversely, reduced fuel costs.

The remaining basic advantage is reduced cost. There were sizeable reductions in production and acquisition costs but only a small reduction in life-cycle costs. None of the cost savings was attributed to the reduced weight.

The life-cycle costs were greatly influenced by introduction time and by the size of the "production buy". It was found that even a six-month delay in a composite hub development effort would negate its financial benefits for the current BLACK HAWK program. Conversely, a larger production buy after the composite hub development effort would increase the financial benefits.

The large reduction in production and acquisition costs implies that a composite hub is potentially very competitive with a metal one,especially on a new aircraft. But before being seriously considered for any highly maneuverable military aircraft a composite hub must be thoroughly evaluated through a flight demonstration program. For this reason a composite hub development effort of limited scope should be undertaken. It would provide the background for the use of a composite hub on a "growth version" of an existing helicopter, or a new generation helicopter, or provide an alternative if a shortage of titanium ever arises.

TABLE 36.

SUMMARY OF ATTRIBUTES

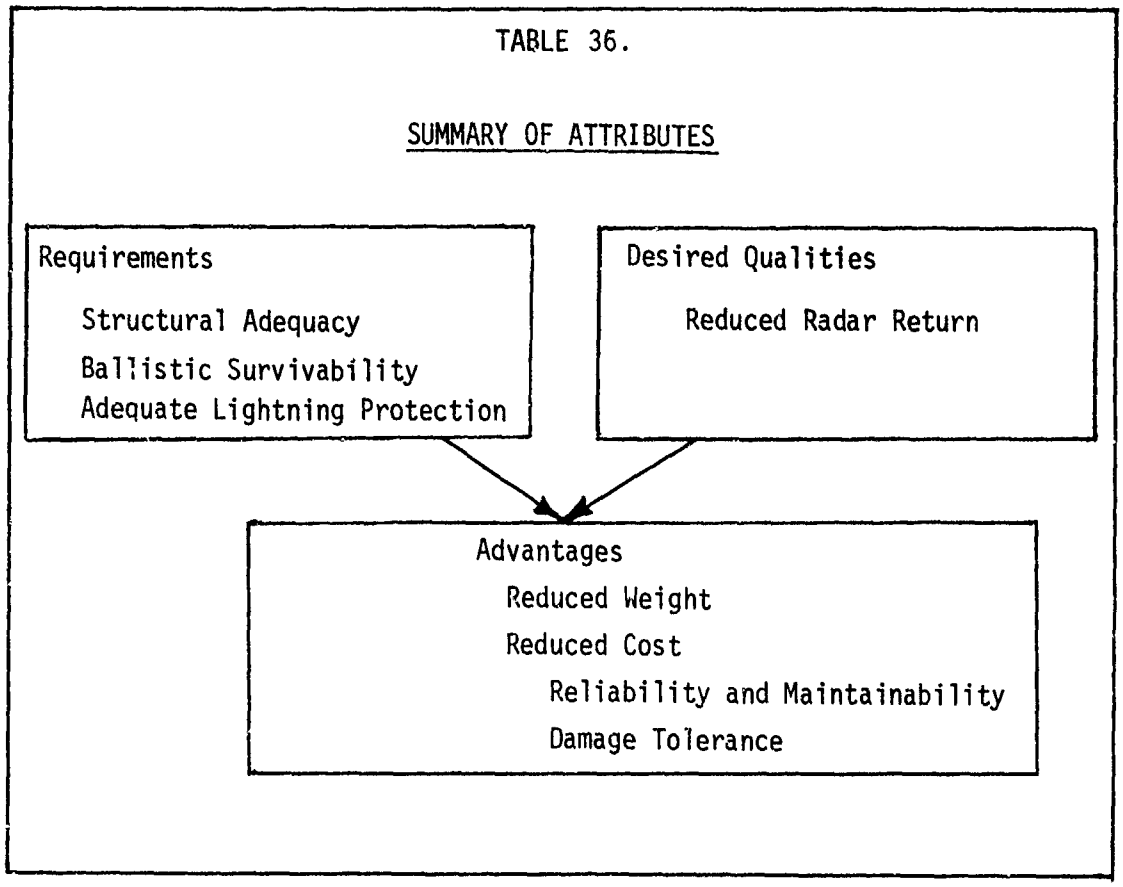

REFERENCES

1. "Main Rotor Head Structural Analysis, UH-60A", SER-70514, Sikorsky Aircraft

2. "Main Rotor Head Loads, CH-53A", SER-65046, Sikorsky Aircraft

3. UH-60A Prime Item Development Specification, November 1, 1976, Contract No. DAAJ01-77-C-000L (P6A)

4. Sikorsky Aircraft Structures Manual

5. "Advanced Composites Design Guide", Rockwell International - Loss Angeles Aircraft Division, Contract No. F33615-71-C-1362, January 1973

6. "Fatigue Properties and Analysis", SER-50586, Sikorsky Aircraft April 1969

7. "Tolerance of Advanced Composites to Ballistic Damage", E. F. Olster and P.A. Roy, ASTM STP546, American Society for Testing and Materials, Philadelphia, Penna., 1973

8. "Foreign Object Impact Damage to Composites", STP 568, American Society for Testing and Materials, January 1975

9. "Service/Maintainability of Advanced Composite Structures", J. D. Labor, Northrop Corp., Contract No. F33615-76-C-3142

10. UH-60A Maintainability Prediction Report, SER-70597, June 10, 1977

11. Navy 3M, SH-3D data, January through December 1975

APPENDIX A. STRESS ANALYSIS

I. Concept Configuration

The hub consists of two plates separated by tubular shear webs. The bifilar is integral with the top plate and, except for four cutouts for the pushrod bearings, is basically flat and circular. The bottom plate is essentially flat and has a square planform shape. The tubular shear webs are structurally tied to the upper and lower plates by bolted and bonded joints. For additional redundancy the tubes are bolted to the shaft extender.

II. Description of the NASTRAN Model

The finite element model shown in Figure A-1 was used to determine deflections, load paths, and stress levels. The model consists of 0.4-inch-thick plate elements (Quad 1 and Tria 1) having material properties consistent with an $(0^{\circ}_2 \pm 45^{\circ})_{sym}$ layup of Type A-S graphite epoxy. Both the plates and the inboard end of the tubes are bolted to the titanium shaft extension. These bolts are tied rigidly to the ground. This represents a completely rigid shaft extension which maximizes the bolt loads and hence is a conservative assumption.

The tubes are bolted and bonded to the upper and lower plates. The connections are represented in the NASTRAN Model by rigid body elements (RBE2) which insure displacement compatibility between appropriate grid points on the hub.

The elastomeric bearing loads are represented by a series of rod elements emanating from the center of the pitch/flap hinge to the periphery of the tube. At the outboard end of each tube is a titanium bearing adapter.

III. Stress Analysis

A stress analysis is presented for the limit and design flight loads. The deflection can be characterized by the displacement of the load application points in each arm (Grid Points 91, 92, 93 and 94). The results are summarized in Table A-1. The axial stress distribution for each loading condition is given in Figures A-2 to A-10.

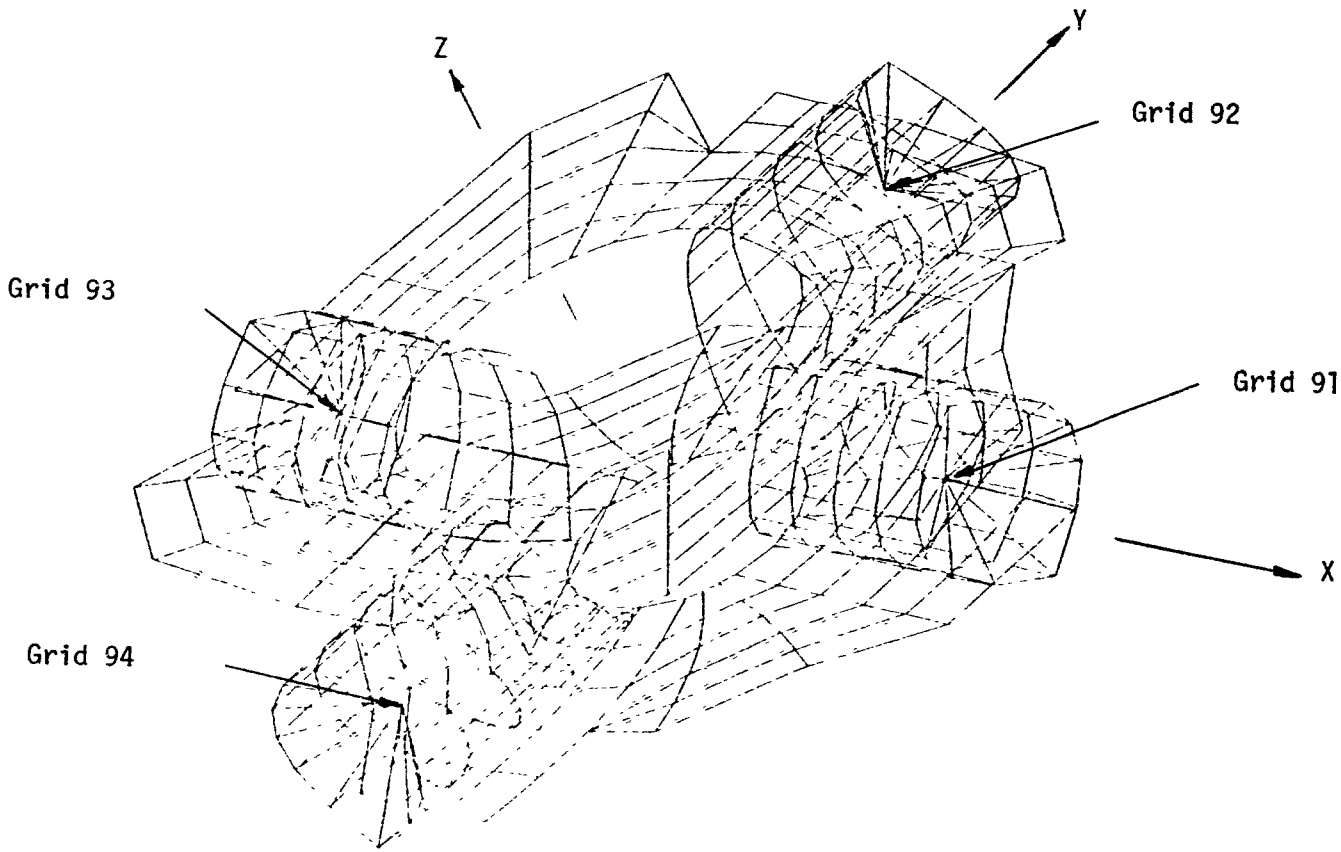

FIGURE A-1. NASTRAN FINITE ELEMENT MODEL FOR THE COMPOSITE HUB

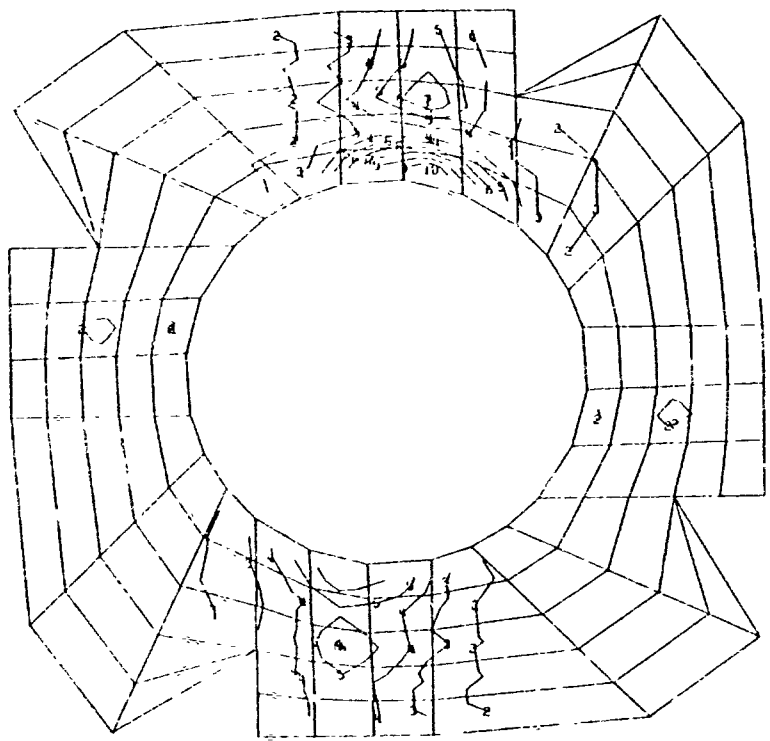

FIGURE A-2. AXIAL STRESS DISTRIBUTION IN THE TOP PLATE FOR THE LIMIT LOAD CONDITION

KEY

10 = f_{max} = 9584 psi

1 = f_{min} = -210 psi

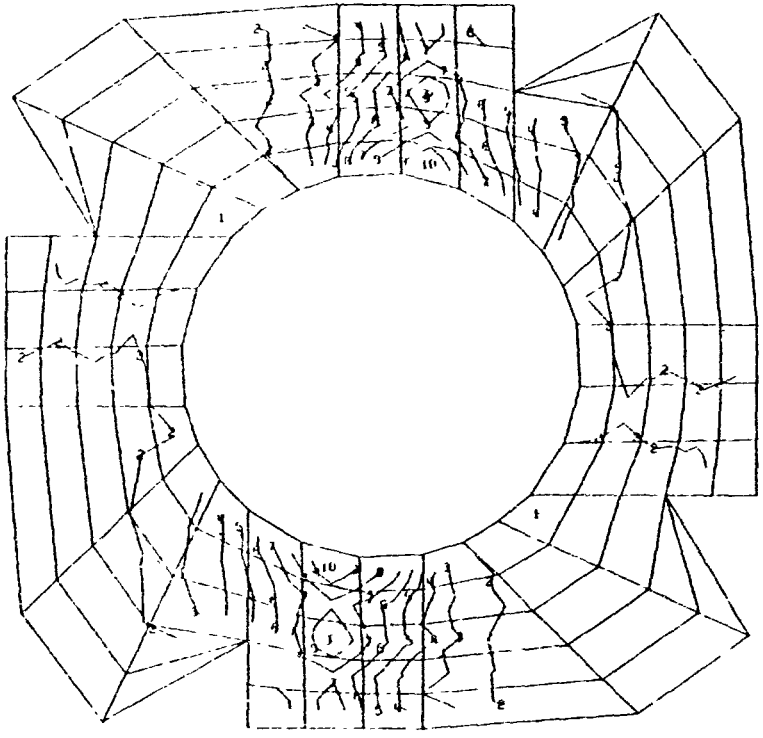

FIGURE A-3. AXIAL STRESS DISTRIBUTION IN THE TOP PLATE FOR THE STEADY COMPONENT OF THE FLIGHT LOADS

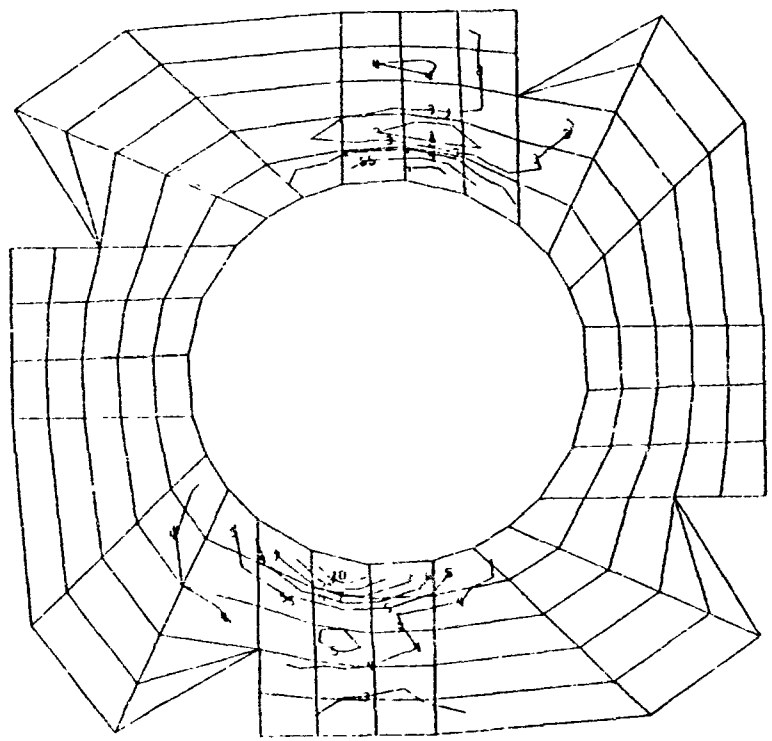

FIGURE A-4. AXIAL STRESS DISTRIBUTION IN THE TOP PLATE FOR THE VIBRATORY COMPONENT OF THE FLIGHT LOADS

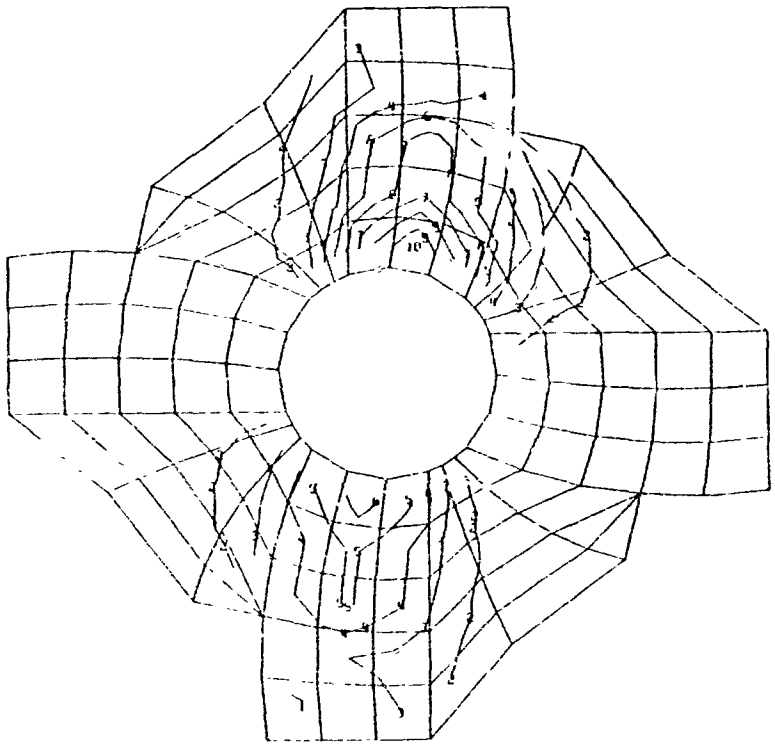

FIGURE A-5. AXIAL STRESS DISTRIBUTION IN THE BOTTOM PLATE FOR THE LIMIT LOAD CONDITION

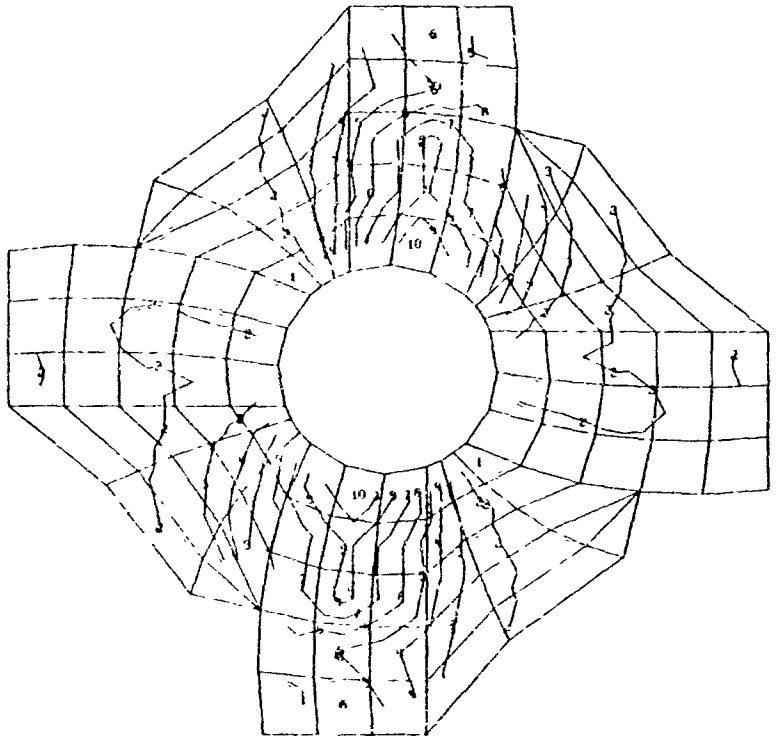

FIGURE A-6. AXIAL STRESS DISTRIBUTION IN THE BOTTOM PLATE FOR THE STEADY COMPONENT OF THE FLIGHT LOADS

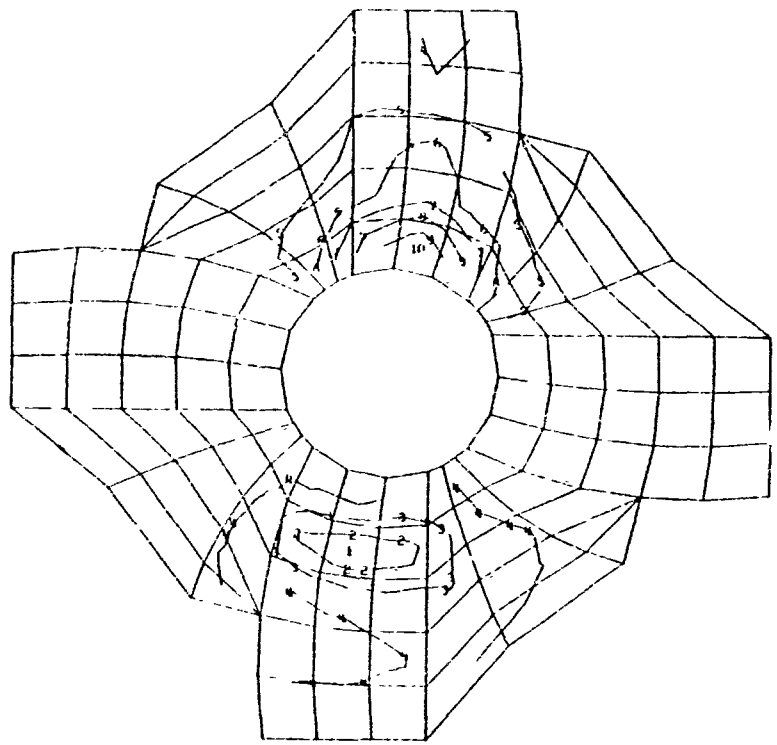

KEY

10 = f_{max} = 3320 psi

1 = f_{min} = -1740 psi

FIGURE A-7. AXIAL STRESS DISTRIBUTION IN THE BOTTOM PLATE FOR THE VIBRATORY COMPONENT OF THE FLIGHT LOADS

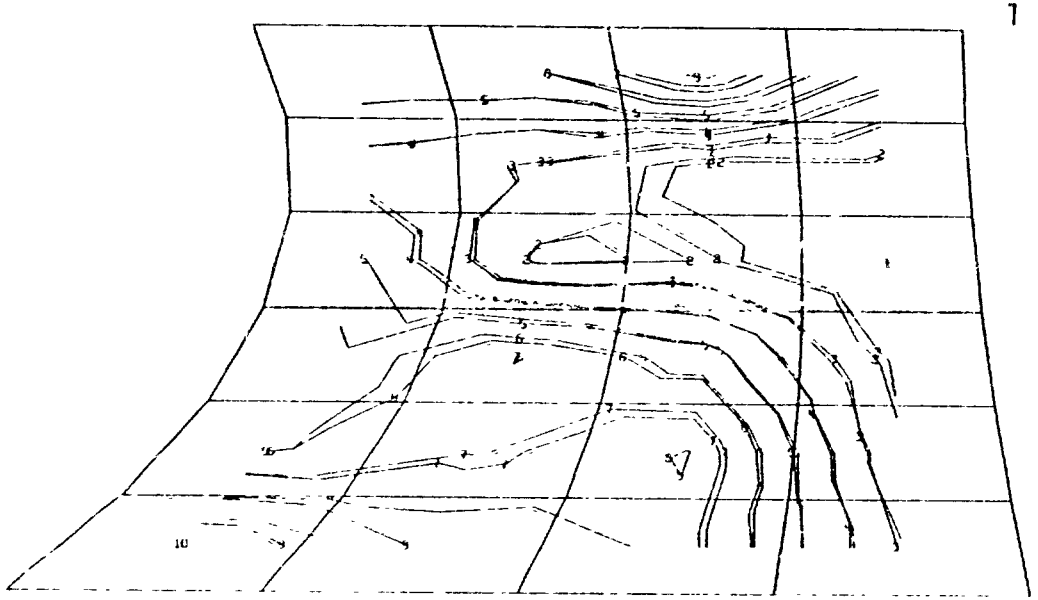

FIGURE A-8. AXIAL STRESS DISTRIBUTION IN THE TUBE FOR THE LIMIT LOAD CONDITION

KEY

10 = f_{max} = 7510 psi

1 = f_{min} = 480 psi

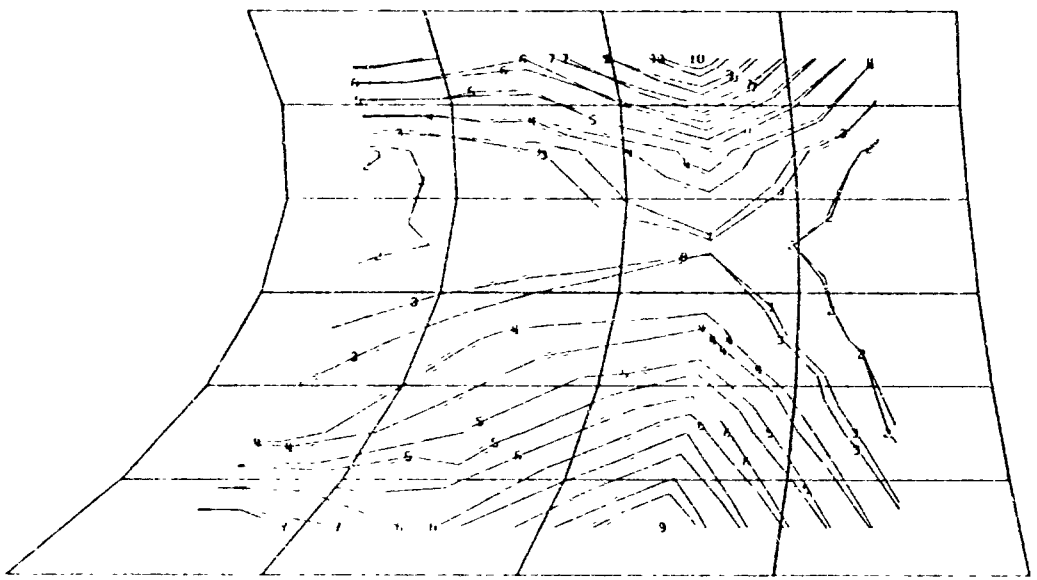

FIGURE A-9. AXIAL STRESS DISTRIBUTION IN THE TUBE FOR THE STEADY COMPONENT OF THE FLIGHT LOADS

KEY

10 = f_{max} = 2489 psi

1 = f_{min} = -980 psi

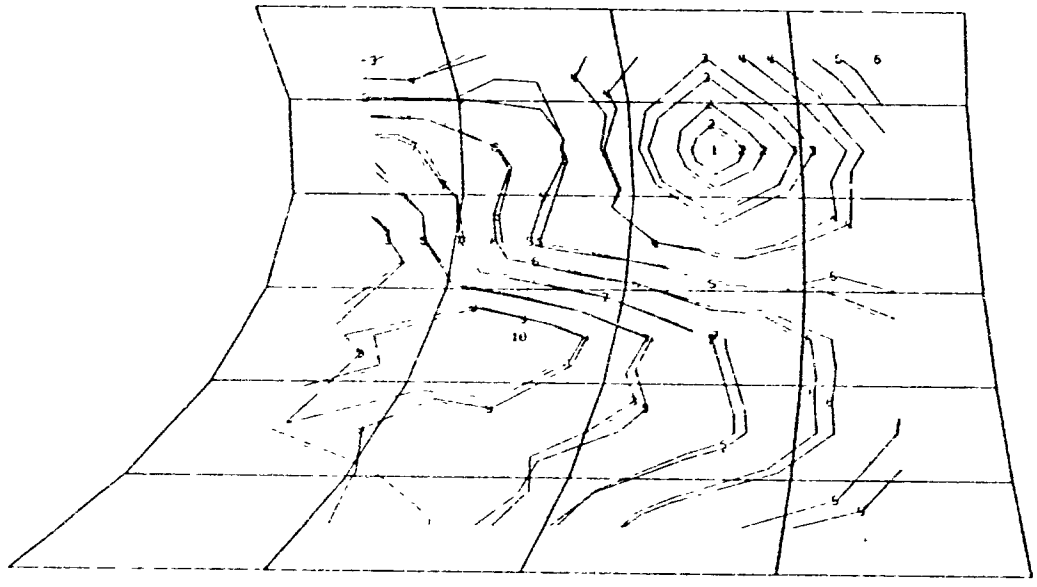

FIGURE A-10. AXIAL STRESS DISTRIBUTION IN THE TUBE FOR THE VIBRATORY COMPONENT OF THE FLIGHT LOADS

TABLE A-1. DEFORMATION FOR SPECIFIC LOADING CONDITIONS

LOAD DESCRIPTION	GRID NO.	DISPLACEMENT X 10^4 in		
		X	Y	Z
Four Times C_F Load Case 500	91	1243	-118	45
	92	118	1243	45
	93	-1243	118	45
	94	- 118	-1243	45
Limit Load Load Case 501	91	485	13	950
	92	-14	481	316
	93	-482	-18	343
	94	19	-481	316
Steady Flight Load Load Case 502	91	316	-58	151
	92	58	316	151
	93	-316	58	151
	94	-58	-316	151
Vibratory Flight Load Load Case 503	91	-15	19	172
	92	1	17	1
	93	17	18	-173
	94	1	-16	0

A. Analysis of the Top Plate

1. Basic Plate Strength

a. Limit Load Analysis

The critical region is located close to the attachment ring (see Figure A-2). The only significant stress is fx.

$fx = 24,400$ psi

$F_{Tu} = 87,500$ psi (Ref. 5, 1.2.1 (28) @ $165^{o}F$)

$$MS_{Axial} = \frac{87,500}{1.5(24,400)} - 1 = 1.38$$

b. Flight Load Analysis

The peak stresses occur close to the attachment rings (see Figures A-3 and A-4). Assuming that the stresses are in phase,

$fx = 9584 \pm 4399$ psi

$Fx_{Vib} = 28,000$ psi (Ref. Figure 11)

$K_E = .94$ = environmental effects

$$MS_{Axial} = \frac{.7(28,000)(.94)}{4399} - 1 = 3.2$$

2. Attachment to Shaft

a. Limit Load Analysis

The peak bolt load is the sum of the restraint forces (SPC Forces). From both nodes of the most highly loaded element (Grid Points 150100 and 150200),

$P = 16,636$ lbs.

The attachment region consists of 0.400 inch of $(0_2 \pm 45)$ GR/EP plus 0.160 inch of 17.7 PH stainless steel laminate. With bushing hole diameter = 1.3 inches,

Check Tension

$p^{tu} = .4\ A^{ns}\ F^{tu}$ *

$p^{tu} = .4x(2.88 \times .16)(222,000)$*

$p^{tu} = 40,918$ lbs

$$MS = \frac{40,918}{1.5(16,636)} - 1 = .63$$

Check Shear Out

$p^{so} = A^{so}\ F^{so}$ *

$p^{so} = 2x(\frac{e}{d} \times D \times t)\ F^{so}$

$p^{so} = 2x(1 \times 1 \times .16)(134,000)$ *

$p^{so} = 42,880$ lbs

$$MS = \frac{42,880}{1.5(16,636)} - 1 = .71$$

Check Bearing

$p^{brg} = A^{brg}\ F^{brg}$ *

$p^{brg} = (1.3 \times .16)(288,000)$ *

$p^{brg} = 59,904$ lbs

$$MS = \frac{59,904}{1.5(16,636)} - 1 = 1.40$$

b. Fatigue Analysis

Loads are obtained in the same way as for the static case.

$P = 11,914 \pm 2903$ lbs

$f_{peak} = K(f_{gross})$

$$f_{peak} = 3 \times \frac{11,914 \pm 2903}{4.18 \times .16}$$

$f_{peak} = 53,441 \pm 13,021$ psi

*Ref. 5

F_{Vib} = 17,500 psi = .7 x 25,000 (Ref. Figure 9)

$$MS = \frac{17,500}{13,021} - 1 = +.25$$

3. Attachment to Tubes

The tubes are bonded and bolted together. This is desirable for maximum strength (see Ref. 5 Pages 1.5.4 (1), 1.3.3 (1) and 1.3.3 (6)). Because the load is shared between the bond and the bolt, the bolt shears are low.

a. Limit Load Analysis

Check Bolt Bearing

The bolt forces are obtained indirectly. The bearing force is proportional to the change in axial stress in the tube.

$$p^{brg} = (\Delta f)\ A$$

$$p^{brg} = (18,291 - 6077)\ (2.3 \times .4)$$

$$p^{brg} = 11,235 \text{ lbs}$$

$$f^{brg} = \frac{P}{A_{brg}} = \frac{11,235}{.4 \times .75}$$

$$f^{brg} = 37,451 \text{ psi}$$

F^{brg} = 100,000 psi (Ref. 5, 1.3.2(23) @ 165°F)

$$MS = \frac{100,000}{1.5(37,451)} - 1 = +.78$$

Check Net Tension

The most conservative assumption for a net tension analysis is that the stress equals the maximum observed on the plate.

$$f_{\text{net tension}} = 18,291 \text{ psi}$$

F^{nt} = 30,000 psi (Ref. 5, 1.3.2(27))

$$MS_{\text{net tension}} = \frac{30,000}{1.5(18,291)} - 1$$

$$MS_{\text{net tension}} = +.09$$

b. Fatigue Analysis

The stresses are determined in the same way as for the static case.

$P = (\Delta f)^* A$

$P_{steady} = (9662 - 7699)(2.3 \times .4)$

$P_{Vib} = (5141 - 1727)(2.3 \times .4)$

$P = 1805 \pm 3134$ lbs

Check Bearing

$$f_{brg} = \frac{P}{.4 \times .75} = 6018 \pm 11{,}196 \text{ psi}$$

$F_{brg} = 50{,}000$ psi (Ref. Fig. 12)

30% reduction due to environment

$$M^{S}_{brg} = \frac{50{,}000 \times .7 \times .7}{11{,}196} - 1 = 1.18$$

Check Net Tension

The most conservative assemption is that the peak stresses in the plate occur at the tube attachment locations.

$f = 9584 \pm 4399$ psi

$f_{peak} = (K)f = (3)f$

f_{peak} $28{,}752 \pm 13{,}197$ psi

$F_{Vib} = 28{,}000$ psi (Ref. Fig. 11)

6% reduction for environment.

$$M.S. = \frac{(.7)(28{,}000)(.94)}{13{,}197} - 1 = +.39$$

*Elements 1106, 1107

B. Analysis of the Bottom Plate

The approach taken is identical to that used for the analysis of the top plate.

1. Basic Plate Strength

a. Limit Load Analysis

From Figure A-5 the stress is:

f_x = 35,918 psi

F_{Tu} = 87,500 psi (Ref. 5, 1.22(28) @ 165°F)

$$MS_{Tension} = \frac{87,500}{1.5(35,918)} - 1 = +.59$$

b. Fatigue Analysis

Again, the most highly loaded region is close to the shaft attachment hole (see Figures A-6 and A-7).

f_x = 13,093 ± 3320 psi

F_{Vib} = 28,000 psi (Ref. Fig. 11)

6% reduction for environment.

$$MS = \frac{28,000 \times .7 \times .94}{3320} - 1 = + \text{ high}$$

2. Attachment to Shaft Extension

a. Limit Load Analysis

Because the bolt ring is smaller in diameter that in the top plate, the bolts are more closely spaced and, therefore, the bolt load is taken to be the peak SPC force.

The attachment region consists of 0.400 inch of $(0_2 \pm 45)$ GR/EP and 0.240 inch of 17.7 PH stainless steel lamina.

This analysis will include the contribution of the composite.

Check Tension

$$P^{TU} = .4(F_M^{TU} A_M^{NS} + F_C^{TU} A_C^{NS}) \text{ (Ref. 5)}$$

$A_M^{NS} = 1.06 \times .24 = .25 \text{ in}^2$

$A_C^{NS} = 1.06 \times .4 = .42 \text{ in}^2$

$P^{TU} = .4(220 \times .25 + 87.5 \times .42)$

$P^{TU} = 36{,}7 \text{ KIPS}$

$P = 15{,}951 \text{ lbs}$

$MS = \frac{36{,}700}{1.5\ (15{,}951)} - 1 = +.53$

Check Shear Out

$P^{SO} = F^{SO} \times A^{SO}$

$P^{SO} = 134{,}000 \times 2 \times 1 \times .24$

$P^{SO} = 64{,}320 \text{ lbs}$

$MS_{\text{Shear out}} = \frac{64{,}320}{1.5(15{,}951)} - 1$

$MS_{SO} = 1.69$

Check Bearing

$P^{BRG} = F^{BRG}\ A^{BRG}$

$P^{BRG} = 288{,}000\ (1.3 \times .24)$

$P^{BRG} = 89{,}856 \text{ lbs}$

$MS_{BRG} = \frac{89{,}856}{1.5(15{,}951)} - 1 = 2.76$

b. Fatigue Analysis

Following the same procedure the bolt force is:

$P = 6808 \pm 1629 \text{ lbs}$

$f_{gross} = \frac{P}{A_{gross}} = \frac{P}{2.36 \times .24}$

$f_{peak} = k\, f_{gross} = 3\, f_{gross}$

$f_{peak} = 36{,}059 \pm 8628$ psi

$F_{VIB} = 28{,}000$ psi (Ref. Fig. 9)

$$MS_{Vib} = \frac{28{,}000 \times .7}{8628} - 1 = 1.27$$

3. Attachment to the Tube

a. Limit Load Analysis

$P = \Delta f^{*} A$

$P = (6336 - 1561)\ (.4 \times 2.3)$

$P = 4393$ lbs

Check Bearing

$$f_{brg} = \frac{P}{A_{brg}} = \frac{4393}{.4 \times .75}$$

$f_{brg} = 14{,}643$ psi

$F_{brg} = 100{,}000$ psi (Ref. 5, 1.3.2(23) @ $165^{o}F$)

$$MS_{brg} = \frac{100{,}000}{1.5 \times 14{,}643} - 1 = +3.55$$

Check Net Tension

$f_{net\ tension} = 17{,}473$ psi (at element 5102)

$F^{NT} = 30{,}000$ psi (Ref. 5, 1.3.2 (27))

$$MS_{NT} = \frac{30{,}000}{1.5\ (17{,}473)} - 1 = .14$$

b. Fatigue Analysis

$P = \Delta f^{**} A$

$P_{steady} = (9086 - 5786)\ (.4 \times 2.3)$

*Stress in Elements 5103 and 5104
**Near Element 5501

$P_{VIB} = (3596 - 1469)\ (.4 \times 2.3)$

$P = 3036 \pm 1956$ lbs

Check Bearing

$$f_{brg} = \frac{P}{A_{brg}} = \frac{3036 \pm 1956}{.75 \times .4}$$

$f_{brg} = 10{,}120 \pm 6520$ psi

$F_{brg} = 50{,}000$ psi (Ref. Fig. 12)

Use 30% environmental reduction

$$MS_{brg} = \frac{50{,}000 \times .7 \times .7}{6520} - 1 = 2.05$$

Check Tension

$f_{gross} = 13{,}093 \pm 3320$ psi

$f_{peak} = k\ f\ gross = 3\ f\ gross$

$f\ peak = 39{,}279 \pm 9960$ psi

$F_{VIB} = 28{,}000$ psi (Ref. Fig. 11)

Use 6% reduction for environment

$$MS = \frac{28{,}000 \times .7 \times .94}{9960} - 1 = .84$$

C. Analysis of the Tube

1. Attachment to the Upper Ring of the Shaft Extension

The tube is bolted to the upper ring of the shaft extension with two 1-inch-diameter bolts. Since the NASTRAN Model has only one grid point to represent these two bolts, the bolt force is half of the SPC force.

The attachment region has 0.400 inch of $(0^0_2 \pm 45^o)$ GR/EP and 0.090 inch of 17.7 PH stainless steel.

a. Limit Load Analysis

P = 1/2 (13,158) = 6579 lbs (Grid Point 1003)

Check Tension

$$p^{nt} = .4\ F^{tu} \times A_{net}$$

$$p^{nt} = .4 \times 222{,}000 \times 2.88 \times .090$$

$$p^{nt} = 23{,}016 \text{ lbs}$$

$$MS = \frac{23{,}016}{1.5(6579)} - 1 = 1.33$$

Check Shear Out

$$p^{so} = F^{so}\ A^{so}$$

$$p^{so} = 134{,}000 \times 2 \times 1 \times .09$$

$$p^{so} = 24{,}120 \text{ lbs}$$

$$MS = \frac{24{,}120}{1.5(6579)} - 1 = 1.44$$

Check Bearing

$$p^{brg} = F^{brg}\ A^{brg}$$

$$p^{brg} = 288{,}000 \times 1.3 \times .090$$

$$p^{brg} = 33{,}696 \text{ lbs}$$

$$MS = \frac{33{,}696}{1.5(6579)} - 1 = 2.41$$

b. Fatigue Analysis

$P = 5043 \pm 1822$ lbs (Grid Point 1001)

$$f_{gross} = \frac{P}{A_{gross}} = \frac{P}{4.18 \times .090}$$

$$f_{peak} = 3\ f_{gross} = 40{,}215 \pm 14{,}529 \text{ psi}$$

$F_{Vib} = 28{,}000$ psi (Ref. Fig. 9)

$$MS = \frac{28{,}000 \times .7}{14{,}529} - 1 = +.35$$

2. Attachment to the Lower Ring of the Shaft Extension

The thickness and layup of the graphite epoxy is 0.400 inch and $(0^o_2 \pm 45^o)$ respectively. Reinforcement of 17.7 PH stainless steel totalling 0.090 inch is present, and the following analysis, conservatively, disregards the contribution of the GR/EP in this area.

a. Limit Load Analysis

P = 11,347 lbs (Grid Point 1011)

Check Net Tension

$$p^{nt} = .4 \left(F^{tu}_m A^n_m + F^{tu}_c A^n_c\right)$$

$$p^{nt} = .4 \left(222{,}000 \times 2.06 \times .09 + 87{,}500 \times 2.06 \times .4\right)$$

$$p^{nt} = 45{,}300 \text{ lbs}$$

$$MS = \frac{45{,}300}{1.5 \times 11{,}347} - 1 = 1.67$$

Check Shear Out

$$p^{so} = F^{so} A^{so}$$

$$p^{so} = 134{,}000 \left(2 \times 1 \times .09\right)$$

$$p^{so} = 24{,}120 \text{ lbs}$$

$$MS = \frac{24{,}120}{1.5 \times 11{,}347} - 1 = .41$$

Check Bearing

$$p^{brg} = F^{brg} A^{brg}$$

$$p^{brg} = 288{,}000 \times \left(1.3 \times .09\right)$$

$$p^{brg} = 33{,}696 \text{ lbs}$$

$$MS = \frac{33{,}696}{1.5 \times 11{,}347} - 1 = .97$$

b. Fatigue Analysis

P = 5879 $\pm$ 966 lbs (Grid Point 1013)

$$f_{gross} = \frac{P}{A_{gross}} = \frac{P}{3.36 \times .090}$$

$$f_{peak} = K f_{gross} = 3 f_{gross}$$

$$f_{peak} = 58,323 \pm 9583 \text{ psi}$$

F_{Vib} = 25,000 psi (Ref. Fig. 9)

$$MS = \frac{25,000 \times .7}{9583} - 1 = +.84$$

3. Attachment to the Plates

Both the tubes and the plates are $(0^{\circ}_2 \pm 45^{\circ})$ GR/EP and are 0.4 inch thick. The analysis of each plate considered the bolt loads and bearing stresses. The bearing stresses are identical to those in the plates and exhibit positive margins of safety. Therefore only tension stresses will be examined.

a. Limit Load Analysis

The worst case exists near a bolt hole. The peak stress occurs near the attachment to the lower lug. It is conservative to take this stress as the net stress near a hole in the tube.

f_{net} = 13,875 psi

F_{nt} = 30,000 psi (Ref. 5, 1.3.2(23))

$$MS = \frac{30,000}{1.5(13,875)} - 1 = .43$$

b. Fatigue Analysis

The peak vibratory stress occurs at element 2100.

f_{gross} = 5697 ± 2489 psi

$f_{peak} = K f_{gross} = 3 f_{gross}$

f_{peak} = 17,091 ± 7467 psi

F = 28,000 psi (Ref. Fig. 11)

Use 6% reduction for environment

$$MS = \frac{28,000 \times .7 \times .94}{7467} - 1 = 1.46$$

4. Attachment to Bearing Adapters

The bearing adapters are bonded and bolted with six 3/4-inch-diameter and two 1-inch-diameter bolts. Conservatively, the bond will be neglected. The primary load is due to C_F. The vertical shear force is included but is of much less significance.

a. Limit Load Analysis

Bolt Load = P

$$P = \frac{A_B C_F}{A_T} + \frac{Vd\ y\ D^2}{I}$$

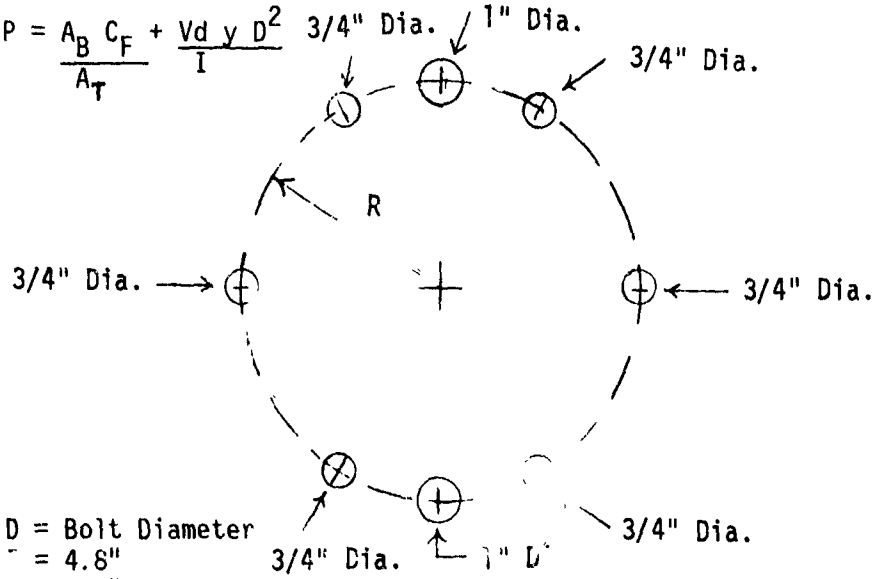

D = Bolt Diameter
= 4.8"
d = 2.0"

$I_{bolt\ pattern}$:

$$I = \frac{\pi}{4} \times 4\ (4.8 \sin 60^0)^2 \times .75^2 + 2\ (4.8)^2 \times \frac{1^2}{4} \times \pi$$

$$= 66.69\ in^4$$

$$I/y = \frac{84.96}{4.8} = 13.89\ in^3$$

$$A_B = \pi(1.0)^2$$

$$A_T = [\pi(.75^2)]\ 6 + [\pi(1.0^2)2]$$

$$P = \left(\frac{1^2}{.75^2 \times 6 + 1^2 \times 2}\right) 107{,}000 + \frac{32{,}400 \times 2 \times 1^2}{13.89}$$

$$= 30{,}031\ lbs$$

$$f_{brg} = \frac{P}{A_{brg}}$$

$A_{brg} = 1 \times (.5 + .5) = 1 \text{ in}^2$

as shared by the bottom plate and the tube

$$f_{brg} = \frac{30,031}{1} = 30,031 \text{ psi}$$

$F_{brg} = 100,000$ psi (Ref. 5, 1.3.2(23) @ 165^{o}F)

$$MS_{brg} = \frac{100,000}{1.5(30,031)} - 1 = 1.22$$

At an intermediate bolt:

$A_{brg} = .5 \times .75 = .375 \text{ in}^2$

$$P = \left[\frac{.75^2}{6 \times .75^2 + 2 \times 1^2}\right](107,000) + \frac{2,400 \times 2 \times (4.8 \sin 60^{o}) \times .75^2}{84.96}$$

$P = 12,981$ lbs

$$f_{brg} = \frac{P}{A_{brg}} = \frac{12,981}{.375} = 34,616 \text{ psi}$$

$F_{brg} = 100,000$ psi (Ref. 5, 1.3.2(23) @ 165^{o}F)

$$MS = \frac{100,000}{1.5(34,616)} - 1 = +.93$$

Check Shear Out at this Intermediate Bolt

$$f_{so} = \frac{P}{A_{so}} = \frac{12,981}{(2 \times .75) \times 2 \times .5}$$

$f_{so} = 8654$ psi

$F_{so} = 19,000$ psi (Ref. 5, 1.3.2(23))

$$MS = \frac{19,000}{1.5(8654)} - 1 = .46$$

Check Net Tension at this Intermediate Bolt

$$f_{nt} = \frac{P_{nt}}{(w - d)t}$$

$$f_{nt} = \frac{12,981}{((2\pi \times 4.8/8) - .75)(.5)}$$

$f_{nt} = 8597$ psi

$F_{nt} = 30,000$ psi (Ref. 5, 1.3.2(27))

$$MS_{nt} = \frac{30,000}{1.5(8597)} - 1 = 1.32$$

b. Flight Load Analysis

At an intermediate bolt -

$$P_{steady} \leq \frac{69,700}{8} = 8712 \text{ lbs}$$

$$P_{Vib} \leq \frac{6000 \times 2" \times (4.8 \sin 60^{0})}{84.96}$$

$P = 8712 \pm 587$ lbs

Check Bearing

$$f_{brg} = \frac{P}{A_{brg}} = \frac{8712 \pm 587}{.75 \times .5}$$

$f_{brg} = 23,232 \pm 1565$ psi

$F_{brg} = 50,000$ psi (Ref. Fig. 12)

Use 30% reduction for environment

$$MS = \frac{50,000 \times .7 \times .7}{1565} - 1 = +HIGH$$

Check Net Tension

$$f_{gross} = \frac{P}{A_{gross}}$$

$$f_{gross} = \frac{8712 \pm 587}{.5 \times 3.76} = 4634 \pm 312 \text{ psi}$$

$$f_{peak} = K f_{gross}\ 3\ f_{gross}$$

$$f_{peak} = 13{,}902 \pm 937 \text{ psi}$$

F = 28,000 psi (Ref. Fig. 11)

Use 6% reduction for environment

$$MS = \frac{28{,}000 \times .7 \times .94}{937} - 1 = +HIGH$$

D. Analysis of the Shaft Extension

1. Configuration of the Conical Section

The geometry below waterline 305 has not changed from the current production version and, therefore, it has adequate margins. The geometry of the conical region is dictated by edge distance requirements of the upper and lower plates, and the air transportability requirement for the aircraft. The wall thickness of the conical section is designed to keep the stress levels less than or equal to those in the present shaft extension. The primary stresses arise from head moment and, therefore, the section modulus is equal to or greater than that of the present shaft. The resulting geometry is given in Table A-2.

Equations for Shaft Extension Geometry:

$$S = \frac{I}{C} = \frac{\pi(R_o^4 - R_i^4)}{4R_o}$$

$$R_1 = \left[R_o^4 - \frac{4}{\pi} SR_o\right]^{1/4}$$

$$A = \pi\left[R_o^2 - R_i^2\right]$$

TABLE A-2. SHAFT EXTENSION GEOMETRY

STATION*	ORIGINAL SHAFT			NEW SHAFT		
	R_o(in)	R_i(in)	A(in^2)	R_o(in)	R_i(in)	A(in^2)
a	4.80	4.3	14.29	5.0	4.56	13.32
b	4.80	3.8	27.01	5.0	4.55	13.32
c	4.70	3.8	24.03	5.0	4.55	13.32
d	4.75	4.0	20.61	5.1	4.68	13.00
e	4.65	4.15	13.82	5.4	5.03	12.08
f	4.50	4.00	13.35	5.75	5.43	11.20
g	4.40	3.80	15.46	6.10	5.82	10.48
h	4.50	3.80	18.25	6.42	6.17	9.88
i	4.60	3.80	21.11	6.80	6.58	9.28
j				7.15	6.95	8.76
k				7.45	7.27	8.40
l				7.80	7.64	8.00

*Refer to Figure A-11 for locations.

$\mathcal{C}_{\ell_1}$ = centerline new shaft

$\mathcal{C}_{\ell_2}$ = centerline old shaft

$\mathcal{C}_{\ell_1}$ & $\mathcal{C}_{\ell_2}$ coincide. They are displaced here to avoid superimposing the two shaft configurations on one another.

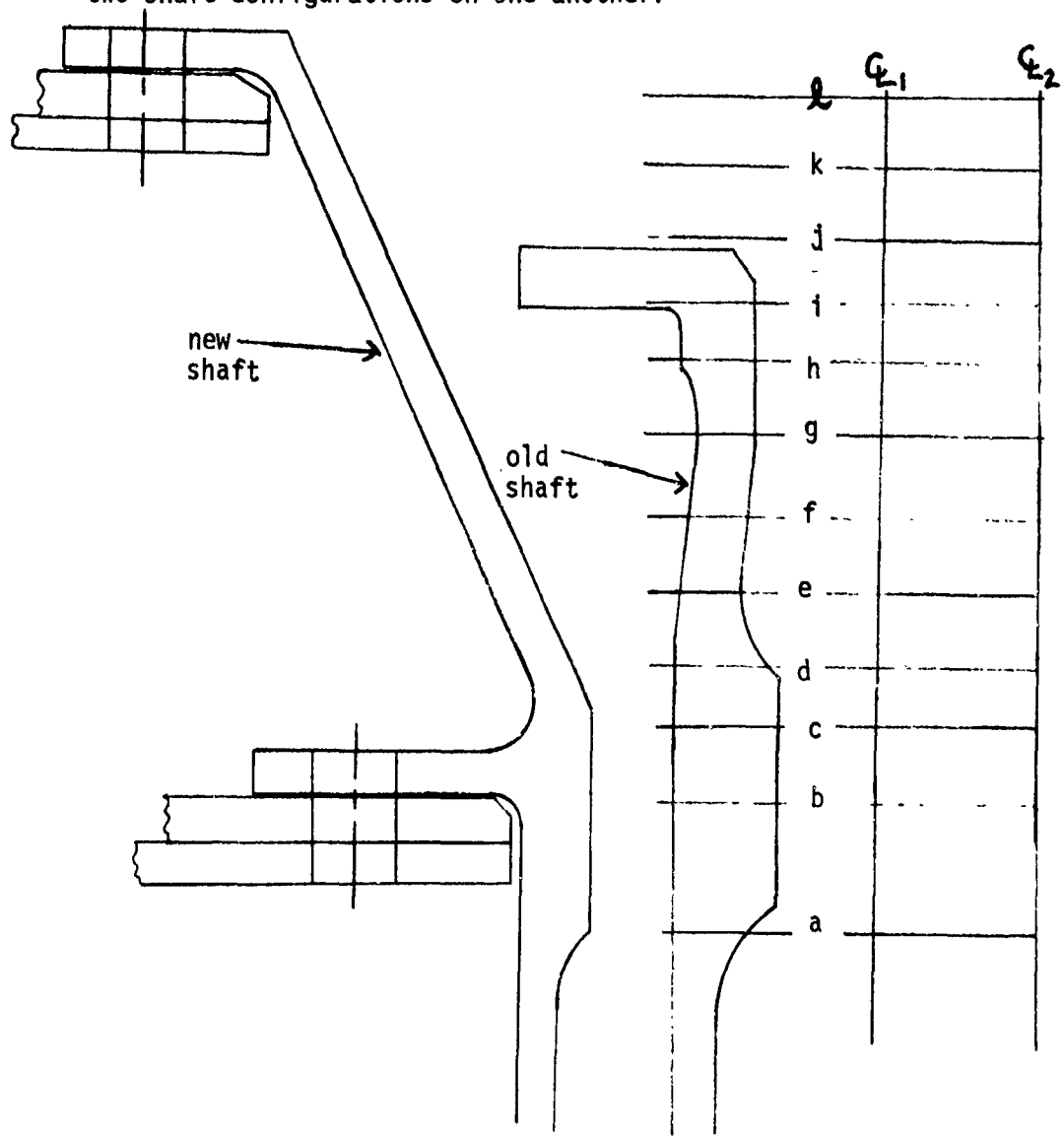

FIGURE A-11. SHAFT EXTENSION CONFIGURATIONS

2. Upper Ring of Shaft Extension

a. Limit Load Analysis

P_1 = Bolt Force from the Top Plate

P_2 = Bolt Force from Top Lug of Tube

P_1 = 16,636 lbs

P_2 = 6579 lbs

$P_T = P_1 + P_2$ = 23,215 lbs

Check Bolt Bearing

T = 0.3 inch

P = 23,215 lbs

$$f_{brg} = \frac{P}{t \times D} = \frac{23,215}{1 \times .3} = 77,383 \text{ psi}$$

F_{brg} = 197,000 psi (Ref. 4)

$$MS = \frac{197,000}{1.5(77,383)} - 1 = +.69$$

Check Net Tension

$$f_{net} = \frac{P}{A_{net}} = \frac{P}{(w-d)\ t}$$

$$f_{net} = \frac{23,215}{3.18 \times .3} = 24,334 \text{ psi}$$

F_{net} = 130,000 psi (Ref. 4)

$$MS = \frac{130,000}{1.5(24,334)} - 1 = +2.56$$

Check Shear Out

$$f_{so} = \frac{P}{Aso} = \frac{P}{2\left[D \times \frac{e}{D} \times t\right]}$$

$$F_{s} = \frac{23,215}{2 \times 1 \times 1 \times .3} = 38,691 \text{ psi}$$

F_{so} = 79,000 psi (Ref. 4)

$$MS = \frac{79,000}{1.5(38,691)} - 1 = +.36$$

b. Fatigue Analysis

$P_1 = 11,914 \pm 2903$ lbs

$P_2 = 5043 \pm 1822$ lbs

$P_t = 16,957 \pm 4725$ lbs

$$f_{gross} = \frac{P_t}{A_{gross}}$$

$$f_{gross} = \frac{16,957 \pm 4725}{4.18 \times .3}$$

$f_{gross} = 13,522 \pm 3767$ psi

$F_{gross\ lug} = \pm 6000$ psi (Ref. Fig. 10)

$$MS = \frac{6000 \times .7}{3767} - 1 = +.11$$

3. Lower Ring of Shaft Extension

a. Limit Load Analysis

P_1 = Load from Bottom Plate

P_2 = Load from Lower Lug of Tube

$P_1 = 15,951$ lbs

$P_2 = 11,347$ lbs

$P_T = P_1 + P_2 = 27,298$ lbs

Thickness of Lug = .35 inch

Check Bolt Bearing

$$f_{brg} = \frac{P}{t \times D} = \frac{27,298}{1 \times .35} = 77,994 \text{ psi}$$

F_{bru} = 197,000 psi (Ref. 4)

$$MS = \frac{197,000}{1.5(77,994)} - 1 = +.68$$

Check Net Tension

$$f_{net} = \frac{P}{Anet} = \frac{P}{(w-d)\ (t)}$$

$$f_{net} = \frac{27,298}{.35 \times 1.36} = 57,348 \text{ psi}$$

F_{net} = 130,000 psi (Ref. 4)

$$MS = \frac{130,000}{1.5(57,348)} - 1 = +.51$$

Check Shear Out

$$f_{so} = \frac{P}{A_{so}} = \frac{P}{2\left[D \times \frac{e}{D} \times t\right]}$$

$$f_{so} = \frac{27,298}{2 \times 1 \times 1 \times .35} = 38,997 \text{ psi}$$

F_{so} = 79,000 psi (Ref. 4)

$$MS = \frac{79,000}{1.5(38,997)} - 1 = +.35$$

b. Fatigue Analysis

P_1 = Load from Bottom Plate

P_2 = Load from Top Plate

P_1 = 6808 $\pm$ 1629 lbs

P_2 = 5879 $\pm$ 966 lbs

P_T = 12,687 $\pm$ 2595 lbs

$$f_{gross} = \frac{P_T}{A_{gross}}$$

$$f_{gross} = \frac{P_T}{.35 \times 2.36}$$

$$f_{gross} = 15,359 \pm 3141 \text{ psi}$$

$$F_{gross\ lug} = \pm 6000 \text{ psi (Ref. Fig. 10)}$$

$$MS = \frac{6000 \times .7}{3141} - 1 = .33$$

E. Analysis of the Bearing Adapter

The bearing adapter is Ti-6AL-4V and has the same dimensions at the outboard region as the present hub. The attachment to the elastomeric bearings, therefore, need not be analyzed.

The most critical bolt hole is at the bottom of the adapter. For loads, refer to Section C.4 where P was shown to be 23,567 pounds.

1. Limit Load Analysis

Check Bolt Bearing

$$f_{brg} = \frac{P}{t \times D} = \frac{23,567}{1 \times .3}$$

$$f_{brg} = 78,556 \text{ psi}$$

$$F_{bru} = 197,000 \text{ psi (Ref. 4)}$$

$$MS = \frac{197,000}{1.5(78,556)} - 1 = +.67$$

Check Net Tension

$$f_{net} = \frac{P}{A_{net}}$$

$$f_{net} = \frac{23,567}{(2.7-1)(.3)} = 46,209 \text{ psi}$$

$$F_{net} = 130,000 \text{ psi (Ref. 4)}$$

$$MS = \frac{130,000}{1.5(46,209)} - 1 = + .87$$

Check Shear Out

$$f_{so} = \frac{P}{A_{so}} = \frac{P}{2 \times D \times \frac{e}{d} \times t}$$

$$f_{so} = \frac{25,567}{2 \times 1 \times 1 \times .3} = 39,278 \text{ psi}$$

$F_{so} = 79,000$ psi (Ref. 4)

$$MS = \frac{79,000}{1.5(39,278)} - 1 = +.34$$

2. Fatigue Analysis

$$P_{steady} = \frac{A_B}{A_T} C_F \quad \text{(See Section C.4 of this Appendix)}$$

$$P_{steady} = \frac{.75^2}{\left[.75^2 \times 6 + 1^2 \times 2\right]} \times 69,700 \text{ lbs}$$

$P_{steady} = 7,294$ lbs

$$P_{Vib} = \frac{Vd\ y\ D^2}{I} \quad \text{(See Section C.4 of this Appendix)}$$

$V = \pm 6000$ lbs

$I = 84.96 \text{ in}^4$

$y = 4.8$ in

$d = 1.4$ inches = distance from flap hinge to bolt ℄

D = bolt diameter = .75 in.

$P_{Vib} = 267$ lbs

$P = 7,294 \pm 267$ lbs

$$f_{gross} = \frac{P}{.3 \times 2.7} = 9005 \pm 330 \text{ psi}$$

$F_{Vib} = 6500$ psi (Ref. Fig. 10)

$$MS = \frac{6500 \times .7}{330} - 1 = +\text{HIGH}$$

F. Analysis of the Damper Lug

The damper lug is shown in Figure A-12. It is an aluminum forging which supports the bolt running from the top to the bottom plate. The loads are substantial only during startup when a 17,000 lb force is applied to the ball. The following conservative assumptions are made:

1. The bolt EI does not assist the damper support in restraining bending.

2. The wall of each tube, which is bolted to a flange on the damper support, is not assumed to assist in limiting displacements.

a. Starting Load Analysis

$$\theta = \frac{M\ell}{EI} \quad \frac{P/2 \times 3.5' \times 8/2}{10 \times 10^6 \times 27.8}$$

$P = 17{,}000$ lbs

$\theta = 4.28 \times 10^{-4}$ radians

$\delta = R\theta = 3.5'' \times \theta = 1.49 \times 10^{-3}$ inches

δ is acceptable

$$f_t = \frac{MC}{I} = \frac{(P/2 \times 3.5) \times 2.5}{27.8}$$

$f_t = 2675$ psi

$F_{tu} = 60{,}000$ psi (Ref. 4)

$$MS = \frac{60{,}000}{1.5(2675)} - 1 = +HIGH$$

b. Fatique Analysis

$$f_t = \frac{MC}{I} = \frac{(P/2 \times 3.5'') \times 2.5}{27.8}$$

$P = \pm 750$ lbs

$f_t = \pm 118$ psi

$F_{Vib} = 17{,}000$ psi (Ref. 6)

$$MS = \frac{17{,}000 \times .7 \times .7}{118} - 1 = +HIGH$$

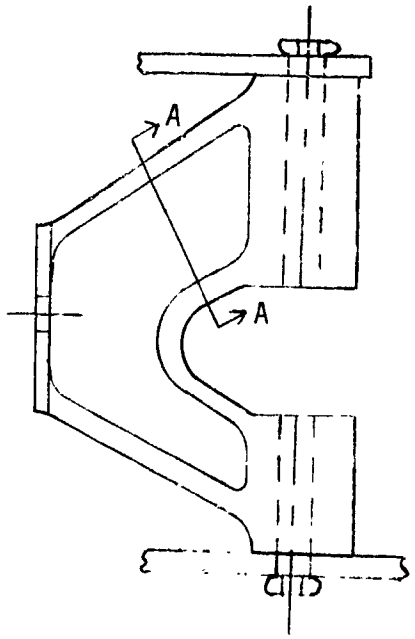

$I_{AA} = 2Ad^2 + 1/12bh^3$

$I_{AA} = 2 \times .9 \times 2 \times 2.5^2 + 1/12 \times 1 \times 4^3$

$I_{AA} = 27.8\ in^4$

$E = 10 \times 10^6$ psi

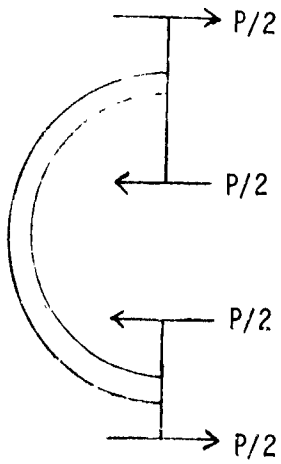

Idealization

FIGURE A-12. DAMPER LUG

Analysis for bolt bearing stresses in the composite plates due to the damper bolt.

a. Starting Load Analysis

$$f_{brg} = \frac{P}{A_{brg}}$$

$$f_{brg} = \frac{1/2 \times 17{,}000 \text{ lbs}}{.75 \times .5}$$

f_{brg} `2,666 psi

F_{brg} = 100,000 psi (Ref. 5, 1.3.2(23) @ 165°F)

$$MS = \frac{100{,}000}{1.5(22{,}666)} - 1 = +1.50$$

b. Fatigue Analysis

$P = \pm 750$ lbs

$$f_{brg} = \frac{1/2\ P}{A_{brg}} = \frac{1/2 \cdot 750}{.75 \times .5}$$

$f_{brg} = \pm 1000$ psi

F_{brg} = 50,000 psi (Ref. Fig. 12)

Use 30% reduction for environment

$$MS = \frac{50{,}000 \times .7 \times .7}{1000} - 1 = +HIGH$$

G. Analysis of the Bifilar Attachment

The bifilar is an integral part of the upper plate. The bushings are replaceable (stainless steel), and the metal cover plate is titanium. The bushing/plate system applies compressive loads to the composite. The bushings distribute the pin loads over the composite. The bifilar loads are summarized in SER-70514, Appendix B. The appropriate loads are given below:

Limit Loads

P_{radial} = 3023 lbs

$P_{vertical}$ = 215 lbs

$P_{tangential}$ = 1252 lbs

Flight Loads

P_{radial} = 1288 ± 340 lbs

$P_{vertical}$ = ± 172 lbs

$P_{tangential}$ = ± 443 lbs

Stiffening and strengthening by the metal cover plate will be conservatively neglected.

a. Limit Load Analysis

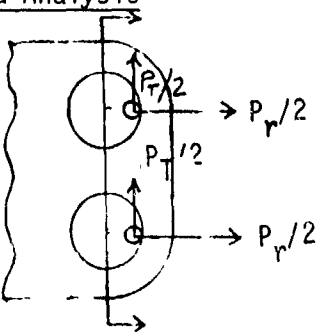

P_v is out of the plane of the paper.

Axial Stress

$$f_a = \frac{P}{A} + \frac{M_f}{S}$$

$$f_a = \frac{P_r}{A} + \frac{(Pr \times \quad)}{S}$$

$$f_a = \frac{3023}{2 \times .5} + \frac{215 \times 1}{1/6 \times 2 \times .5^2}$$

f_a = 5603 psi

Shear Stress

$$f_s = \frac{P_T}{A} = \frac{1252}{2 \times .5} = 1252 \text{ psi}$$

F_a = 87,500 psi (Ref. 5, 1.2.2(28) @ 165°F)

F_s = .7 x 10,000 = 7000 psi conservatively using the shear strength of unidirectional material.

$$MS = \frac{1}{\left[\left(\frac{5603}{87,500}\right)^2 \left(\frac{1252}{7000}\right)^2\right]^{1/2}} - 1$$

$$MS = + 4.26$$

b. Fatigue Analysis

Axial Stress

$$f_a = \frac{P_R}{A} + \frac{M_f}{S}$$

$$f_a = \frac{1288 \pm 340}{2" \times .5"} + \frac{\pm 172 \times 1}{1/6 \times 2 \times .5^2}$$

$$f_s = \frac{P_T}{A} = \frac{\pm 443}{2 \times .5}$$

$$f_a = 1288 \pm 2404 \text{ psi}$$

$$f_s = \pm 443 \text{ psi}$$

F_a = 18,000 psi (Ref. Fig. 11)

F_s = 1400 psi (Ref. SER-79158, Appendix A, Ref. 1, Pg. 77)

$$MS = \frac{1}{\left[\left(\frac{2404}{18,000 \times .7}\right)^2 + \left(\frac{443}{1400 \times .7}\right)^2\right]^{1/2}} - 1$$

$$MS = + 1.03$$

Analysis of Bolts

1. Hub to Shaft Fasteners - Upper Bolt Ring.

Bolts: 1" Dia. - Stainless Steel

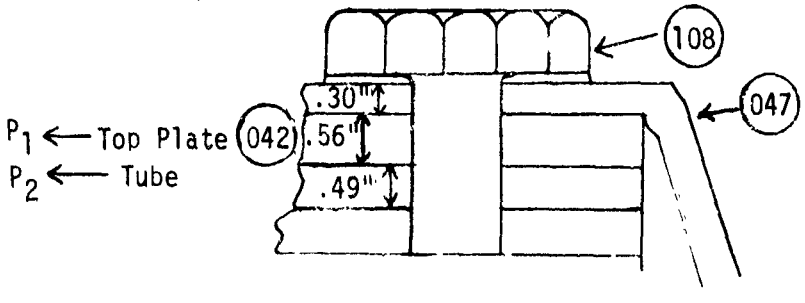

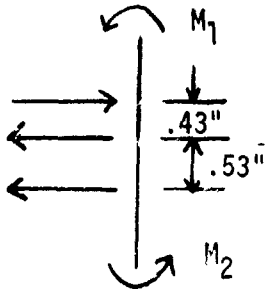

$M_1 + M_2 = P_1 \times .43 + P_2 \times .96$

$M_1 = M_2 = M$

$M = \frac{1}{2}(P_1 \times .43 + P_2 \times .96)$

Static Analysis

$P_1 = 16{,}636$ lbs

$P_2 = 6579$ lbs

$M = \frac{1}{2}(.43 \times 16{,}636 + 6579 \times .96)$

$M = 6734$ in-lbs

$V = P_1 + P_2 = 23{,}215$ lbs

$M_{ult} = 25{,}900$ in-lbs (Ref. 4)

$V_{ult} = 74{,}600$ lbs (Ref. 4)

$$MS_{shear} = \frac{74{,}600}{1.5(23{,}215)} - 1 = 1.10$$

$$MS_{bending} = \frac{25{,}900}{1.5(6734)} - 1 = 1.50$$

Fatigue Analysis

$P_1 = 11{,}914 \pm 2903$ lbs

$P_2 = 5043 \pm 1822$ lbs

$P_T = 16{,}957 \pm 4725$ lbs

$M = \frac{1}{2}(P_1 \times .43 + P_2 \times .96)$

$M = 4982 \pm 1498$ in-lbs

P = Preload

$$P = \frac{T}{.2D} = \frac{6850}{.2 \times 1} = 34{,}200 \text{ lbs}$$

$A = \pi r^2 = .785$ in^2

For bending take into account for the bushing.

$$I = \frac{\pi r^4}{4} = \frac{\pi(1.3/2)^4}{4} = .14 \text{ in}^4$$

$$y = .5 \text{ in}$$

$$S = \frac{I}{y} = .28 \text{ in}^3$$

$$f_z = \frac{P}{A} + \frac{M}{S}$$

$$f = \frac{34,200}{.785} + \frac{(4982 \pm 1498)}{.28}$$

$$f = 61,360 \pm 5350 \text{ psi}$$

$$f_{Vib} = 12,000 \text{ psi (Ref. Pg. 5.0.6)}$$

$$MS = \frac{12,000 \times .7}{5350} - 1 = .57$$

2. Hub to Shaft Fasteners - Lower Bolt Ring

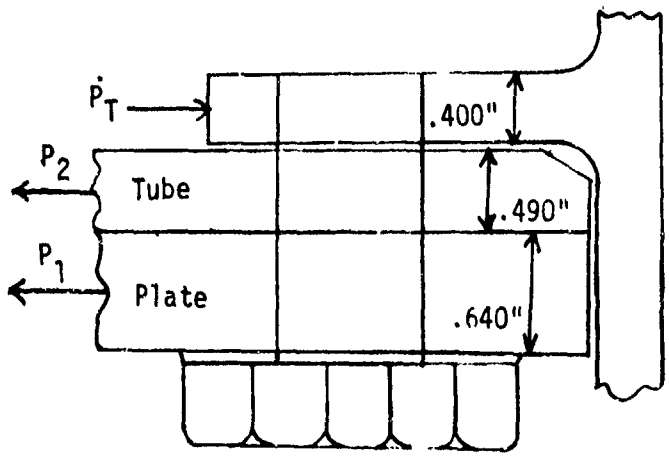

P_1 static = 15,951 lbs

P_1 fatigue = 6808 ± 1629 lbs

P_2 static = 11,347 lbs

P_2 fatigue = 5879 ± 966 lbs

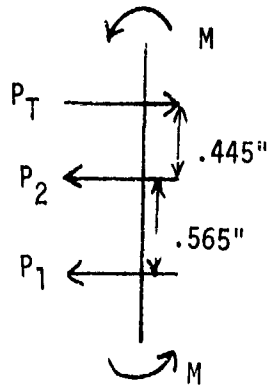

$M = \frac{1}{2} P_2 \times .445 + P_1 (.445 + .565)$

$V = P_T$

Static Analysis

$M = 10{,}579$ in-lbs

$V = 27{,}298$ lbs

$M_{ult} = 25{,}900$ in-lbs (Ref. 4)

$M_{ult} = 74{,}600$ lbs (Ref. 4)

$$MS_{shear} = \frac{74{,}600}{1.5(27{,}298)} - 1 = .82$$

$$MS_{bending} = \frac{25{,}900}{1.5(10{,}579)} - 1 = .64$$

Fatigue Analysis

$M = 4746 \pm 1037$ in-lbs

$f = \frac{P}{A} + \frac{My}{I}$ Same as with the bolt on the top (Page 177)

Preload is same; bending moment is less, therefore MS is higher.

MS > .57 (See Page 179)

3. Bearing End ℄ To Tube - Intermediate Bolt

3/4" Dia. bolt

Titanium 6Al-4V

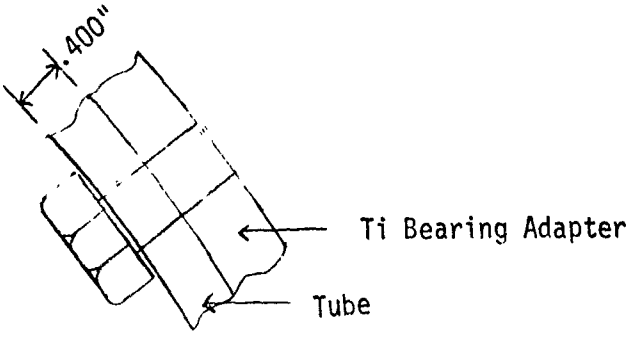

Steady

P = 14,368 lbs

Vibratory

P = 8712 ± 238 lbs

Limit Analysis

V = 14,368 lbs

V_{ult} = 31,800 lbs (Ref. 4)

$$MS = \frac{31,800}{1.5(14,368)} - 1 = .48$$

Bending:

M = P x .4" = 14,368 x .4

M = 5747 in-lbs

M_{ult} = 19,900 in-lbs (Ref. 4)

$$MS = \frac{19,900}{1.5(5747)} - 1 = 1.3$$

Fatigue Analysis

The restraining moments are computed in the same manner as before

$M = \frac{1}{2}(8712 \pm 238)(.4) = (3484 \pm 95)$

$S = \frac{\pi r^3}{4} = \frac{\pi(3/8)^3}{4} = .0414 \text{ in.}^3$

$P = \frac{T}{.2D} = \frac{3130}{.2x.75} = 20{,}866 \text{ lbs}, \quad A = \pi r^2 = \pi(3/8)^2 = .442 \text{ in.}^2$

$f = \frac{M}{S} + \frac{P}{A}$

$f = \frac{\frac{1}{2}(3484 \pm 95)}{.0414} + \frac{20{,}866}{.442}$

$f = 89{,}291 \pm 1146 \text{ psi}$

$P_{Vib} = 4000 \times 2.23 = 8920 \text{ psi}$ (Ref. 6, Pg. 5.09)

$MS = \frac{.7 \times 8920}{1146} - 1 = 4.47$

4. Damper Bolts

3/4" Dia. Titanium Bolt

$P_{steady} = 17{,}000 \text{ lbs}$

$P_{Vib} = 0 \pm 750 \text{ lbs}$

Static Analysis

Shear

$V = \frac{1}{2}P = \frac{1}{2} \times 17{,}000 \text{ lbs}$

$V = 8500 \text{ lbs}$

$V_{ult} = 41{,}900 \text{ lbs}$ (Ref. 4)

$MS_{shear} = \frac{41{,}900}{1.5(8500)} - 1 = 2.28$

Bending

The bolt will bend the same amount as the damper lug (See Page 173)

$$\frac{d\theta}{dx} = \frac{4.28 \times 10^{-4}}{4} \text{ rad/inch}$$

$$F_b = E\, y \frac{d\theta}{dx}$$

$$f_b = (16 \times 10^6)\ (3/8)\ \frac{(4.2 \times 10^{-4})}{4}$$

$$f_b = 630 \text{ psi}$$

$$F_{ult} = 130{,}000 \text{ psi (Ref. 4)}$$

$$MS = \frac{130{,}000}{1.5\ (\ 630)} - 1 = + \text{HIGH}$$

Very little bending occurs as was the intent of the support.

Fatigue Analysis

$$f_s = \frac{V}{A_s} = \frac{\pm \frac{1}{2}(750)}{\pi\,(3/8)^2}$$

$$f_s = 848 \text{ psi}$$

$$MS = \frac{1}{\left[4\left(\frac{f_s}{F_s}\right)^2\right]^{1/2}}$$

F_s = chafing endurance limit

F_s = .7 x 8920 = 6244 (Ref. 6, Pg. 5.0.9)

$$MS = \frac{1}{\left[4\left(\frac{848}{6244}\right)^2\right]^{1/2}} - 1 = 2.68$$

Shim Analysis

Stainless steel shims having a taper of .100 inch in thickness per 1.00 inch in length are embedded in the top plate, and tubes in the region where these components attach to the shaft extension. A typical layup is shown below:

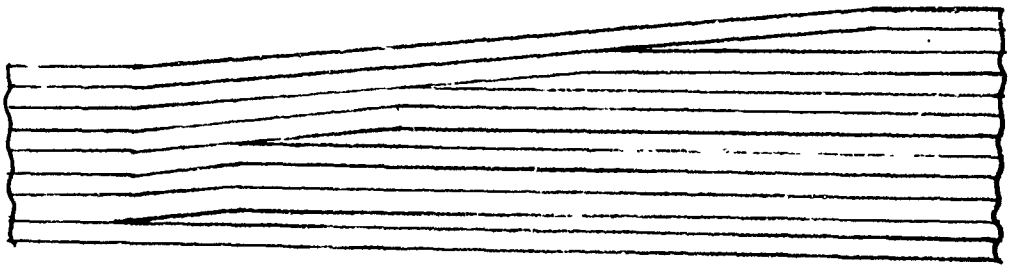

The most critical region is at the tip of the longest shim because there the EA change is the greatest. The stresses are computed using Y004B, a lap shear computer analysis. The analytical model is shown below:

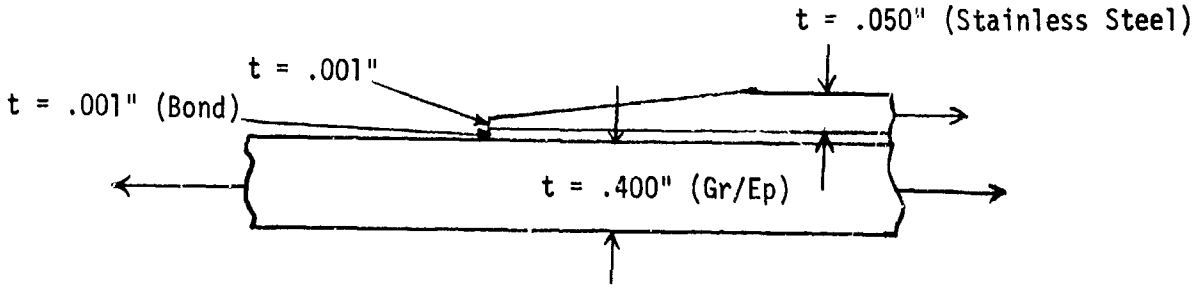

τ = peak shear stress

f = applied axial stress

From Y004B $\frac{\tau}{f}$ = .14

Since the laminates are buried, the bond area is increased by a factor of 2. Hence, $\frac{\tau}{f}$ = .07.

Analysis of Top Plate

Static Analysis

f_{max} = 24,405 psi

$\tau_{max} = .07\ f_{max}$ = 1708 psi

τ_{all} = 10,000 psi (Static Allowable)

Use 30% environmental reduction

$$MS = \frac{10{,}000 \times .7}{1.5\ (1708)} - 1 = 1.73$$

Fatigue Analysis

$f_{max} = 9548 \pm 6399$

$\tau_{max} = .07\ f_{max} = 670 \pm 307$ psi

τ_{all} = 1300 psi (Ref. Fig. 13)

Use 30% reduction factor for environment

$$MS = \frac{.7 \times 1300 \times .7}{307} - 1 = 1.07$$

Analysis of Bottom Plate

Static Analysis

f_{max} = 35,918 psi

$\tau_{max} = .07\ f_{max}$ = 2514 psi

τ_{all} = 10,000 psi

Use 30% environmental reduction factor

$$MS = \frac{10{,}000 \times .7}{1.5\ (2514)} - 1 = + .85$$

Fatigue Analysis

$f_{max} = 13{,}093 \pm 3320$

$\tau_{max} = .07\ f_{max} = 916 \pm 232$

$\tau_{all} = 1200$ (Ref. Fig. 13)

Use 30% environmental factor

$$MS = \frac{1200 \times .7 \times .7}{232} - 1 = 1.52$$

Tube - Attachment to Top Ring

Static Analysis

$f_{max} = 5172$ psi

$\tau_{max} = .07\ f_{max} = 362$ psi

$\tau_{all} = 10{,}000$ psi

Use 30% environmental factor

$$MS = \frac{10{,}000 \times .7}{1.5\ (362)} - 1 = +HIGH$$

Fatigue Analysis

$f_{max} = 3964 \pm 1432$

$\tau_{max} = .07\ f_{max} = 277 \pm 100$

$\tau_{all} = 1400$ (Ref. Fig. 13)

Use 30% environmental factor

$$MS = \frac{1400 \times .7 \times .7}{100} - 1 = + HIGH$$

Tube Attachment to Lower Ring

Static Analysis

$f_{max} = 16{,}686$ psi

$\tau_{max} = .07\ f_{max} = 1168$ psi

τ_{all} = 10,000 psi

Use 30% envircnmental reduction

$$MS = \frac{10{,}000 \times .7}{1.5\ (1168)} - 1 = + \text{HIGH}$$

Fatigue Analysis

$f_{max} = 4982 \pm 818$

$\tau_{max} = .07\ f_{max} = 348 \pm 57$

τ_{all} = 1500 (Ref. Fig. 13)

Use 30% reduction for environment

$$MS = \frac{1500 \times .7 \times .7}{57} - 1 = + \text{HIGH}$$

APPENDIX B. ANALYSIS AFTER A BALLISTIC HIT

The most critical "hit" is one which damages the lower portion of the most highly loaded arm. The assumption for this analysis is that a 3 inch x 8 inch region of the lower plate and its attachment to the shaft as well as the redundant attachment of the tube to the shaft are destroyed.

The stresses in the top and bottom plate and the tube are shown in Figures B-1, B-2 and B-3 respectively. Compared to the undamaged hub (refer to Appendix A) these stresses have increased by a factor of 2, or 6 if the stress concentration is included.

Several changes have been made in the analysis. First, because the limit load condition is so much higher than the minimum flight head moment, the analysis was performed for limit load only; fatigue stresses were estimated by ratioing head moments. Limit M_H = 657,000 in.-lbs. and 3^o flapping, which was used for the 30 minute safe flight requirement, M_H = 91,400 in.-lbs. (See Table 9, Flapping Angle Spectrum, Basic Report). Therefore, fatigue stresses are $\frac{91,400}{65,700}$ times the limit load stresses.

Another difference is that a less conservative and more realistic approach was taken for stress analysis. The critical regions of the composite are close to the shaft attachment rings. The NASTRAN Model was 0.40 inches throughout. The actual hub in this region is 0.56 and 0.64 inch thick for the top and bottom plate respectively. For axial (membrane) stresses, the actual stress is reduced proportionally to the thickness ratio; i.e., $f_{actual} = f_{model} \frac{.4}{t_{actual}}$.

For bending (flexural) stresses the actual stress is reduced by the square of the thickness ratio; i.e. $f_{actual} = f_{model} \left(\frac{.4}{t_{actual}}\right)^2$.

For static stresses, the allowables were reduced, not by 1.5 as for the normal analysis, but by 1.12 as is standard for a yield type of situation.

Analysis of the Top Plate

Limit Load

The peak stress is close to the attachment to the shaft. From Figure B-2, f_{max} = 59,200 psi. From a detailed analysis of the individual element stresses it was found that nearly all of the stress was associated with flexure.

Therefore,

$$f = \left(\frac{.40}{.56}\right)^2 \quad (59,200) = 30,204 \text{ psi}$$

$$MS_{ult} = \frac{87,500}{(1.12)(30,204)} - 1 = + 1.58$$

Fatigue Analysis

Fatigue stresses are:

$$f_{Vib} = \frac{91,400}{657,000} = 30,204 \text{ psi}$$

$$f_{Vib} = \pm 4228 \text{ psi}$$

F_{Vib} = 28,000 psi (Figure 11)

$$MS = \frac{28,000 \times .7 \times .94}{4228} - 1 = + \text{HIGH}$$

Analysis of the Bottom Plate

Limit Load

The maximum stress occurs at the edge of the damage, near the shaft attachment. The stresses from this "far field" analysis do not reflect local stress concentration effects. Therefore, these stresses will be multiplied by $K_T = 3$. From Figure B-2 the maximum stress is:

f_{max} = 49,300 psi

A detailed study of the stresses in the element shows that approximately half is due to bending and half is due to axial extension. Therefore,

$$f_T = \tfrac{1}{2}\left(\frac{.40}{.64}\right) f_{max} + \tfrac{1}{2}\left(\frac{.40}{.64}\right)^2 f_{max}$$

f_T = 25,035 psi

$f_{peak} = K_T f_T = 3 \times 25,035 = 75,105$ psi

$$MS = \frac{87,500}{1.12\ (75,105)} - 1 = + .04$$

Fatigue

$$f_{vib} = \frac{91,400}{657,000} \quad 75,105 = 10,402 \text{ psi}$$

F_{vib} = 28,000 (Figure 11 of Basic Report)

$$MS = \frac{28,000 \times .7 \times .94}{10,402} - 1 = .77$$

(No other regions are as critical on the hub).